

5-2016

Developing And Using Methyl-Specific Antibodies To Study The Biological Roles Of Arginine Methylation

Vidyasiri Vemulapalli

Follow this and additional works at: https://digitalcommons.library.tmc.edu/utgsbs_dissertations



Part of the [Cell Biology Commons](#), [Medicine and Health Sciences Commons](#), and the [Molecular Biology Commons](#)

Recommended Citation

Vemulapalli, Vidyasiri, "Developing And Using Methyl-Specific Antibodies To Study The Biological Roles Of Arginine Methylation" (2016). *Dissertations and Theses (Open Access)*. 648.
https://digitalcommons.library.tmc.edu/utgsbs_dissertations/648

This Dissertation (PhD) is brought to you for free and open access by the MD Anderson UTHealth Houston Graduate School at DigitalCommons@TMC. It has been accepted for inclusion in Dissertations and Theses (Open Access) by an authorized administrator of DigitalCommons@TMC. For more information, please contact digcommons@library.tmc.edu.

DEVELOPING AND USING METHYL-SPECIFIC ANTIBODIES TO STUDY
THE BIOLOGICAL ROLES OF ARGININE METHYLATION

By

Vidyasiri Vemulapalli, M.S.

APPROVED:

Mark Bedford, Ph.D.
Supervisory Professor

David Johnson, Ph.D.

Richard Wood, Ph.D.

Taiping Chen, Ph.D.

Mark McArthur, DVM, DACVP

APPROVED:

Dean, The University of Texas

Graduate School of Biomedical Sciences at Houston

DEVELOPING AND USING METHYL-SPECIFIC ANTIBODIES TO STUDY
THE BIOLOGICAL ROLES OF ARGININE METHYLATION

A

DISSERTATION

Presented to the Faculty of
The University of Texas
Health Science Center at Houston
and
The University of Texas
MD Anderson Cancer Center
Graduate School of Biomedical Sciences
in Partial Fulfillment
of the Requirements
for the Degree of
DOCTOR OF PHILOSOPHY

by

Vidyasiri Vemulapalli, M.S.

Houston, Texas

May, 2016

DEDICATION

This dissertation work is lovingly dedicated to my mother, Padmavathi, who passed away from cancer during my doctoral studies. Her constant, unconditional love had given me strength and sustained me during the first few years of my Ph.D. I dedicate this dissertation to my dearest husband, Ratnakar, who inspired me to continue on, and stay strong during those hard times. I also dedicate this work to my father, Poornachandra Rao, who instilled in me a love for learning and provided me with the scaffolding to pursue higher education. Finally, I dedicate this dissertation to my brother and my parents-in-law for their loving support.

ACKNOWLEDGEMENTS

First and foremost, I would like to thank my mentor, Dr. Mark Bedford, for taking me on as a graduate student in his lab, training me, and importantly helping me in accomplishing my scientific goals. I was extremely fortunate in having him as my mentor. His enthusiasm towards research has been contagious and motivational for me, especially in helping me push myself forward during the tough times. I thank him in every possible way for spending his precious time in helping with my research, answering my questions, reviewing my scientific paper, dissertation and many write-ups during the course of my Ph.D.

I am also fortunate to have the help and guidance of my advisory committee members. Dr. David Johnson, Dr. Taiping Chen, Dr. Richard Wood, and Dr. Mark McArthur provided many useful suggestions for my projects and helped me improve my scientific writing and speaking skills. I specially want to thank Dr. David Johnson for providing me the opportunity to rotate in his lab, where I learned a number of cell culture and mouse techniques under the excellent guidance of Dr. Anup Biswas.

My success in graduate school would not have been possible without the help and support of my lab members. Dr. Donghang Cheng is the expert in the lab and the go-to person for everybody. I was fortunate to be guided by him and to collaborate with him on my main Ph.D. project. He is not only an excellent mentor, but also a great friend who took care of me during the time my mother passed away. Dr. Yanzhong Yang (Frankie) was another highly talented post-doc in the lab. Although he did not directly guide me in my project, I learned a great deal from his presence in the lab. I would also like to thank Alexsandra Espejo for teaching the molecular biology basics during my first lab rotation in the Bedford lab. Aimee Iberg, another amazing student in the Bedford lab, is my role model and an excellent friend. Cari Sagum (DB), Karynne Black, and Sitaram Gayatri also became very dear friends over

the past few years and I really cherish the time I spent with them. Nobody can make me laugh like they do.

Finally, I want to thank my family without whose support, I could not have finished my Ph.D. I lost my mother to breast cancer during my second year of Ph.D and it was a very difficult time for me. My husband, whom I met five months after my mother's death, gave me a lot of comfort and strength, which I really needed to continue my Ph.D. study further. I am also thankful to my father, brother and my parents-in-law for their constant help, encouragement and moral support.

**Developing and using methyl-specific antibodies to study
the biological roles of arginine methylation**

Vidyasiri Vemulapalli, Ph.D.

Supervisory Professor: Mark T. Bedford, Ph.D.

Arginine residues can be modified in three different ways to produce asymmetric dimethylarginine (ADMA), symmetric dimethylarginine (SDMA), and monomethylarginine (MMA). These modifications are catalyzed by a family of nine protein arginine methyltransferases (PRMT1-9), which are of three types (I, II, and III). The majority of Type I enzymes asymmetrically dimethylate Glycine- and Arginine-rich (GAR) motifs, except for PRMT4, which methylates Proline-, Glycine-, and Methionine-rich (PGM) motifs. The same substrates (GAR or PGM motifs) can also be dimethylated by PRMT5 in a symmetric fashion. However, it is not clear whether there are dedicated residues within these motifs for ADMA and SDMA, or if the two enzyme types (I and II) compete for the same arginine residue. In addition, very little is known about MMA, which commonly occurs as an intermediate in the pathway to ADMA and SDMA generation. But, occasionally some substrates are solely monomethylated due to the Type III activity of PRMT7. This project aimed at clarifying the dynamics of different methylation types using methylarginine-specific antibodies and PRMT null cell lines. By performing methyl-specific antibody Western and amino acid analysis, we were able to show that loss of PRMT1, which removes 90% of ADMA, causes a global rise in MMA and SDMA levels. Hence, we concluded that there is a dynamic interplay among the three types of methylation, and that ADMA acts as a dominant mark preventing the occurrence of MMA and SDMA on the same substrates.

The second project also involved methyl-specific antibodies, however, it was aimed at discovering novel PRMT4 substrates. PRMT4, also referred as coactivator-associated arginine methyltransferase (CARM1), functions as a regulator of transcription and splicing by

methylation of a diverse array of substrates. In order to broaden our understanding of CARM1's mechanistic actions, we generated CARM1 substrate motif antibodies, and used immunoprecipitation coupled with mass spectrometry to identify novel cellular targets for CARM1, including Mediator Complex Subunit 12 (MED12) and the lysine methyltransferase KMT2D/MLL2. Both of these proteins are implicated in enhancer function. We identified the primary CARM1-mediated MED12 methylation site as arginine 1899. Using methyl-specific antibodies to this site, we found that MED12 methylation positively correlates with CARM1 levels. ChIP-seq studies reveal that CARM1 and its activity are tightly associated with ER α -specific enhancers and positively modulate transcription of estrogen (E2)-regulated genes. Using a cell-free biotinylated DNA pulldown assay, we demonstrated that CARM1 and MED12 are co-recruited to a *GREB1* estrogen response element (ERE), and in cells, methylated MED12 efficiently assembles on a multicopy engineered ERE array in response to E2 treatment. Additionally, we show that MED12 interacts with the Tudor domain-containing effector molecule, TDRD3, in a CARM1-dependent fashion. These findings reveal an arginine methylation regulatory node on the Mediator complex that may facilitate the communication between DNA-bound transcription factors and RNA polymerase II.

Table of Contents

Chapter 1: Introduction.....	1
1.1 Protein arginine methylation	1
1.1.1 Arginine methylation types and the PRMT family	1
1.1.2 Regulation of PRMTs.....	7
1.1.3 Arginine methylation in human disease.....	8
1.2 PRMT1	9
1.3 CARM1	13
1.4 Mediator Complex	22
1.4.1 MED12	24
2.1 Antibodies.....	29
2.2 Plasmids and peptides.....	29
2.3 Cell lines	30
2.4 Amino acid analysis	33
2.5 Antibody binding assay	34
2.6 In vitro methylation assay.....	34
2.7 In vitro phosphorylation assay.....	35
2.8 Peptide pull-down assay.....	35
2.9 Immunoprecipitation and Coimmunoprecipitation assays.....	35
2.10 Oligonucleotide pull down assay	37
2.11 Chromatin Immunoprecipitation and quantitative PCR (ChIP-qPCR).....	37
2.12 ChIP-seq analysis	38
2.12.1 Mapping of Reads.....	38
2.12.2 Peak calling and gene annotation	38

2.12.3 Landscape of ChIP-Seq Signal	39
2.12.4 Heatmap and Average Profile of ChIP-Seq Signal around peak center.....	39
2.13 Quantitative Reverse Transcription PCR (RT-qPCR)	39
2.14 Immunofluorescence and Image Analysis.....	40
Chapter 3: Loss of PRMT1 causes substrate scavenging by other PRMTs.....	43
3.1 Mono-methyl arginine antibodies reveal methylation type switching with PRMT1 loss.....	43
3.2 MMA and SDMA levels reach a maximum within 4-6 days after PRMT1 loss.....	46
3.3 Amino acid analysis confirms the global accumulation of MMA and SDMA levels with PRMT1 loss.....	49
Chapter 4: CARM1 Methylates Mediator to Promote Estrogen Receptor-Regulated Transcription	57
4.1 Developing and characterizing CARM1 Substrate antibodies	57
4.2 Using ADMA ^{CARM1} antibodies to identify CARM1 substrates.....	62
4.3 Mediator subunit 12 is methylated at Arginine 1899 by CARM1 <i>in vivo</i>	68
4.4 Methylated MED12 interacts with the effector molecule TDRD3.....	75
4.5 Genome-wide analysis of CARM1, MED12 and H3R17me2a in MCF-7 cells	79
4.6 The dynamics of CARM1 and MED12 recruitment to EREs.....	87
Chapter 5: Discussion	92
5.1 Substrate specificity of PRMTs	92
5.2 Investigating the MMA mark	93
5.3 The dominant ADMA activity of PRMT1 keeps the global MMA and SDMA levels in check.....	96
5.4 CARM1 methylates a distinct motif	99
5.5 CARM1 primarily associates with enhancers, but is also found at promoters	103

5.6 How does CARM1 methylation of MED12 regulate its function?	105
Chapter 6: Future studies	107
Chapter 7: Significance	113
8. References.....	116
9. Vita	133

List of Illustrations

Figure 1: Types of arginine methylation.....	2
Figure 2: The protein arginine methyltransferase family	4
Figure 3: Kinetic mechanism for PRMT1 catalysis.....	12
Figure 4: CARM1 coactivates NR-dependent gene expression	15
Figure 5: Classification of CARM1 substrates.....	17
Figure 6: Basic function and modular structure of the Mediator complex.	21
Figure 7: Domain structure of MED12.	25
Figure 8: Loss of PRMT1 or inhibition of global methylation by AdOx reveals an	44
Figure 9: Loss of other Type I enzymes (PRMT3, 4, and 6) or reduction of Type II	45
Figure 10: Arginine methylation trends in inducible PRMT1-knockout MEFs.	47
Figure 11: Expression analysis of PRMTs in the absence of PRMT1.	48
Figure 12: Quantification of MMA, ADMA, SDMA and arginine levels in protein	51
Figure 13: Workflow for the two-dimensional quantification of MMA, ADMA, SDMA,	52
Figure 14: Reverse-phase HPLC methods optimized to quantify OPA-derivatives of	53
Figure 15: Characterization of CARM1 substrate antibodies.	59
Figure 16: Histone peptide array analysis of CARM1 substrate antibodies.....	61
Figure 17: Identification of novel CARM1 substrates.	64
Figure 18: Validation of CARM1 substrates.....	67
Figure 19: Characterization of the meMED12 antibodies.....	69
Figure 20: Binding specificity of methyl-MED12 antibody determined by OPAL.....	71
Figure 21: CARM1 - Mediator interactions.....	73
Figure 22: MED12 methylation does not affect CDK8 kinase activity.....	74
Figure 23: MED12 - TDRD3 interactions	76
Figure 24: MED12 methylation status in breast cancer subtypes.....	78

Figure 25: ChIP-seq analysis of CARM1, MED12, and H3R17me2a in MCF-7 cells.	81
Figure 26: Overlap between ER peaks and promoter peaks.....	82
Figure 27: Regulation of ChIP-seq target genes by MED12 methylation.	84
Figure 28: Confirmation of ChIP-seq peaks for the target genes.	85
Figure 29: MED12 methylation levels do not correlate with ER levels.	86
Figure 30: E2-dependent recruitment of methylated MED12 to the ER-target gene,.....	89
Figure 31: E2-dependent recruitment of methylated MED12 to TFF1, IGFBP4, and.....	91
Figure 32: Co-immunoprecipitation of GFP-PRMTs with endogenous PRMT1.....	94
Figure 33: Hyper-monomethylation of SmB/SmB' upon PRMT5 loss.....	95
Figure 34: Dynamic interplay between the three types of arginine methylation.....	98
Figure 35: Alignment of CARM1-methylated motifs.	100
Figure 36: MED12 associates with activating ncRNAs in a CARM1-dependent manner....	108
Figure 37: Mutant MED12 shows reduced interaction with activating ncRNAs.	109
Figure 38: MED12 associates with activating ncRNAs in a TDRD3-dependent manner. ...	110
Figure 39: Testing the efficacy of PRMT inhibitors using methyl-specific antibodies.....	114

List of Tables

Table 1: List of phenotypes for mice lacking prmt1-8 genes.	6
Table 2: Antibodies used in the first study.	31
Table 3: Antibodies used in the second study.....	32
Table 4: Primers used for ChIP-qPCR assays.....	41
Table 5: Primers used for RT-qPCR assays.....	42
Table 6: Average fold change in MMA, ADMA and SDMA levels upon the loss of.....	55
Table 7: Comparison of the relative levels of MMA, ADMA, and SDMA in different	56

List of Abbreviations

ADMA	Asymmetrical dimethyl arginine
AdoMet	Adenosyl Methionine
AdOx	Adenosine dialdehyde
APP	Amyloid precursor protein
AR	Androgen receptor
AREs	AU-rich elements
AURKA	Aurora Kinase A
BAF155	BRG1 associated factor 155
BMP	Bone morphogenic protein
BTG	B-cell Translocation Gene
<i>C. elegans</i>	<i>Caenorhabditis elegans</i> ; common nematode
CA150	Transcription elongation regulator 1
CARM1	Co-activator associated arginine methyltransferase 1
CAS3	CARM1 substrate 3
CBP	RNAPII C-terminal Binding Protein
CCNE1	Cyclin E1
CDK8	Cyclin-dependent kinase 8
CITED2	CBP/p300-interacting transactivator 2
<i>D. melanogaster</i>	<i>Drosophila melanogaster</i> ; common fruit fly
<i>D. rerio</i>	<i>Danio rerio</i> ; common fresh water zebra fish
DAL-1	Differentially expressed in adenocarcinoma of lung 4
DDAH	Dimethylarginine dimethylaminohydrolase
DMEM	Dulbecco's modified eagle medium

DN1	Double negative population 1
DN2	Double negative population 2
E2	Estrogen
EBNA2	Epstein-Barr Nuclear Antigen 2
ELK1	ETS domain-containing protein Elk1
EMT	Epithelial to mesenchymal transition
ERE	Estrogen response element
ER α	Estrogen receptor alpha
ESCs	Embryonic stem cells
FBS	Fetal bovine serum
FBW7	F-Box And WD Repeat Domain Containing 7
FKBP4	FK506 Binding protein 4
G9a	Histon lysine N-methyltransferase (EHMT2)
GAPDH	Glyceraldehyde-3-phosphate dehydrogenase
GAR	Glycine and arginine rich
GPS2	G-Protein Pathway suppressor 2
GR	glucocorticoid receptor
GREB1	Growth regulation by estrogen in breast cancer 1
GRIP1	Glutamate Receptor Interacting Protein 1
hCAF1	CCR4-associated factor 1
HCV	Hepatitis C-Virus
HIV	Human Immunodeficiency Virus
HMT	Histone methyl transferase
hnRNP	Heterogeneous Nuclear Ribonucleoprotein
HPLC	High pressure liquid chromatography

HRE	Hormone Response element
HSV	Herpes Simplex Virus
HuD	ELAV-Like protein 4
HuR	ELAV-Like protein 1
IFNAR	Interferon α/β Receptor
IGFBP4	Insulin-like growth factor binding protein 4
IP	Immunoprecipitation
IP-MS	Immunoprecipitation coupled with mass spectrometry
IPTG	Isopropyl β -D-1-thiogalactopyranoside
IVTT	In vitro transcription/translation
JMJD6	Jumonji-domain containing protein 6
KD	Knockdown
KMT2D/MLL2	Lysine methyltransferase 2D
KO	Knockout
lncRNA	Long non-coding ribonucleic acid
MAPK	Mitogen activated protein kinase
MED12	Mediator complex subunit 12
MEFs	Mouse embryonic Fibroblasts
MEP50	WD Repeat containing protein 77
miRNA	Micro RNA
MMA	Monomethyl arginine
MRE11	Double-strand break repair protein MRE11
mRNA	Messenger RNA
Myf5	Myogenic Factor 5
NBS1	Nibrin

NF- κ B	Nuclear Factor Kappa B
NHEJ	Non homologous end joining
NO	Nitric Oxide
NOB1	NIN1 Binding protein
NOS	Nitric Oxide synthase
NR	Nuclear Hormone Receptor
NS3	Non-structural Protein 3
OHT	4-hydroxytamoxifen
OPA	O-phthaldialdehyde
p160	Steroid Receptor Co-activator family
p300	E1A binding protein p300
p53	Tumor Protein 53
PABP	Poly A Binding Protein
PBS	Phosphate buffered saline
pCAF	p300/CBP-associated factor
PPAR γ	Peroxisome Proliferator-activated receptor gamma
PRMT	Protein arginine methyl transferase
pTEFb	Positive transcription elongation factor b
PTM	Post-translational modification
PVDF	Polyvinylidene fluoride
PXR	Pregnane X Receptor
qPCR	Quantitative polymerase chain reaction
RAD50	DNA Repair Protein RAD50
RERM	Rapid equilibrium Random mechanism
REST	Repressor element-1 binding factor

RIPA	Radio immuno precipitation assay
Rme	Methylated arginine or Methyl arginine
RNAPII	RNA Polymerase II
SAH	S-adenosyl-L-homocysteine
SAM	S-adenosyl-L-methionine
SDMA	Symmetrical dimethyl arginine
SF3B4	Splicing factor 3B subunit 4
SILAC	Stable Isotope labeling by amino acids in cell culture
SMAD	Transforming Growth Factor-Beta-Signaling Protein
SNAI1	Protein Snail Homolog
snRNP	Small nuclear ribonucleoprotein
SRC	Steroid Receptor Coactivator
SREBP1	Sterol regulatory element binding protein 1
TAF15	TATA Box Binding Protein-Associated Factor
TARPP	Thymocyte cAMP-regulated phosphoprotein
TDRD3	Tudor domain-containing protein 3
TFF1	Trefoil factor 1
TGFβ	Transforming growth factor β
TPR	Tetra tri co-peptide repeat
TR3	Nuclear receptor subfamily 4 group A member 1
U1C	U1 small nuclear ribonucleoprotein C
WWP2	WW Domain Containing E3 Ubiquitin ligase 2
XLID	X-linked Intellectual disability
YAP	Yes-associated protein

Chapter 1: Introduction

1.1 Protein arginine methylation

Proteins acquire functional diversity from a limited repertoire of polypeptides by undergoing post-translational modifications (PTMs). These modifications regulate the stability, activity, localization, and binding ability of proteins with its interactors (Deribe et al, 2010). Protein arginine methylation is a post-translational modification that modulates important cellular functions like transcription, splicing, signal transduction, and DNA repair (Bedford & Clarke, 2009). It is catalyzed by a family of enzymes called protein arginine methyltransferases (PRMTs), which methylate about 0.5% of total arginine residues in mammalian cells, making it a prevalent modification (Dhar et al, 2013). PRMTs transfer methyl group(s) (CH_3 -) from S-adenosyl-L-methionine (SAM) to the terminal nitrogen(s) of the guanidino group of an arginine residue, giving rise to a methylated protein and the byproduct, S-adenosyl-L-homocysteine (SAH) (Bedford & Clarke, 2009). Methylation of an arginine residue does not affect its positive charge, but it changes its shape, increases bulkiness and hydrophobicity, which in turn affects its protein-protein interactions, both positively and negatively. For example, methylation of histone H3 tail promotes its interaction with the Tudor domain of TDRD3 (Yang et al, 2010), whereas methylation of the Sam68 proline-rich motifs inhibits its interaction with the SH3 domain of p59^{fyn} and PLC γ -1 (Bedford et al, 2000).

1.1.1 Arginine methylation types and the PRMT family

There are three types of methyl-arginine species in cells (Figure 1). ω - N^G , N^G -asymmetric dimethylarginine (ADMA) is the most prevalent type. Here, two methyl groups

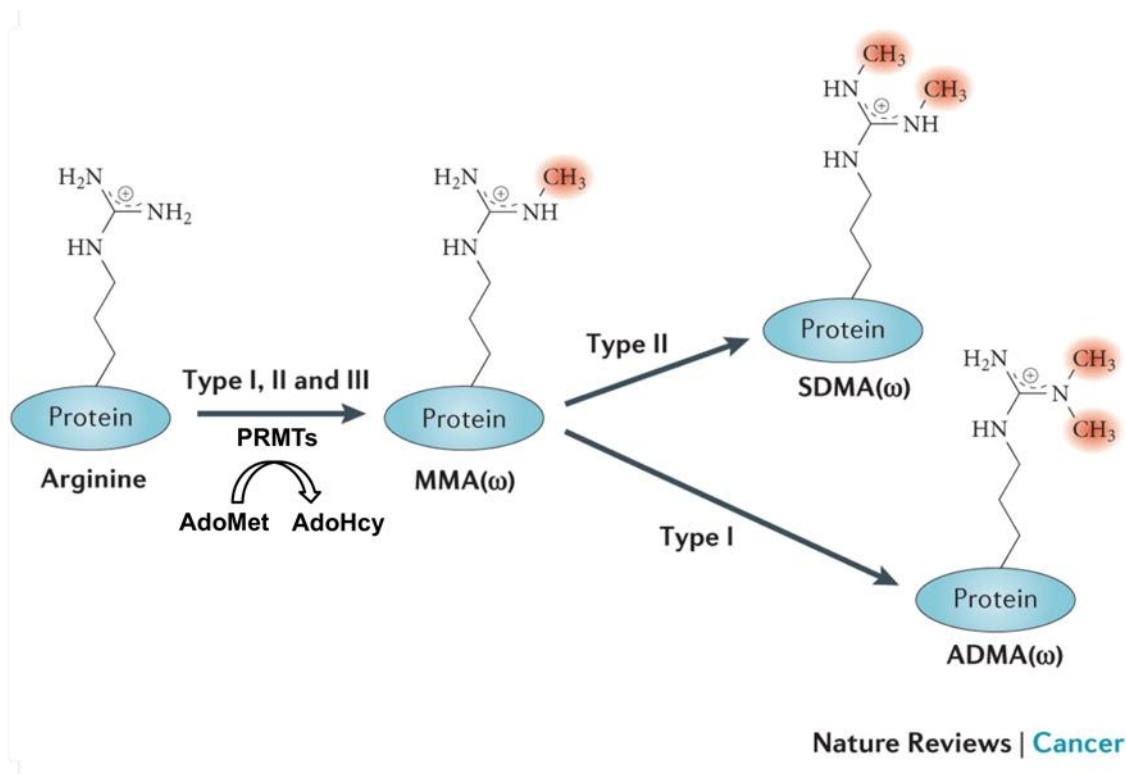


Figure 1: Types of arginine methylation.

The three types of methyl-arginine species occurring in cells are ω -N^G-monomethyl arginine (MMA), ω -N^G,N^G-asymmetric dimethylarginine (ADMA), and ω -N^G,N^G-symmetric dimethylarginine (SDMA).

Figure 1 is adapted from Yang Y, Bedford MT (2013) Protein arginine methyltransferases and cancer. *Nat Rev Cancer* **13**: 37-50.

Permission has been acquired from the journal to use this figure.








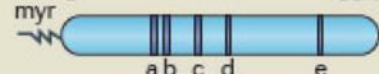
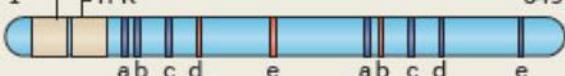
PRMT (locus)	Domain structures of human enzymes*
PRMT1 (19q13.3)	1 316 
PRMT2 (21q22.3)	1 433 
PRMT3 (11p15.1)	1 531 
CARM1 (19p13.2)	1 608 
PRMT5 (14q11.2)	1 637 
PRMT6 (1p13.3)	1 375 
PRMT7 (16q22.1)	1 692 
PRMT8 (12p13.3)	1 394 
PRMT9 (4q31.23)	1 843 

Figure 2: The protein arginine methyltransferase family

The mammalian genome contains nine *PRMT* genes. All enzymes harbor five signature motifs (indicated by dark blue vertical lines, a-e. 'a' stands for Motif I: VLD/EVGXGXG; 'b' stands for Post I: V/IXG/AXD/E; 'c' stands for Motif II: F/I/VDI/L/K; 'd' stands for Motif III: LR/KXXG; 'e' stands for THW loop. The red vertical lines b, d, and e in PRMT9 are motifs with poor sequence similarity with the indicated PRMT motifs. TPR stands for tetratricopeptide repeats. The fourth member of the PRMT family, PRMT4, is otherwise called as co-activator associated arginine methyltransferase (CARM1).

Figure 2 is adapted from Yang Y, Bedford MT (2013) Protein arginine methyltransferases and cancer. Nat Rev Cancer 13: 37-50.

Permission has been acquired from the journal to use this figure.

are added to one of the terminal nitrogen atoms of the guanidinium group. The other two types occur less commonly in cells. They are ω - N^G, N^G -symmetric dimethylarginine (SDMA), where two methyl groups are added to each of the terminal nitrogen atoms of the guanidine group, and ω - N^G -monomethyl arginine (MMA), which has a single methyl group on one of the terminal nitrogen atoms. The mammalian genome encodes a family of nine PRMT enzymes (Figure 2), which can be classified into three types: Type I enzymes (PRMT1, 2, 3, 4, 6 and 8) generate ADMA, Type II enzymes (PRMT5 and 9) generate SDMA and the Type III (PRMT7) enzyme forms MMA residues in mammalian cells. All PRMTs harbor five signature motifs that are responsible for their methyltransferase activity, and a few additional features to facilitate their unique functions. For example, protein domains like SH3, Zn finger, proline-rich motif and TPRs, in PRMT2, 3, 8 and 9 enzymes, respectively, aid in substrate recognition; the myristoyl group at the N-terminus of PRMT8 regulates its subcellular localization.

All PRMTs are ubiquitously expressed, except for PRMT8, which is only expressed in brain (Lee et al, 2005a). However, they also undergo alternative splicing to produce tissue-specific isoforms. Knockout mice were generated for PRMT1-8 and they show dramatic and lethal phenotypes, indicating their essential roles in the organism's development and survival. *Prmt1*- and *Prmt5*-knockout mice die very early during development; *Carm1*-knockout mice die at birth and show differentiation defects among many cell types, whereas *Prmt2*-, *Prmt3*-, *Prmt6*-, *Prmt7*- and *Prmt8*-knockout mice are viable with a few abnormalities (refer to Table 1). Additionally, all knockout mice display hypomethylation of their respective substrates, indicating the non-redundant nature of these PRMTs (Yang & Bedford, 2013).

<i>Prmt</i>	Knockout mouse phenotype	References
<i>Prmt1</i>	Embryonic lethal by E6.5. Required for post-implantation development.	(Pawlak et al, 2000; Yu et al, 2009)
<i>Prmt2</i>	Viable. Null MEFs have increased NF- κ B activity and are more resistant to apoptosis.	(Yoshimoto et al, 2006)
<i>Prmt3</i>	Viable. Embryos are smaller, but attain normal size in adulthood.	(Swiercz et al, 2007)
<i>Carm1</i>	Perinatal lethality. Embryos are smaller and have differentiation defects in T-cells, adipocytes, chondrocytes, muscle and lungs. The enzyme-dead knock-in phenocopies the null.	(Dacwag et al, 2009; Ito et al, 2009; Kawabe et al, 2012; Kim et al, 2004; O'Brien et al, 2010; Yadav et al, 2008; Yadav et al, 2003)
<i>Prmt5</i>	Embryonic lethal by E6.5. Required for embryonic epiblast cell differentiation.	(Tee et al, 2010)
<i>Prmt6</i>	Viable. Primary knockout MEFs undergo rapid senescence.	(Neault et al, 2012)
<i>Prmt7</i>	B cell-specific knockout mice are viable and fertile. Impaired splenic B-cell development and decreased IgG1 and IgA production.	(Ying et al, 2015)
<i>Prmt8</i>	Viable. Abnormal motor behaviors such as hindlimb clasping and hyperactivity. Altered cerebellar structure and stunted growth of Purkinje cell dendrites.	(Kim et al, 2015)

Table 1: List of phenotypes for mice lacking prmt1-8 genes.

Adapted and modified from Yang Y, Bedford MT (2013) Protein arginine methyltransferases and cancer. Nat Rev Cancer 13: 37-50.

Permission has been acquired from the journal to use this figure.

1.1.2 Regulation of PRMTs

The activity of PRMTs can be regulated through various mechanisms. Certain PTMs have been shown to regulate PRMT activity. CARM1 undergoes phosphorylation during mitosis, which prevents dimerization and blocks its enzymatic activity (Feng et al, 2009). PRMT5 undergoes a pathological phosphorylation, as seen in patients with myeloproliferative disease, which disrupts its interaction with MEP50 and abolishes its activity (Liu et al, 2011). PRMT1, CARM1, PRMT6 and PRMT8 are auto-arginine methylated, although the functional significance of this methylation remains unknown (Dillon et al, 2013; Frankel et al, 2002; Gui et al, 2011; Kuhn et al, 2011; Sayegh et al, 2007). N-terminal myristoylation was shown to target PRMT8 to the plasma membrane (Lee et al, 2005a). Secondly, PTMs on histone tails can block or promote methylation of neighboring arginine residues. For example, histone H3K18 acetylation by CBP primes the H3 tail for R17 dimethylation by CARM1 (Daujat et al, 2002). H3K9 acetylation blocks H3R8 dimethylation by PRMT5 (Pal et al, 2004). The presence of H3R8me2a or me2s mark in turn prevents H3K9 methylation by G9a (Rathert et al, 2008). Another mode of regulation is through protein-protein interactions. Interaction between PRMT5 and MEP50 is required for the methyltransferase activity of PRMT5 (Friesen et al, 2002). PRMT3 interaction with the tumor suppressor, DAL-1, inhibits its activity (Singh et al, 2004). MicroRNA-mediated expression control is another mode of regulation for PRMTs. For example, the expression of PRMT5 is inhibited by miR-25, -32, -92, and -92B (Pal et al, 2007; Wang et al, 2008). In addition, PRMTs also regulate the expression of microRNAs (Mallappa et al, 2011). Lastly, PRMT activity can be indirectly modulated by the actions of enzymes that could reverse arginine methylation on proteins. One such enzyme, Jumonji-domain containing 6 (JMJD6), was shown to demethylate H3R2me2 and H4R3me2 marks (Chang et al, 2007; Gao et al, 2015). However, later studies could not reproduce this work, which makes arginine demethylation a controversial topic (Webby et al, 2009). If arginine demethylases do exist,

their discovery would help us better understand and appreciate the dynamic and regulatory nature of arginine methylation.

1.1.3 Arginine methylation in human disease

The deregulation of PRMTs is observed in many diseases. PRMT1 and CARM1 are elevated in breast, prostate, and colon cancers (Cheung et al, 2007; El Messaoudi et al, 2006; Hong et al, 2004; Kim et al, 2010b; Majumder et al, 2006). PRMT1 is also involved in blood cancers, by interacting with AML1-ETO and promoting its transcriptional activation (Shia et al, 2012). CARM1 functions by methylating the oncogenic protein AIB1, which stabilizes and enhances its activity (El Messaoudi et al, 2006; Lahusen et al, 2009). PRMT5 is overexpressed in gastric cancers, lymphomas and leukemias (Kim et al, 2005; Pal et al, 2007; Wang et al, 2008; Wei et al, 2012). PRMT5 co-operates with SNAIL to downregulate the expression of E-cadherin, an adhesion molecule lost during the epithelial-mesenchymal transition (EMT) process in metastatic cancers (Hou et al, 2008). Deregulated arginine methylation is also implicated in cardiovascular diseases. Nitric oxide (NO) is an important signaling molecule in cardiovascular, immune, and nervous systems. Nitric oxide synthase (NOS) catalyzes the generation of NO from L-arginine. The free methylarginine species (produced by the proteolysis of methylated proteins), MMA and ADMA, but not SDMA, were shown to inhibit NOS activity (Stuhlinger et al, 2001). The enzyme dimethylarginine dimethylaminohydrolase (DDAH) converts MMA/ADMA to citrulline and monomethylamine/dimethylamine, and maintains their intracellular pool size. Deregulation of PRMT or DDAH enzymes may cause a reduction in NO levels, resulting in endothelial dysfunction and atherosclerosis. In fact, PRMT1 was shown to be overexpressed in the hearts of coronary heart disease patients (Chen et al, 2006). The significance of arginine methylation in viral pathogenesis is evident from the fact that a large number of viral proteins are PRMT

substrates (E.g. HIV proteins Rev, Tat, nucleocapsid; HSV protein ICP27; HCV protein NS3 and EBNA2) (Boulanger et al, 2005; Kwak et al, 2003). In the HIV cell culture model, methylation of the viral proteins was shown to increase the virus infectivity (Kwak et al, 2003). Arginine methylation may function by increasing the interactions between viral and host proteins, and possibly disrupting host cellular functions.

Section 1.2 serves as the background for Chapter 3

1.2 PRMT1

PRMT1 is the major Type I enzyme, accounting for about 90% of global arginine methylation in mammalian cells (Tang et al, 2000a). It is involved in a multitude of biological processes like RNA processing, protein trafficking, signaling, transcriptional activation and DNA repair (Bedford & Clarke, 2009). These versatile functions of PRMT1 are achieved through its ability to methylate multiple classes of cellular proteins (Nicholson et al, 2009). The major class of proteins methylated by PRMT1 is RNA-binding proteins, which include hnRNPs, fibrillarin, nucleolin, PABPII, Sam68, SLM-1, SLM-2, QKI-5, GRP33, and TAF15 (Bedford & Richard, 2005). Methylation of these proteins seems to be required for their proper localization and RNA processing ability (Cote et al, 2003). Many signaling pathways are also influenced by PRMT1-mediated methylation. Insulin treatment of myotubes was shown to translocate PRMT1 to the plasma membrane, where it methylates several membrane-associated proteins (Iwasaki & Yada, 2007). PRMT1 synergizes with CARM1 and GRIP1 to enhance Nuclear hormone receptor (NR) -mediated transcription. It methylates the histone H4 (at Arg3), which further enables H4 acetylation by p300 to enhance transcriptional activation by NRs (Wang et al, 2001). ER α is also methylated by PRMT1, which is required for its interaction with PI3K, Src, and FAK (Le Romancer et al, 2008). PPAR γ coactivator (PGC-1 α) methylation by PRMT1 induces its target genes (Teyssier et al, 2005). The

transcription factors, YY1, p53 and NF- κ B, associate with and recruit PRMT1 to their target promoters to methylate the histone H4 tail (at Arg3), suggesting that H4R3me2a is not a random event and it functions in activating specific gene programs (An et al, 2004; Hassa et al, 2008; Rezai-Zadeh et al, 2003). PRMT1 also methylates SPT5, which then decreases its interaction with RNA polymerase II to regulate transcription elongation, in response to viral and cellular factors (Kwak et al, 2003). The activity of PRMT1 is tightly regulated, which happens mainly through association with various proteins. The binding of PRMT1 with BTG1, BTG2, IFNAR1, ILF3 and hCAF1 promotes its methyltransferase activity (Abramovich et al, 1997; Lin et al, 1996; Miyata et al, 2008; Robin-Lespinasse et al, 2007; Tang et al, 2000b), whereas binding with the orphan nuclear receptor TR3 inhibits its activity (Lei et al, 2009). Interaction with the pregnane X receptor (PXR) results in nuclear accumulation of PRMT1 (Xie et al, 2009).

To study the *in vivo* functions of PRMT1, a *Prmt1* null allele was generated in mice, which resulted in embryonic lethality (at E6.5) (Pawlak et al, 2000; Yu et al, 2009). MEFs deficient in PRMT1 showed a delay in cell cycle progression, spontaneous DNA damage, checkpoint defects, aneuploidy, and polyploidy (Yu et al, 2009). The knockout cells also displayed hypomethylation of PRMT1 substrates including Sam68 and MRE11 (Yu et al, 2009). Hypomethylation of MRE11 impairs its exonuclease activity, but does not affect complex formation with RAD50 and NBS1 (Boisvert et al, 2005a). Additionally, the recruitment of HR protein, Rad51, to DNA damage foci is also reduced upon PRMT1 loss (Yu et al, 2009). Another DNA damage response protein, 53BP1, which promotes NHEJ-mediated repair, is also methylated by PRMT1 at the GAR motif and this methylation regulates its oligomerization and interaction with DNA (Boisvert et al, 2005b). These findings underscore the importance of PRMT1 in genome maintenance and DNA damage response pathway.

The crystal structure of the rat PRMT1 enzyme has been solved and it revealed that the dimerization of this enzyme is required for AdoMet binding and enzymatic activity (Zhang

& Cheng, 2003). It also showed that the enzyme has three peptide binding channels, which may explain how PRMT1 can methylate arginine residues within various sequence contexts (E.g. RG, RGG, RXR, and other non-GAR motifs) and possess such a wide spectrum of substrates. Indeed, surface-scanning mutational analysis identified differential enzymatic activity towards different substrates (E.g. H4 versus GAR) (Lee et al, 2007).

Most of the Type I and Type II PRMTs are known to catalyze substrates in a distributive manner i.e. they transfer the first methyl group to the substrate and release it before rebinding to the monomethylated substrate to facilitate the addition of the second methyl group (Antonyasamy et al, 2012; Kolbel et al, 2009; Lakowski & Frankel, 2008; Wang et al, 2014b). On the contrary, a processive enzyme maintains the interaction with its substrate until both mono- and dimethylation events occur. However, PRMT1 catalyzes by neither of these mechanisms. If it works in a fully processive manner, ADMA generation is obligatory i.e. the concentration of the monomethyl intermediate should not rise above the concentration of the enzyme. However, the reaction contained equimolar amounts of MMA and ADMA products even in the presence of excess unmodified substrate (Osborne et al, 2007). If it functions in a distributive fashion, the monomethyl intermediate should have a much higher affinity for PRMT1 than an unmodified substrate. Nevertheless, this is not the case (Osborne et al, 2007). By performing initial velocity, product inhibition and dead-end inhibition studies, Thompson and Zheng groups confirmed that PRMT1 functions in a partially processive fashion by utilizing a rapid equilibrium random (RER) mechanism (explained in Figure 3) (Feng et al, 2011; Obianyo et al, 2008).

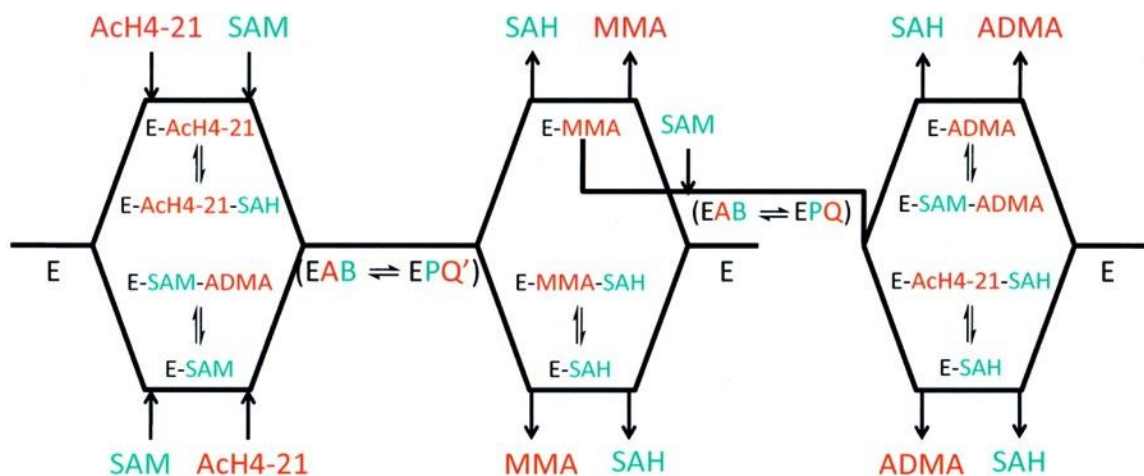


Figure 3: Kinetic mechanism for PRMT1 catalysis.

RER is a type of kinetic mechanism for bisubstrate enzyme reactions where substrates (denoted by A and B) and products (denoted by P and Q) bind to and dissociate from enzyme (E) very rapidly. In the first step, PRMT1 (E) binds to AcH4-21 peptide (A) and SAM (B) to catalyze the first methyl transfer ($EAB \rightarrow EPQ'$, $P = SAH$ and $Q' = MMA$). In the next step, either SAH dissociates prior to MMA release, which allows binding of second SAM to the original E-MMA complex and formation of ADMA product ($EAB \rightarrow EPQ$ sequentially, $Q = ADMA$), or, MMA dissociates prior to SAH release, which then rebinds with a new EB complex to undergo the second methylation event ($EAB \rightarrow EPQ'$, $EBQ' \rightarrow EPQ$). This explains the presence of monomethyl intermediates in the PRMT1 methylation reactions.

Figure 3 is adapted from Obianyo O, Osborne TC, Thompson PR (2008) Kinetic mechanism of protein arginine methyltransferase 1. Biochemistry 47: 10420-10427

Permission has been acquired from the journal to use this figure.

Sections 1.3 and 1.4 serve as the background for Chapter 4

1.3 CARM1

CARM1, also known as PRMT4, was first identified in a yeast two-hybrid screen for GRIP1-binding proteins (Chen et al, 1999). GRIP1/SRC-2 belongs to the p160 family of co-activators (SRC-1, SRC-2, and SRC-3), which facilitate nuclear hormone receptor-mediated transcription. Upon hormone stimulation, nuclear hormone receptors (NRs) homodimerize, bind to their cognate hormone response elements (HREs) and recruit p160 co-activators, which further bring in p300/CBP and pCAF to acetylate histones. Acetylated histones then recruit SWI/SNF chromatin remodeler complex to increase the accessibility of local chromatin. NRs also recruit Mediator complex, which communicates with the basal transcription machinery to facilitate transcription initiation (Stallcup et al, 2003). By using Luciferase reporter assays, Stallcup group showed that the co-expression of CARM1 along with GRIP1 significantly enhanced HRE-driven reporter gene expression (Figure 4A). They also showed that mutating CARM1 to disrupt its methyltransferase activity substantially reduced reporter gene expression (Figure 4A), indicating that CARM1 may function as a secondary co-activator by methylating its substrates (Chen et al, 1999). Further studies demonstrated that CARM1 methylates p160 coactivators (Feng et al, 2006), the histone acetyltransferases (p300/CBP) (Daujat et al, 2002; Xu et al, 2001), and the histone H3 (H3R17me2a) (Chen et al, 1999), and these methylation events influenced NR-mediated transcription positively (Figure 4B). On the other hand, CARM1 methylation of CBP/p300 disables its interaction with CREB, thereby preventing CREB-dependent gene activation (Xu et al, 2001). In this context, CARM1 indirectly acts as a transcriptional co-repressor. Aside from this, CARM1 was shown to coactivate NF- κ B, p53, β -catenin and Sox2 transcription factors (An et al, 2004; Covic et al, 2005; Ou et al, 2011; Zhao et al, 2011). Furthermore, ChIP studies using H3R17me2a (a CARM1 deposited mark) antibody showed elevated

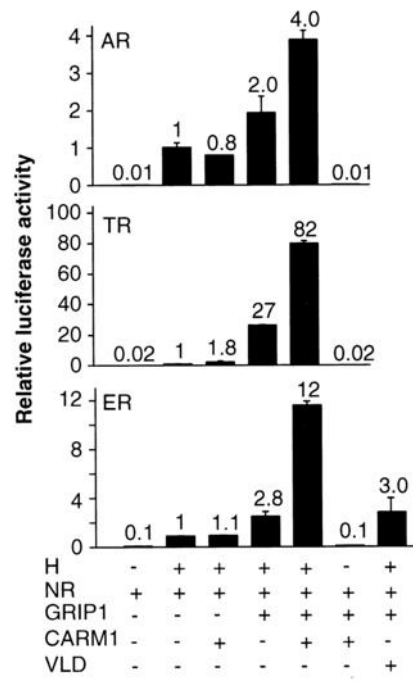
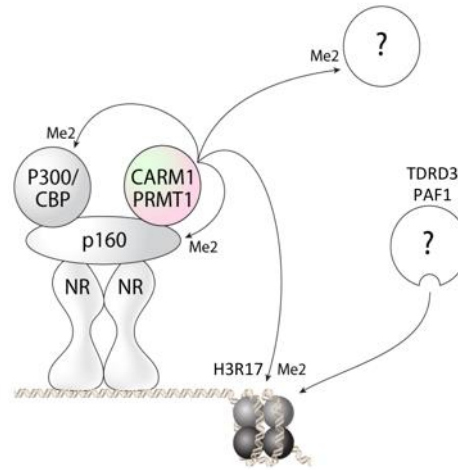
A**B**

Figure 4: CARM1 coactivates NR-dependent gene expression

(A) CV-1 cells were transiently transfected with nuclear hormone receptor (NR) (i.e. androgen receptor (AR), thyroid hormone receptor β 1 (TR) or, estrogen receptor (ER)), GRIP1, CARM1, VLD, and luciferase reporter gene expressing vectors and grown in charcoal-stripped serum before activating with dihydrotestosterone for AR, triiodothyronine for TR, and estradiol for ER. Luciferase activities were enhanced 2- to 27-fold by coexpression of GRIP1 with NR, and further enhanced 2- to 4-fold by coexpression of CARM1 with GRIP1 and NR.

(B) Ligand-activated nuclear receptors, through a p160 scaffold, recruit CARM1, which partially stimulates transcription by remodeling chromatin (H3R17me2a) in the vicinity of the gene as well as by modifying non-chromatin substrates (SRC-1, SRC-2, SRC-3 and p300/CBP). This methylation is interpreted by effector molecules (E.g. TDRD3 'reads' H3R17me2a) that help promote the coactivator function of CARM1.

Figure 4A is adapted from Chen D, Ma H, Hong H, Koh SS, Huang SM, Schurter BT, Aswad DW, Stallcup MR (1999) Regulation of transcription by a protein methyltransferase. Science 284: 2174-2177

Permission has been acquired from the journal to use this figure.

levels at a number of gene promoters including pS2, E2F1, CCNE1, aP2, Oct 4, Sox2, CITED2, and Scn3b (Bauer et al, 2002; Carascossa et al, 2010; El Messaoudi et al, 2006; Fietze et al, 2008; Kleinschmidt et al, 2008; O'Brien et al, 2010; Wu et al, 2009; Yadav et al, 2008). Therefore, CARM1 functions as a general transcriptional coactivator.

Gene ablation studies in mice revealed that CARM1 is vital for existence (Yadav et al, 2003). Although the knockout embryos are outwardly developmentally normal (except for their smaller size), they display a number of cellular differentiation defects such as a partial block in T-cell development (Kim et al, 2004) and improper differentiation of lung alveolar cells (O'Brien et al, 2010) and adipocytes (Yadav et al, 2008). Enzyme-dead CARM1 knock-in mice phenocopy the null mice, indicating that CARM1's enzymatic activity is required for most of its *in vivo* functions (Kim et al, 2010a). Thus a detailed knowledge of the spectrum of proteins that are methylated by CARM1 is critical for an in-depth understanding of how this enzyme functions in these different settings.

1.3.1 Identification of CARM1 substrates

Multiple strategies have been used to identify CARM1 substrates including *in vitro* substrate screens, candidate approaches, modification-specific antibodies and MS-based proteomic approaches. The classification of CARM1 substrates based on the functions as well as screening strategies is shown in Figure 5. The first *in vitro* screen utilized high-density protein macroarrays to identify CARM1 substrates. To prepare high-density protein macroarrays, a human fetal brain cDNA library was cloned into a His-tagged bacterial expression vector and transformed into E. Coli. The transformants were gridded onto PVDF filters in a duplicate pattern, grown on agar plates overnight, and induced with IPTG for protein expression. The filters containing cells were then treated with sodium hydroxide and sodium chloride solutions, which break open the bacteria and release the protein onto the filter. The filters (containing 10,000 his-tagged proteins in duplicates) were then incubated

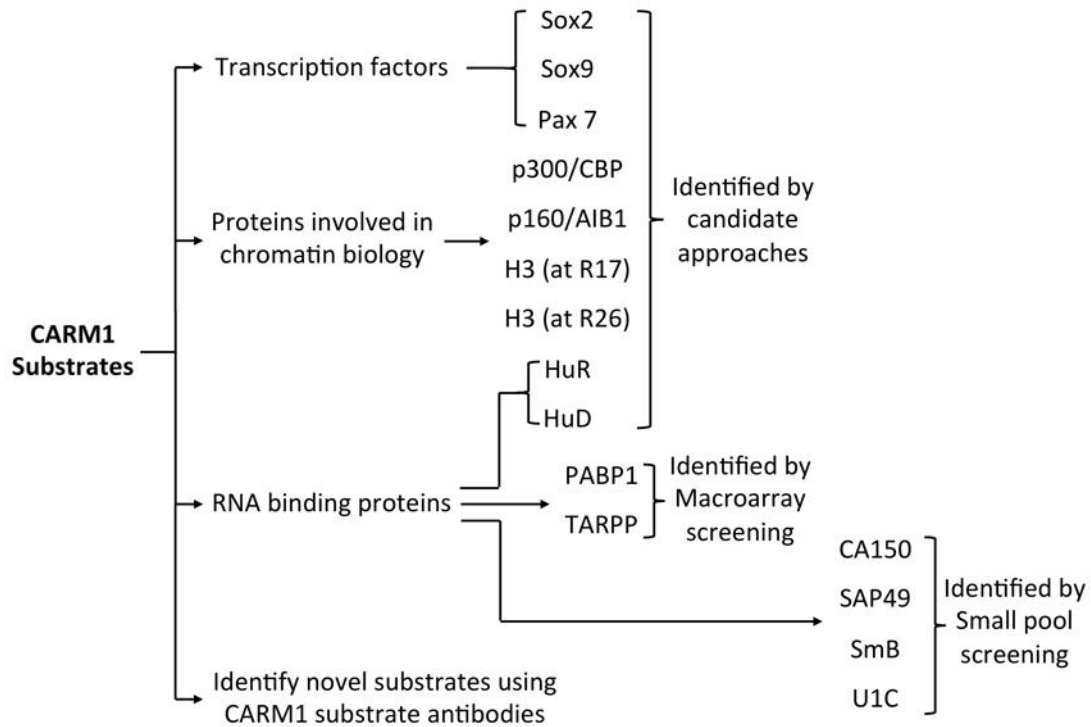


Figure 5: Classification of CARM1 substrates.

Proteins methylated by CARM1 can be functionally divided into three classes. Transcription factors (class I) and chromatin regulators (class II) were identified by candidate approaches, whereas most of the RNA binding substrates (class III) were revealed by macroarray and small pool screening strategies. In this current study, we aimed at identifying novel substrates for CARM1 using substrate motif antibodies.

with recombinant CARM1 and radioactively labeled S-adenosyl-L-methionine ([³H]AdoMet), washed and exposed to film overnight. This large-scale *in situ* methylation screen identified thymocyte cAMP-regulated phosphoprotein (TARPP), polyA binding protein (PABP1), and CARM1 substrate 3 (CAS3) as CARM1 substrates (Lee & Bedford, 2002). CARM1 knockout mice undergo a partial developmental block in the early thymocyte progenitors (DN1 to DN2 transition) (Kim et al, 2004; Li et al, 2013). It is speculated that the arginine methylation of TARPP, whose expression is initiated at the DN2 stage, may contribute to the maturation of thymocyte progenitors. PABP1 binds the mRNA 3' polyA tail and the translation initiation factor to form a closed loop structure that promotes mRNA translation and regulates stability. CAS3 is an uncharacterized protein and is the product of the BC043098 cDNA clone. The functions of methylation on PABP1 and CAS3 are yet to be identified.

The second approach was a small pool expression screening, modified to identify CARM1 substrates. Here, a plasmid cDNA library from a mouse B-cell hybridoma (containing 14,000 clones) was generated and divided into pools, each containing ten clones. In vitro transcription/translation (IVTT) reactions were performed on these plasmid pools using reticulocyte lysate. Besides the transcription/translation machinery, the lysate also contains arginine methyltransferases. Hence, addition of radioactively labeled methyl donor, S-adenosyl-L-methionine ([³H]AdoMet) to the IVTT reactions, would label the methyl-accepting protein products. As expected, the IVTT screen generated labeled proteins, which were visualized by fluorography. To identify the methylated proteins, the plasmid pools were deconvoluted and single plasmids were sequenced. This approach identified eleven methylated proteins, which were further characterized by *in vitro* methylation reactions using recombinant PRMTs to determine the specific enzymes responsible for methylating each substrate. Of the eleven identified substrates, four were CARM1 substrates – snRNP core protein (SmB), splicing factor 3B subunit 4 (SF3B4/SAP49), U1 snRNP protein (U1C), and transcription elongation regulator 1 (TCERG1/CA150). The ability of CARM1 to methylate

several splicing factors and RNA binding proteins underscores its importance in RNA processing and splicing. In fact, CARM1-mediated methylation of CA150 was shown to regulate alternative splicing by promoting exon skipping (Cheng et al, 2007).

Most PRMTs (PRMT1, 3, 5, 6 and 8) recognize and methylate a GAR (Glycine and Arginine-rich) motif (Yang & Bedford, 2013), which has facilitated the development of methylarginine-specific antibodies that can be used to identify and help characterize substrates for this class of PRMTs. The first methyl-GAR motif antibodies (ADMA and SDMA) were developed by Stephane Richard's group, and used in immunoprecipitation-coupled mass spectrometry (IP-MS) experiments to identify novel methylated proteins (Boisvert et al, 2003). This approach has recently been expanded upon with the development of additional antibodies that recognize MMA and ADMA motifs using redundant peptide libraries with fixed methylarginine residues as antigens (Guo et al, 2014). A screen for CARM1 substrates using one of these ADMA-specific antibodies identified the chromatin-remodeling factor, BAF155, as methylated by CARM1. Arginine methylation of BAF155 targets it to genes of the c-myc pathway, and enhances breast cancer progression and metastasis (Wang et al, 2014a).

An alternative (antibody independent) approach to identifying methylated proteins is based on a modification of the "stable isotope labeling by amino acids in cell culture" (SILAC) technique, called heavy methyl SILAC (Ong et al, 2004a). Heavy methyl SILAC exploits the fact that methionine is taken up by the cell and converted to the sole biological methyl donor, AdoMet. Thus, if [$^{13}\text{CD}_3$]methionine is used in these experiments, heavy methyl groups are incorporated into *in vivo* methylated proteins. Using this approach, in combination with methylarginine enrichment techniques, a large number of PRMT substrates have recently been identified (Geoghegan et al, 2015; Uhlmann et al, 2012), which comprised the novel CARM1 substrates found in the current study such as MED12, MLL2 and GPS2.

Other known CARM1 substrates were identified by candidate approaches. HuR and HuD are RNA-binding proteins that bind AU-rich elements (AREs) of labile mRNAs to stabilize

them. CARM1 methylates HuD to inhibit its ability to stabilize p21 mRNA, thereby maintaining the PC12 cells in a proliferative state and preventing neuronal differentiation (Fujiwara et al, 2006). CARM1 methylates HuR and enhances its ability to regulate the turnover of cyclin A, cyclin B1, c-fos, SIRT1 and p16 mRNAs, thereby regulating replicative senescence (Li et al, 2002; Pang et al, 2013). CARM1 was also shown to regulate muscle differentiation. During muscle regeneration, satellite stem cells differentiate into Myf5⁺ satellite myogenic cells and fuse into myofibers. The expression of Myf5 requires the activation of the transcription factor, Pax7. CARM1 interacts with and methylates Pax7, which then binds MLL1/MLL2 proteins of the MLL/ASH2L HMT complex and recruits it to the Myf5 promoter to induce its expression (Kawabe et al, 2012). CARM1 also methylates the C-terminal domain of RNA polymerase II. Mutation disrupting this methyl site causes misexpression of snRNAs and snoRNAs, suggesting that CARM1 methylation of CTD facilitates the transcription of select RNAs (Sims et al, 2011).

CARM1 has unique substrate specificity, and it does not methylate GAR motifs (Cheng et al, 2007; Lee & Bedford, 2002). Thus, to facilitate the rapid identification of new CARM1 substrates, we developed CARM1-motif antibody screening strategies to enrich for CARM1-methylated proteins. The H3R17me2a antibody (Millipore) was raised against the asymmetric dimethylarginine 17 mark on histone H3. Immunoblotting protein extracts with this antibody, however, detected many differentially recognized proteins between wild-type and CARM1 knockout embryos (Cheng et al, 2012; Yadav et al, 2003). These proteins were further confirmed to be CARM1 substrates (Cheng et al, 2007). Hence, we speculated that CARM1-methylated motifs, have a rather loose consensus sequence, and can be used to raise pan antibodies that would potentially recognize unknown CARM1 substrates. Using a cocktail of CARM1 methylated motifs as an antigen, we demonstrated that pan CARM1-

motif antibodies can be developed. Furthermore, we identified MED12, MLL2, GPS2 and SLM2 as novel CARM1 substrates, as well as a number of previously characterized CARM1 substrates.

1.4 Mediator Complex

Eukaryotic gene expression is largely dependent on transcription factors (TFs), which bind to the proximal promoter or the distal enhancer regions of the genes through their DNA binding domains. Through their activation domains, TFs bind the Mediator complex, which relays regulatory signals directly to RNA polymerase II (RNAPII) (Figure 6A). Mediator is a large, multi-subunit complex that is conserved from yeast to humans. In addition to gene activation, Mediator also regulates chromatin architecture, transcription elongation and repression. Genetic, biochemical and structural studies have identified that the mammalian Mediator complex comprises 30 individual subunits that are arranged in four modules – head, middle, tail and kinase (Figure 6B). Head, middle and tail modules form the stable core structure, henceforth referred as “core Mediator”. The head and middle modules mainly associate with the RNAPII machinery, whereas the tail module binds with activator proteins and regulates various transcriptional programmes (Malik & Roeder, 2010). For example, MED1 associates with the ligand-inducible nuclear receptors (NRs) such as Thyroid, Estrogen, Glucocorticoid and PPAR γ receptors (Ge et al, 2008; Ge et al, 2002; Hittelman et al, 1999; Kang et al, 2002; Malik et al, 2002; Rachez et al, 1999). Studies on *Med1*^{-/-} cells highlighted the importance of MED1 in PPAR γ -mediated adipogenesis, GR-mediated steatosis, TR α -mediated thermogenesis etc. Similarly, MED23 was shown to interact with MAPK-regulated factor, ELK1 (Wang et al, 2005). Therefore, *Med23*^{-/-} MEFs cannot induce ELK1 target genes (such as *Egr2*) and consequently fail to undergo insulin-triggered adipogenesis (Wang et al, 2005). Another tail module subunit, MED15, interacts with SREBP1

and modulates lipid metabolism (Yang et al, 2006). The kinase module associates in a reversible manner with the core Mediator to form “CDK-Mediator”. Structural and biochemical studies suggest that the kinase module binds core Mediator at the same surface, as does RNAPII, thereby preventing the formation of Mediator-RNAPII holoenzyme (Tsai et al, 2013). Therefore, the kinase module has been attributed a repressive role in transcription, however, studies on individual kinase subunits, which include MED13, MED12, CDK8 and Cyclin C, proved that they function both in transcription activation and repression (Taatzjes, 2010). The dissociation of the kinase module is regulated by the FBW7-mediated proteosomal turnover of MED13, the subunit that physically links the kinase to the core Mediator (Davis et al, 2013). Apart from this scaffolding function, MED13 is also involved in developmental gene regulation. It was shown to repress Wnt- and Notch-target genes in many metazoan model systems including *C. elegans*, *D. melanogaster* and *D. rerio* (Carrera et al, 2008; Janody & Treisman, 2011). CDK8 functions through multiple mechanisms to regulate transcription, both positively and negatively. CDK8 phosphorylates TFIIH, which in turn inhibits its kinase activity towards CTD of RNAPII and represses transcription (Akoulitchiev et al, 2000). CDK8 phosphorylates histone H3 (at Ser 10), which inhibits methylation at H3K9, thereby preventing recruitment of HP1 to chromatin for epigenetic silencing (Fischle et al, 2005). CDK8 promotes transcription by enhancing co-activator recruitment. SMAD proteins activated by ligand-induced TGF β and BMP receptors are recruited to the target gene enhancers and are phosphorylated by CDK8, which then recruit YAP protein to facilitate efficient transcription. After transcription, the same phospho mark on SMAD proteins is recognized by the ubiquitin ligases to facilitate their degradation (Alarcon et al, 2009). CDK8 positively regulates serum-responsive and hypoxia-related genes by stimulating RNAPII elongation through recruitment of pTEFb (Donner et al, 2010; Galbraith et al, 2013). Additionally, target genes for p53, Thyroid receptor and phospho-C/EBP β are positively regulated by CDK8 (Belakavadi & Fondell, 2010; Donner et al, 2007; Mo et al, 2004). CDK8 also represses genes by phosphorylating and inactivating TFs (E.g.

E2F1, SREBP1) (Morris et al, 2008; Zhao et al, 2012). It also phosphorylates other TFs (E.g. Notch ICD, Gcn4, and Msn2) subjecting them to ubiquitin-mediated proteosomal degradation (Fryer et al, 2004; Rawal et al, 2014).

1.4.1 MED12

The kinase module gene, *MED12*, is located on X-chromosome (at Xq13) and encodes a 2212 aa (240kDa sized) protein. This protein can be divided into four distinct domains: leucine-rich (L) domain, leucine-serine-rich (LS) domain, proline-glutamine-leucine-rich (PQL) domain and a poly-glutamine (Opa) domain (Figure 7). MED12 is highly conserved among eukaryotes, particularly in mammals, with 96% identity between mouse and human amino acid sequences (Philibert & Madan, 2007). *Med12* gene is essential for early mouse development. The null embryos are arrested at the head-fold stage (E7.5), since they cannot induce mesoderm formation (Rocha et al, 2010). The hypomorphic mutants expressing less than 10% MED12 protein die at E10.5 and have defects in neural tube closure, axis elongation, somitogenesis and heart formation. Both canonical Wnt/ β -catenin and non-canonical Wnt/PCP pathways are disrupted in these hypomorphic mutants. This is expected as MED12 physically interacts with β -catenin to activate the transcription of Wnt-responsive genes (Kim et al, 2006). MED12 was also reported to interact with Nanog and coregulates its target genes. RNAi-mediated *Med12* knockdown was shown to reduce the expression of Nanog and its target genes in embryonic stem (ES) cells, which then start the differentiation process (Tutter et al, 2009). In contrast to this, *Med12*^{+/+}, *Med12*^{-/-} and *Med12*^{hypo} ES cells showed unaltered expression of Nanog and its target genes, suggesting that MED12 is not required for ES cell pluripotency (Rocha et al, 2010). Nevertheless, MED12 is involved in the transcriptional regulation of many signaling pathways. Indeed, the *C. elegans* ortholog of

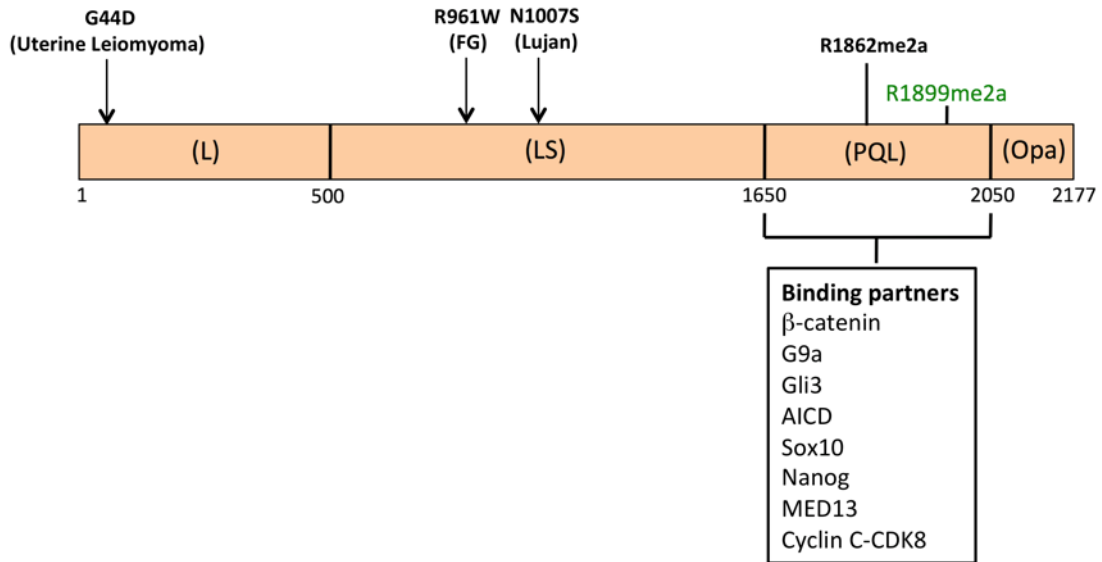


Figure 7: Domain structure of MED12.

L → Leucine-rich domain, LS → Leucine- and Serine-rich domain, PQL → Proline-, Glutamine- and Leucine-rich domain, Opa → Opposite paired domain. FG- (R961W) and Lujan-related (N1007S) mutations are found in LS domain, the most common uterine leiomyoma-linked (G44D) mutation is found in the L domain. The methylation site (R1862) associated with cancer drug sensitivity is present in the PQL domain. The methylation site (R1899) identified in the current study is also present in the PQL domain. All known interactors bind MED12 at its PQL domain.

MED12, *dpy-22*, was identified to be one of the six highly connected 'hub' genes (all of which encode chromatin regulators) that interact with numerous components of diverse signaling pathways and serve as modifier genes in multiple mechanistically unrelated genetic diseases (Lehner et al, 2006). Sox10 is a transcription factor required for terminal differentiation of myelinating glia. MED12 interacts with Sox10 and induces genes necessary to drive the myelination of neurons. Glia-specific deletion of *Med12* in mice showed defects in terminal differentiation and myelin gene expression of both Schwann cells and Oligodendrocytes (Vogl et al, 2013). Amyloid precursor protein (APP), a transmembrane protein associated with Alzheimer's disease, is cleaved by γ -secretase to produce amyloid- β (A β) peptide and APP intracellular domain (AICD). Although the events of amyloid- β plaque formation and consequent neuronal death have been well studied, little is known about the mechanism by which AICD activates its target genes, which are associated with disease pathology. AICD was shown to recruit Mediator complex via interaction with MED12 to activate its target genes. Disruption of this interaction abrogates the transactivation potential of AICD, suggesting that MED12 plays a crucial role in the pathophysiology of Alzheimer's disease (Xu et al, 2011). In addition to this, MED12 is implicated in a number of neurological disorders. Exonic polymorphisms have been associated with neuropsychiatric diseases including schizophrenia and psychosis (Philibert, 2006; Sandhu et al, 2003). Recurrent missense mutations in *MED12* have been shown to cause X-linked intellectual disability (XLID) syndromes such as Optiz-Kaveggia (or FG) syndrome and Lujan-Fryns (or Lujan) syndrome (Graham & Schwartz, 2013; Risheg et al, 2007; Schwartz et al, 2007). In addition to mental retardation, these two syndromes share many overlapping characteristics like macrocephaly, dysgenesis of corpus callosum, hypotonia, craniofacial dysmorphisms, seizures and behavioural problems. To understand the molecular mechanisms by which R961W (FG) and N1007S (Lujan) mutations could contribute to XLID phenotypes, Boyer group identified MED12 binding partners and studied the biological significance of these interactions. Sonic hedgehog (Shh) acts like a

morphogen that controls the left-right, dorso-ventral axes patterning, limb patterning and development of brain, spinal cord and most other organs. The Boyer group showed that Shh-activated Gli3 recruits Mediator complex via interaction with MED12, wherein enzymatically active CDK8 suppresses Gli3 transactivation activity. R961W and N1007S mutations in *MED12* prevent recruitment of CDK-Mediator to the target gene promoters, thereby hyperactivating Gli3-dependent Shh signaling that may possibly contribute to XLID phenotypes (Zhou et al, 2006; Zhou et al, 2012). Repressor element-1 binding factor (REST) is a transcription factor that represses the expression of neuron-specific genes in terminally differentiated non-neural tissues or undifferentiated neural precursors. RE1-bound REST recruits Mediator complex via interactions with MED19 and MED26, wherein MED12 acts as a direct interface for G9a recruitment and H3K9 dimethylation, leading to epigenetic silencing of REST-target genes. FG- and Lujan-related *MED12* mutations disrupt the epigenetic restrictions imposed by REST, possibly contributing to XLID phenotypes (Ding et al, 2009; Ding et al, 2008). Studies by Sheikattar group showed that Mediator interacts with ncRNA-activating (ncRNA-a), a novel class of lncRNAs that activate their neighboring genes using a cis-mediated mechanism. NcRNA-a3 and -a7 interact with MED12 to recruit Mediator and deposit CDK8-mediated H3S10 phosphorylation at the promoters of a3 and a7 target genes (SNAI1, AURKA, and TAL1) for transcriptional activation. They also showed that FG-related *MED12* mutations significantly diminish interactions with ncRNA-a, which may possibly contribute to XLID (Lai et al, 2013). In addition to neurological disorders, *MED12* is also frequently mutated in human cancers like uterine leiomyomas, breast and prostate cancers (Schiano et al, 2014). Uterine leiomyoma-linked mutations in *MED12* were shown to disrupt its interaction with Cyclin C-CDK8 resulting in loss of Mediator-associated kinase activity (Turunen et al, 2014). Furthermore, MED12 is linked to drug resistance in different cancer types. Cytoplasmic MED12, independent of the Mediator complex, was shown to interact with the immature form of TGF β R2 and prevent it from undergoing glycosylation and plasma

membrane association. Therefore, loss of MED12 activates TGF β signaling that further causes MEK/ERK activation, which is sufficient to confer multidrug resistance in colon and lung cancers (Huang et al, 2012). Using genome-scale CRISPR-Cas9 knockout (GeCKO) library screening, another group identified *MED12* as the top hit among genes whose loss results in drug resistance in melanoma cells (Shalem et al, 2014).

Chapter 2: Materials and Methods

Contents of this chapter are partially based on Dhar S*, Vemulapalli V*, Patananan AN, Huang GL, Di Lorenzo A, Richard S, Comb MJ, Guo A, Clarke SG, Bedford MT (2013) Loss of the major Type I arginine methyltransferase PRMT1 causes substrate scavenging by other PRMTs. *Sci Rep* **3**: 1311. (* indicates equal contribution authors)

According to Nature Scientific Reports, the author retains the ownership of copyright to reproduce the contribution or extracts from the original article.

2.1 Antibodies

The details of all the antibodies used in this study are described in tables 2 and 3.

2.2 Plasmids and peptides

The generation of GFP-PRMT1, GFP-PRMT2, GFP-PRMT3, GFP-CARM1, GFP-PRMT5, GFP-PRMT6 (Frankel et al., 2002) and GFP-PRMT8 (Lee et al., 2005) constructs has been described previously. GFP-PRMT7 and GFP-PRMT9 constructs were generated by cloning the human PRMT7 or PRMT9 cDNA into pEGFP-C1 (Clontech) vector. GST-PABP1 (Lee and Bedford, 2002), GST-CARM1 (Frankel et al., 2002), FLAG-CA150 (Cheng and Bedford, 2006), GST-Tudor (TDRD3) (Yang and Bedford, 2010), and GST-Tudor (SMN) (Kim et al., 2006) have been described previously. The other GST-Tudor constructs used in the pull-down experiments were generated by cloning the Tudor domains of SPF30, SPIN1, SND1,, and TDRKH, separately, into a pGEX-6p-1 vector (Biomatik). Recombinant H3 protein used in the *in vitro* methylation assay was purchased from New England Biolabs. The p3XFLAG-MED12 plasmid was a gift from Thomas Boyer (University of Texas Health Science Center at San Antonio). The MLL2^a fragment (3619-4285 aa) was amplified from human cDNA

using gene-specific primers and subcloned into a p3XFLAG-CMV-7.1 vector. FLAG-GPS2 was a gift from Darryl Zeldin (NIEHS). SLM2 plasmid was a gift from Stéphane Richard (McGill University). FLAG-PABP1 and FLAG-SF3B4 were generated by cloning the cDNAs from GST-PABP1, and His-SF3B4 (Cheng et al, 2007; Lee & Bedford, 2002). SRC-1, SRC-2, and SRC-3 constructs were kindly provided by Bert O'Malley (Baylor College of Medicine). FLAG-MED12-R1899K and FLAG-MLL2^a-R3727K mutants were generated using a QuikChange II XL Site-Directed Mutagenesis Kit, Agilent Technologies. Biotinylated peptides encompassing residues 1891-1907 of the MED12 protein with unmodified- or asymmetrically dimethylated- Arg1899 were purchased from CPC Scientific.

2.3 Cell lines

The generation of *Carm1*^{+/+} and *Carm1*^{-/-} MEF lines has been described previously (Yadav et al., 2003). The tamoxifen-inducible *Prmt1*^{fl/-} ER-Cre MEF line was a gift from Stéphane Richard (McGill University). These MEFs were treated with 2μM 4-hydroxytamoxifen, which stabilizes ER*-Cre (A fusion protein between the estrogen receptor ligand-binding domain and the Cre recombinase) and translocates it to the nucleus, which then excises the floxed *Prmt1* allele to generate PRMT1 knockout MEFs. The generation of *Prmt3*^{+/+} and *Prmt3*^{-/-} MEF lines has been described previously (Swiercz et al., 2005). *Prmt6*^{+/+} and *Prmt6*^{-/-} MEF lines were created by immortalizing MEFs from PRMT6 WT and KO mice, according to standard 3T3 protocol. PRMT6 KO mouse was a gift from Stéphane Richard (McGill University). HeLa-shPRMT5 cell lines were a gift from Sharon Dent (UT MD Anderson Cancer Center). The tetracycline-inducible T-REx-CARM1-293 cell line

Antibody Name	Company	Catalog #	Antibody type	Host Species	WB Dilution
MMA1	Cell Signaling	8711	Monoclonal	Rabbit	1:2000
MMA2	Cell Signaling	8015	Monoclonal	Rabbit	1:1000
MMA3	Cell Signaling		Monoclonal	Rabbit	1:1000
MMA4	Cell Signaling		Monoclonal	Rabbit	1:1000
MMA5	Cell Signaling		Monoclonal	Rabbit	1:1000
ADMA	Cell Signaling	Not yet commercially released	Polyclonal	Rabbit	1:500
SDMA	Cell Signaling	Not yet commercially released	Polyclonal	Rabbit	1:1000
H3R17me2a	Millipore	07-214	Polyclonal	Rabbit	1:1000
Y12	A gift from Robin Reed	N/A	Monoclonal	Mouse	1:100
PRMT1	A gift from Stephane Richard	N/A	Polyclonal	Rabbit	1:1000
PRMT3	N/A	N/A	Polyclonal	Rabbit	1:500
CARM1	Bethyl	A300-421A	Polyclonal	Rabbit	1:2000
PRMT5	Active Motif	61001	Polyclonal	Rabbit	1:2000
PRMT6	Bethyl	A300-929A	Polyclonal	Rabbit	1:1000
PRMT7	A gift from Said Sif	N/A	Polyclonal	Rabbit	1:500
GFP	Life technologies	A6455	Polyclonal	Rabbit	1:1000

Table 2: Antibodies used in the first study.

Antibody Name	Company	Catalog #	Antibody type	Host Species	WB Dilution
ADMA-1 ^{CARM1}	Cell Signaling	Not yet commercially released	Polyclonal	Rabbit	1:500
ADMA-2 ^{CARM1}	Cell Signaling	Not yet commercially released	Polyclonal	Rabbit	1:500
ADMA-3 ^{CARM1}	Cell Signaling	Not yet commercially released	Polyclonal	Rabbit	1:500
ADMA-4 ^{CARM1}	Cell Signaling	Not yet commercially released	Polyclonal	Rabbit	1:500
CARM1	Bethyl	A300-421A	Polyclonal	Rabbit	1:2000
PRMT5	Active Motif	61001	Polyclonal	Rabbit	1:2000
PRMT6	Bethyl	A300-929A	Polyclonal	Rabbit	1:1000
PRMT7	A gift from Said Sif	N/A	Polyclonal	Rabbit	1:500
FLAG	Sigma	F7425	Polyclonal	Rabbit	1:2000
FLAG	Sigma	F3165	Monoclonal	Mouse	1:2000
SRC1	Cell Signaling	2191	Monoclonal	Rabbit	1:1000
SRC3	BD Transduction	611105	Monoclonal	Mouse	1:250
MED12	Bethyl	A300-774A	Polyclonal	Rabbit	1:500
meMED12 ^a	Cell Signaling	Not yet commercially released	Monoclonal	Rabbit	1:500
meMED12 ^b	Cell Signaling	Not yet commercially released	Monoclonal	Rabbit	1:500
mePABP1	Generated in our lab	N/A	Polyclonal	Rabbit	1:250
TDRD3	Generated in our lab	N/A	Monoclonal	Mouse	1:500
GST	Generated in our lab	N/A	Polyclonal	Rabbit	1:2000
MED4	A gift from Thomas Boyer	N/A	Polyclonal	Rabbit	1:1000
MED30	A gift from Thomas Boyer	N/A	Polyclonal	Rabbit	1:1000
CDK8	A gift from Thomas Boyer	SC-1521	Polyclonal	Goat	1:500
pH3S10	Cell Signaling	9701	Polyclonal	Rabbit	1:1000
ER α	Abcam	sc-543	Polyclonal	Rabbit	1:1000

Table 3: Antibodies used in the second study.

(Cheng et al, 2007) has been described previously. The MCF-7-Tet-on-shCARM1 cell line was a gift from Wei Xu (University of Wisconsin, Madison). MCF-7, HeLa and HEK293T cell lines were obtained from ATCC. All cell lines were maintained in Dulbecco modified Eagle medium containing 10% fetal bovine serum. PRMT1 MEFs were supplemented with 3 μ g/ml blasticidin and PRMT5 KD cells were supplemented with 5 μ g/ml puromycin.

2.4 Amino acid analysis

35–180 mg of wet weight packed MEFs and 100 μ L of 6 N HCl were added to a 6 x 50-mm glass tube. Hydrolysis was carried out in a Waters Pico-Tag Vapor-Phase apparatus in a vacuum vial with an additional 200 μ L of 6 N HCl for 18 h at 110°C. After hydrolysates were vacuum dried, resuspended in 100 μ L of water, and centrifuged to remove any debris, 75 μ L was added to 250 μ L of citrate buffer (0.2 M Na⁺, pH 2.2) and loaded onto a 0.9 x 8 cm column of PA-35 sulfonated polystyrene beads (6–12 μ m, Benson Polymeric Inc., Sparks, NV). The column was equilibrated and eluted with citrate buffer (0.35 M Na⁺, pH 5.27) at 55°C and a flow rate of 1 mL/min. Individual fractions from 50 to 80 min that included the known elution positions of ADMA, SDMA, MMA, and arginine were then derivatized with OPA for fluorescence detection after separation on reverse-phase HPLC.

Amino acids were labeled with OPA by mixing 60 μ L of 1 mL cation exchange column fraction with 20 μ L of 0.4 M potassium borate (pH 10.3), and 10 μ L of OPA reagent (10 mg/mL OPA powder (Sigma, P0657) in 900 μ L methanol, 100 μ L 0.4 M potassium borate (pH 10.3), and 10 μ L b-mercaptoethanol). After incubating the mixture at room temperature for 200 s, 5 μ L of 0.75 M HCl was added and the sample was vortexed by hand for 5 s. The resulting fluorescent isoindole derivatives were separated and quantified using reverse-phase HPLC (HP 1090 II liquid chromatograph coupled to a Gilson Model 121 fluorometer with excitation and emission filters of 305–395 nm and 430–470 nm, respectively, and a setting of 0.01 RFU).

An Alltech Adsorbosphere OPA HR (5 mm, 4.6-mm inner diameter, 250-mm length) was used with 90 μ L sample injection volumes at room temperature and a flow rate of 1.5 ml/min. Solvent A consisted of 50 mM sodium acetate, pH 7.0, and solvent B of 100% methanol. Two HPLC gradients were used to optimize the quantification of MMA, ADMA, and SDMA (Figure 14). In situations where the fluorometer was overloaded with too much sample, such as in the case of some fractions associated with the arginine peak, a 1000-fold dilution of the cation exchange fraction was made in pH 5.27 sodium citrate buffer. Methylated arginine species were detected based on the HPLC retention time for standards and were confirmed by spiking the appropriate standard to the sample. Graphpad was used to calculate the area under the curve for the amino acid of interest. The total amount of a certain amino acid was calculated by summing every cation exchange fraction's HPLC run that had the appropriate peak present.

2.5 Antibody binding assay

CARM1 substrate antibodies were incubated with histone peptide arrays for 90–180 min at 4°C and washed with PBS. Arrays were then probed with the Alexa Fluor 647 labeled secondary antibody (Invitrogen) for 30–60 min at 4°C, washed with PBS, dried and scanned using a Typhoon TRIO+ imager (GE Healthcare). Binding intensities were measured using ImageQuant array software (GE Healthcare).

2.6 In vitro methylation assay

The *in vitro* methylation reactions contained 1 μ g substrate (PABP1, H3 or MED12 peptides), 1 μ g recombinant GST-CARM1, 1 μ L S-adenosyl-L-[methyl- 3 H] methionine (81.7 Ci/mmol from a 6.7 μ M stock solution, Perkin Elmer, NET155001MC) in a final volume of 30 μ L PBS. The reactions were incubated at 30°C for 1.5 h, and boiled in protein loading buffer

for 5 min. The samples were resolved by SDS-PAGE, transferred onto PVDF membranes, treated with En³hance (Perkin Elmer, 6NE970C), and exposed to film for 1-3 days at -80°C.

2.7 In vitro phosphorylation assay

The *in vitro* phosphorylation reactions were performed by incubating 1 µg recombinant H3 protein, MED12 or CDK8 immunoprecipitated protein A/G beads (from a 10 cm plate), 1 µl non-radiolabelled 10mM ATP in a final volume of 50 µl PBS at 37°C for 1.5 h. The reactions were stopped by adding protein loading buffer and boiling for 5 min. The samples were analyzed by Western blotting.

2.8 Peptide pull-down assay

Biotinylated MED12 peptides (20 µg) were immobilized on 20 µl streptavidin agarose beads (Millipore, 16-126) in 500 µl of mild lysis buffer (50 mM Tris-HCl, pH 7.5, 150 mM NaCl, 0.1% Nonidet P-40, 5 mM EDTA, 5 mM EGTA and 15 mM MgCl₂) at 4°C for 2 h. The beads were washed three times with Co-IP buffer and incubated with 4 µg of GST-Tudor protein in 500 µl mild lysis buffer at 4°C for 2 h. After three washes with Co-IP buffer, the beads were boiled in protein loading buffer and subjected to western blot analysis using αGST antibody.

2.9 Immunoprecipitation and Coimmunoprecipitation assays

For screening CARM1 substrates, HEK293T cells (90% confluent) were transiently transfected with expression vectors encoding FLAG-tagged putative CARM1 substrates using Lipofectamine 2000 (Invitrogen). Cells (10 cm plate) were harvested after 24 h, washed with ice-cold PBS and lysed in 1 ml of RIPA lysis buffer (25 mM Tris-HCl (pH 7.6), 150 mM NaCl, 1% Nonidet P-40, 1% Sodium deoxycholate, 0.1% Sodium dodecyl sulfate, 2 mM EDTA) with

protease inhibitor cocktail (Roche). The lysates were incubated with 40 μ l of anti-FLAG M2 affinity gel (Sigma Aldrich, A2220) for 1 h. The beads were washed three times with RIPA buffer, eluted in protein loading buffer.

For the co-IP assays, cells (10 cm plate) were transiently transfected with expression vectors using Lipofectamine 2000 (Invitrogen) according to the manufacturer's instructions. Cells were harvested 30h after transfection and lysed in 1 ml of mild lysis buffer (50 mM Tris-HCl, pH 7.5, 150 mM NaCl, 0.1% Nonidet P-40, 5 mM EDTA, 5 mM EGTA and 15 mM MgCl₂) and immunoprecipitated with the specified antibodies.

For the TDRD3-MED12 co-IP experiment, MCF7-tet-on-shCARM1 cells (Yang et al, 2010) were treated with 1 μ g/ml of Doxycycline for 6 days to knockdown endogenous CARM1 expression. Untreated parental cells were used as controls. Cells were lysed in buffer A (10 mM HEPES, 1.5 mM MgCl₂, 10 mM KCl, 0.5 mM DTT, 0.05%NP40, pH 7.9) supplemented with cocktails of protease inhibitor and phosphatase inhibitor (Pierce) for 10 min on ice. After centrifuging at 4° C at 3000 rpm for 10 min, the supernatant was removed and the pellet was resuspended in 387 μ l of buffer B (5 mM HEPES, 1.5 mM MgCl₂, 0.2 mM EDTA, 0.5 mM DTT, 26% glycerol (v/v), pH7.9) supplemented with 13 μ l of 4.6M NaCl to give 150mM NaCl. After lysing on ice for 10 min, brief sonication was applied to dissolve the pellet. Cell lysates were kept on ice for additional 30 min. After centrifuge at 24,000 g for 20 min at 4° C, the supernatant was collected as nuclear extract for immunoprecipitation using anti-TDRD3 antibody.

The immunoprecipitated samples or cell extracts were separated by SDS-PAGE and transferred onto PVDF membranes. Blots were blocked in PBS-Tween 20 containing 5% nonfat dry milk and then incubated with the appropriate primary antibody in the blocking buffer overnight at 4°C. The blots were then washed, probed with an HRP-labeled secondary antibody and detected using enhanced chemiluminescence (Amersham).

2.10 Oligonucleotide pull down assay

A 364 bp doubly biotinylated fragment from the human *GREB1* gene was made by PCR using pCR4-Topo-GREB or pCR4-Topo-GREB ERE mut as a template and purified by centrifugation through PCR Kleen Spin Columns (Bio-Rad) as detailed in Foulds, C.E. et al. *Mol Cell* 2013. Two micrograms of this fragment were bound to 40 μ l Dynabeads® M280 streptavidin (Invitrogen) in 150 μ l D-PBS as detailed in Foulds, C.E. et al. *Mol Cell* 2013. MCF-7 nuclear extract (NE) was prepared as detailed in Foulds, C.E. et al. *Mol Cell* 2013. We added clarified NE (1 mg) to resuspend beads, 100 nM water-soluble E2 (Sigma), and a 1 mM EDTA/EGTA mix. Reactions were rotated at 4°C for 1.5 hr. Beads were washed two times in NETN and once in D-PBS as detailed in Foulds, C.E. et al. *Mol Cell* 2013. After PBS removal, the final washed endogenous ER-coregulator complexes were resuspended in 20 μ l 2x SDS sample buffer (Pierce) and 9 μ l samples were loaded on a 4–15% Mini-PROTEAN® TGX™ Precast gel (Bio-Rad) for immunoblotting using an ECL Plus kit (Pierce) and X-ray film as detailed in Foulds, C.E. et al. *Mol Cell* 2013. Sources of primary antibodies were the following: ER α (sc-543, Santa Cruz Biotechnology), MED12 (A300-774A, Bethyl Laboratories), meMED12 (Bedford lab rabbit polyclonal), and CARM1 (A300-421A, Bethyl Laboratories).

2.11 Chromatin Immunoprecipitation and quantitative PCR (ChIP-qPCR)

Chromatin was harvested from MCF-7 cells as described previously (Iberg et al, 2008) and ChIP was performed using CARM1, MED12, and H3R17me2a antibodies. Using 2 μ l of ChIP DNA as the template, qPCR was performed on the ABI 7900 HT Fast Real Time PCR System (ABI) with primer sets against the specified genes (Table 4). Data was analyzed using the Sequence Detection System software (ABI). The experimental cycle threshold (Ct) was calibrated against the input product.

2.12 ChIP-seq analysis

2.12.1 Mapping of Reads

Sequenced DNA reads were mapped to human genome hg19 using bowtie (version 0.12.8) [1] and only the reads that were mapped to unique position were retained. 31-63 million reads were generated per sample. 80-97% reads were mapped to human genome, with 59-71% uniquely mapped. To avoid PCR bias, for multiple reads that were mapped to the same genomic position, only one copy was retained for further analysis. In the final, 22-41 million reads were used in peak calling and downstream analyses.

2.12.2 Peak calling and gene annotation

The original peak calling for CARM1/MED12/R17 was done by MACS (version 1.4.2) [2] using total input DNA as control. The window size was set as 300 bp and the p -value cutoff was $1e-6$. The peaks overlapping DAC Blacklisted Regions and Duke Excluded Regions downloaded from UCSC genome browser (<http://genome.ucsc.edu/cgi-bin/hgFileUi?db=hg19&g=wgEncodeMapability>) were removed. Then the peaks from the three factors were merged (allowing at least 1bp overlap) to form a highly confident superset of peaks. For each peak from the superset, if it overlapped the peaks of one of the factors called at p -value $1e-4$, it was marked as occupied by the corresponding factor. For ERa, the peaks were called by MACS with no control used. The window size was set as 300 bp and the p -value cutoff was $1e-10$. The peaks overlapping blacklisted regions were removed. For public CARM1 data, the peaks were called by MACS by comparing CARM1 E2 treated to both CARM1 EtOH treated and total input. The window size was set as 300 bp and the p -value cutoff was $1e-6$. Only peaks that were called by comparing to both controls and didn't overlap blacklisted regions were kept. For venn diagram of public CARM1 vs. our CARM1, the peaks (at p -value $1e-6$) from both were merged (allowing at least 1bp overlap). For each of the

merged peaks, if it overlapped the peaks of one of the CARM1 datasets called at p -value $1e-4$, it was counted as called in the corresponding dataset. Each peak in the superset was assigned to the gene that has the closest transcription start site (TSS) to it. Then the peak was classified by its location to the gene: upstream (-50k to -5k from TSS), promoter (-5k to +0.5k from TSS), exon, intron, TES (-0.5k to +5k from TES) and downstream (+5k to +50k from TES). The gene list used to annotate the peaks is GENCODE release 19 [3].

2.12.3 Landscape of ChIP-Seq Signal

Each read was extended by 150bp to its 3' end. The number of reads on each genomic position was rescaled to normalize the total number of mapped reads to 10M and averaged over every 10bp window. The normalized values were displayed in UCSC genome browser (<http://genome.ucsc.edu/>).

2.12.4 Heatmap and Average Profile of ChIP-Seq Signal around peak center

10kbp upstream and 10kbp downstream from the center of each peak were subdivided into 250 bp bins. For each ChIP-Seq sample, the rpkm (reads per million reads per kilobase) values for each bin were calculated and normalized through z-score transformation to minimize the potential batch effect. The values were then averaged over all peaks to generate average profile or plotted in heatmap by R function heatmap.2.

2.13 Quantitative Reverse Transcription PCR (RT-qPCR)

MCF-7-Tet-on-shCARM1 cells were untreated or treated with doxycycline (1 μ g/ml) for 5 days. The cells were then gently washed with PBS and transferred to phenol red-free DMEM supplemented with 10% charcoal dextran-stripped FBS. The cells were maintained in this

media with or without doxycycline for 3 days. On the 9th day, cells were treated with 50nM E2 for 45 min. Total RNA was extracted using RNeasy Mini kit (74104, Qiagen) and cDNA was synthesized using Superscript III First-Strand Synthesis system (18080-051, Invitrogen). qPCR was then performed using primer sets against the specified genes (Table 5). Data was analyzed using the Sequence Detection System software (ABI). The experimental cycle threshold (Ct) was calibrated against the β -actin control product, and the amount of sample product from Dox-treated cells relative to that of the control cells was determined using the DDCT method (1-fold, 100%).

2.14 Immunofluorescence and Image Analysis

Immunofluorescence experiments were performed as previously described (Bolt et al, 2013). Briefly, cells were fixed in 4% formaldehyde in PEM buffer (80 mM potassium PIPES [pH 6.8], 5 mM EGTA, and 2 mM MgCl₂), quenched with 0.1 M ammonium chloride, permeabilized with 0.5% Triton X-100, non-specific sites were blocked with blotto (5% milk in Tris-buffered saline/Tween 20), and then specific antibodies were added overnight at 4C prior to 30 min of secondary antibody (Alexa conjugates; Molecular Probes) and DAPI staining. Automated imaging was carried out using an IC-200 high throughput microscope (Vala Sciences). Image fields were acquired with a sCMOS 5.5 megapixel camera through a Nikon S Fluor 40x/0.90 NA objective. Z-stacks were imaged at 1 μ m intervals. Nuclear array segmentation and signal quantification were performed using PipelinePilot image analysis software (Biovia) as previously described (Ashcroft et al, 2011; Bolt et al, 2013). Aggregated cells, mitotic cells, and apoptotic cells were removed using filters based on nuclear size, nuclear shape, and nuclear intensity.

Gene Name	Forward Primer	Reverse Primer
<i>GREB1</i> No peak	TTTGCATGGACAGGCCTTGA	GCCCAAACCTTGGCACTTTC
<i>GREB1</i> peak1	GAGAGGGTGGTGACACTTGG	CTGCAGCTGACAGAGGAGAC
<i>GREB1</i> peak2	CTGGCTGCTTCCTGAGTGG	GCGTCAAGCAACTACACTCC
<i>GREB1</i> peak3	TGAGCAAAAGCCACAAAGTAGT	TGCTGCGGCAATCAGAAGTA
<i>GREB1</i> peak4	GGCTCCAGTCCAAGTACACA	AAATGCCACCGTTTCGTGT
<i>FKBP4</i> No peak	CTTCTCAGTAAGCCTGCGGT	GACTATCTGCCGAACCAGGG
<i>FKBP4</i> peak	CTCTGCTGTGGAGCCTGC	TCTCTGATTCTCCCTGGAACCT
<i>IGFBP4</i> No peak	TTTTGGGTCTGGGTGTGTGT	CAGCACCTGAGGAGTGCC
<i>IGFBP4</i> peak	AGGGTTGGGCAAGGAAAAGT	CATGCACTTGGGCACTCTGA
<i>TFF1</i> No peak	CCAGGGCCACCGAGAAC	CATTCTCGGGGTCAGCACC
<i>TFF1</i> peak 1	ACATTTGCCTAAGGAGGCCC	ACCTCACCACATGTCGTCTC
<i>TFF1</i> peak 2	ATTTCTTCTCCACGCCCTGT	GACAGCTGCCAGGTACGG

Table 4: Primers used for ChIP-qPCR assays.

Gene Name	Forward Primer	Reverse Primer
CARM1	CCAGGGTGATGATGAAGGAC	GGGCATCGCCCTCTACA
FKBP4	CTATCGTGGAGGTTGCACTG	CCATAAGGCAGATCCAGGTT
GREB1	CTGTCCAGAGGGTGACATTG	CAGGGATGCTGCTTTAGTGA
IGFBP4	AGGGGCTGAAGCTGTTGTT	CCTGCACACACTGATGCAC
NOB1	TTGGAAGCAGAGTTTGTGG	ATGTGCAGAGGTGTTTCTGG
TFF1	TCCCTCCAGAAGAGGAGTGT	CAGAAGCGTGTCTGAGGTGT
WWP2	GAAAATTGTCAGCTCTCCGC	GTCTTGAAGAACAATGGGGG
GAPDH	AGCCACATCGCTCAGACAC	GCCCAATACGACCAAATCC

Table 5: Primers used for RT-qPCR assays.

Chapter 3: Loss of PRMT1 causes substrate scavenging by other PRMTs

3.1 Mono-methyl arginine antibodies reveal methylation type switching with PRMT1 loss

A panel of five different rabbit monoclonal antibodies (MMA1-5) was generated to recognize endogenous proteins when monomethylated at arginine residues. MMA1 was raised against the arginine-glycine-glycine motif, mono-methylated at arginine residue (Rme1-G-G) and MMA2-5 antibodies were generated against a synthetic peptide library containing mono-methyl arginine flanked by degenerate amino acids (XXXXXRme1XXXXX). To validate these antibodies, we tested them on wild-type and PRMT1-deficient cells. Since PRMT1 is essential for cell viability, we used an inducible-knockout cell line. The MEF cell line, heterozygous for the floxed *Prmt1* allele, was stably transfected with ER*-Cre (Cre recombinase fused to the ligand-binding domain of the mouse estrogen receptor (ER)) (Yu et al, 2009). This *Prmt1^{fl/-}* ER-Cre MEF line can be treated with 4-hydroxytamoxifen (OHT), which stabilizes ER*-Cre and translocates it to the nucleus, which then excises the floxed *Prmt1* allele to generate PRMT1 KO MEFs. These cells were treated for 8 days with OHT, which is a few days (2-4 days) prior to cell death, before harvesting cell extracts. PRMT1 has been known to generate MMA and ADMA marks *in vitro*. We expected that PRMT1 will mono- and di-methylate proteins in cells and the loss of this enzyme will lead to the depletion of both types of methylation. Surprisingly, we found an increase in immunoreactivity with all five MMA antibodies upon PRMT1 removal (Figure 8A). Additionally, we tested the antibodies on HCT116 cells untreated or treated with AdOx for 2 days. Adenosine dialdehyde (AdOx) is a global methylation inhibitor. It functions by inhibiting S-adenosylhomocysteine (SAH) hydrolase, which leads to the accumulation of intracellular SAH levels. This increase in SAH levels results in the feedback inhibition for most methyltransferase reactions. Hence, AdOx treatment should deplete all types of methylation

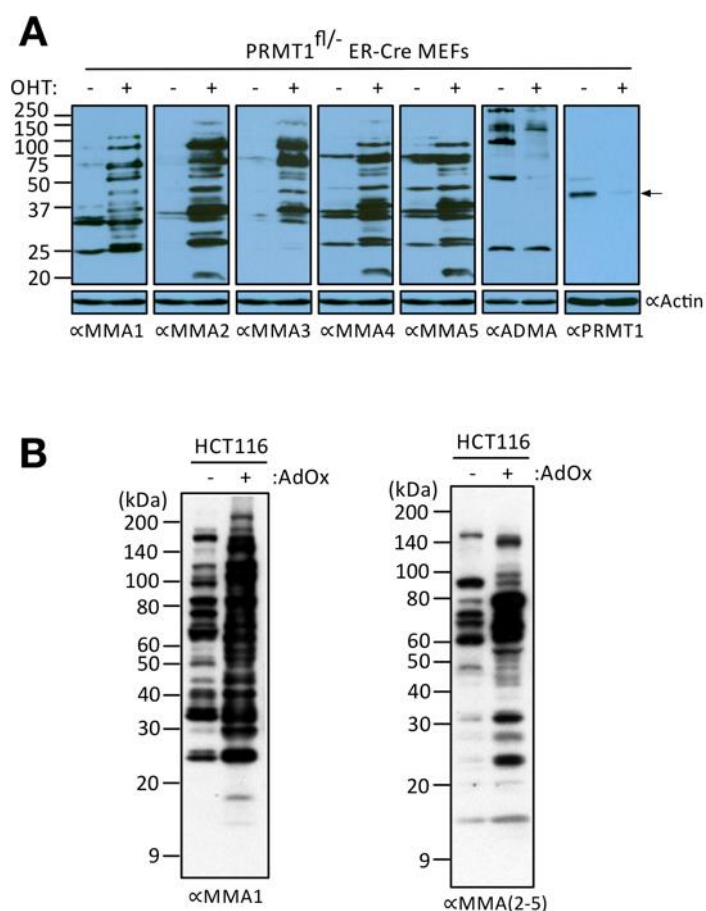


Figure 8: Loss of PRMT1 or inhibition of global methylation by AdOx reveals an accumulation of monomethylated substrates.

(A) *PRMT1*^{fl/-} ER-Cre MEFs were untreated or treated with 4-hydroxytamoxifen (OHT, 2 μ M) for 8 days. Whole cell lysates were prepared and immunoblotted with α MMA1-5, α ADMA, and α PRMT1 antibodies. Arrow indicates the position of the PRMT1 protein. β -actin serves as a loading control.

(B) HCT116 cells were treated with AdOx (20 μ M) for 48 h and whole cell lysates were immunoblotted with α MMA1 and a pool of α MMA2-5 antibodies.

Experiment for figure 8B was performed by Cell Signaling Technology.

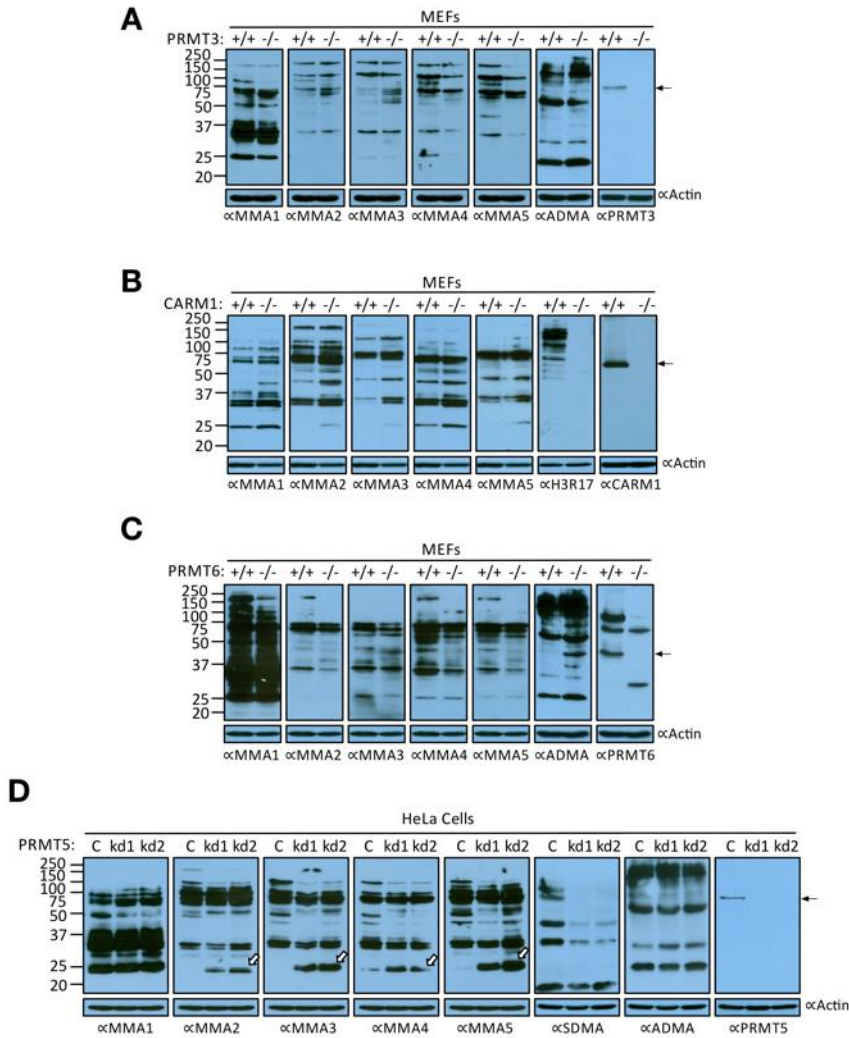


Figure 9: Loss of other Type I enzymes (PRMT3, 4, and 6) or reduction of Type II enzyme (PRMT5) has no effect on global MMA levels.

Whole cell extracts of wild-type (+/+) and PRMT3 **(A)**, CARM1 **(B)** or PRMT6 **(C)** knockout (-/-) MEFs were immunoblotted with α MMA1-5, α ADMA, and α H3R17me2a (Millipore) antibodies. **(D)** HeLa-shControl (C) and HeLa-shPRMT5 (kd1 and kd2) cell extracts were immunoblotted with α MMA1-5, α SDMA, and α ADMA antibodies. All knockout and knockdown cell lines were validated by immunoblotting with their respective α PRMT antibodies. Arrows indicate the position of the PRMTs. β -actin serves as a loading control.

from cellular proteins. However, AdOx-treated cells showed an increased mono-methylation signal relative to the untreated cells (Figure 8B). Perhaps, AdOx induces MMA accumulation by partially inhibiting PRMT1 activity. Next, we wanted to determine if this phenomenon holds true with the removal of other PRMTs. The loss of PRMT3, 4, 6 or the knockdown of PRMT5 did not cause an accumulation of mono-methylated substrates (Figure 9A-D). However, one protein that migrates at 25 kDa, was mono-methylated upon PRMT5 knockdown (indicated by solid white arrows in Figure 9D). From these data, we can conclude that the loss of PRMT1 seems unique in its ability to generate mono-methylated substrates. It is also noteworthy that these antibodies can be used as tools for identifying novel PRMT1 substrates by IP-MS approaches.

3.2 MMA and SDMA levels reach a maximum within 4-6 days after PRMT1 loss

Next, we wanted to study the dynamics of different types of arginine methylation upon the gradual loss of PRMT1. This experiment is possible due to the availability of the inducible-knockout PRMT1 cell line (PRMT1^{fl/-} ER-Cre MEFs). These cells were treated with 4-hydroxytamoxifen (OHT) and harvested after various time points (0-10 days). Two days post treatment, 90% of the PRMT1 protein is lost and by 4 days, the cells are completely devoid of the enzyme (Figure 10D). Concomitant with PRMT1 loss, we observed an increase in MMA signal (Figure 10A). When tested with ADMA antibody, we observed an initial loss of methylation among some substrates (Figure 10B – lower molecular weight bands in 2 d and 4 d lanes), which reappeared later (Figure 10B – 6 d to 10 d lanes). We speculated that the cells could be compensating the loss of PRMT1 by over-expressing other PRMTs. Hence, we tested the expression of various PRMTs at 4 and 8 days after OHT treatment (Figure 11). At 8-day time-point, we observed an increase in PRMT6 and

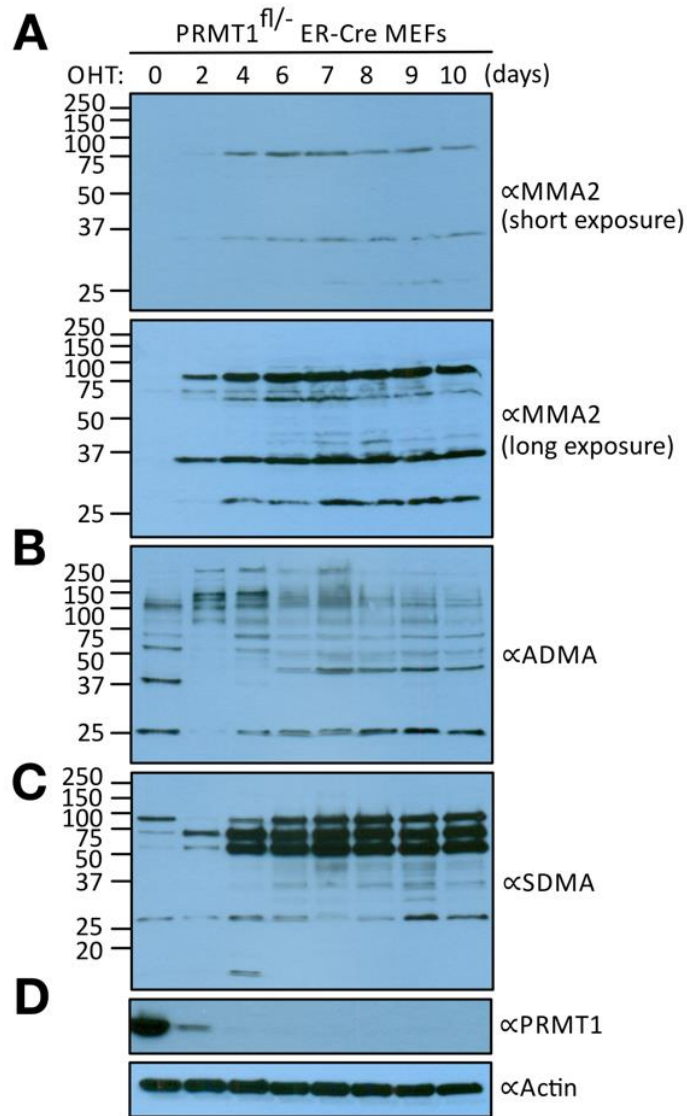


Figure 10: Arginine methylation trends in inducible PRMT1-knockout MEFs.

Prmt1^{fl/-} ER-Cre MEFs were untreated or treated with 4-hydroxytamoxifen (OHT, 2 μ M) and harvested after 0, 2, 4, 6, 7, 8, 9, and 10 days. Whole cell lysates were immunoblotted with α MMA2 (**A**), α ADMA (**B**), α SDMA (**C**) and α PRMT1 (**D**) antibodies. β -actin serves as a loading control.

Experiment for figure 10 was performed by Dr. Surbhi Dhar (a previous post-doc from Dr. Mark Bedford's lab, UT M.D. Anderson Cancer Center)

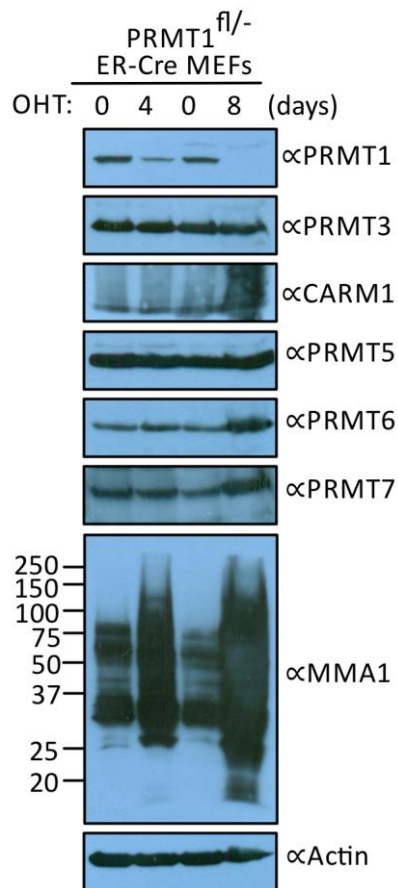


Figure 11: Expression analysis of PRMTs in the absence of PRMT1.

Prmt1^{fl/-} ER-Cre MEFs were untreated or treated with 4-hydroxytamoxifen (OHT, 2 μ M) and harvested after 0, 4, and 8 days. Whole cell extracts were subjected to Western analysis with α PRMT1, α PRMT3, α CARM1, α PRMT5, α PRMT6, α PRMT7 and α MMA1 antibodies.

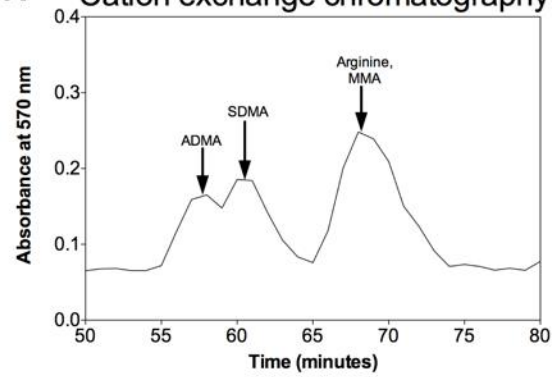
Experiment for figure 11 was performed by Dr. Surbhi Dhar (a previous post-doc from Dr. Mark Bedford's lab, UT M.D. Anderson Cancer Center)

PRMT7 expression levels, suggesting that the cells compensated PRMT1 loss by expressing these 2 enzymes. Additionally, we also noticed streaking of CARM1 by Western analysis, which could imply hyper protein modification (Figure 11). However, at 4-day time-point, the cells showed equal expression of PRMT3, 4, 5, 6, and 7 enzymes. This suggests that the increase in MMA levels upon 4 days of OHT treatment is not due to over-expression of PRMTs. We also evaluated the dynamics of symmetric di-methylation upon PRMT1 gradual loss. Like MMA, SDMA levels have also increased with PRMT1 loss (Figure 10C).

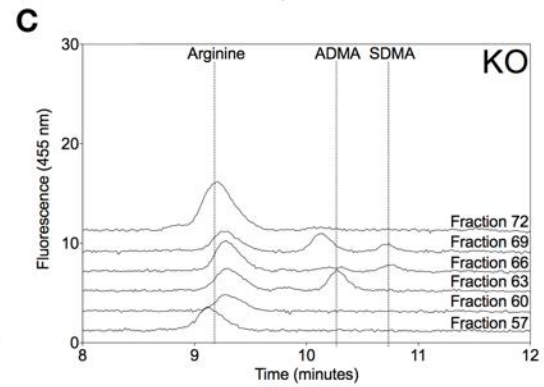
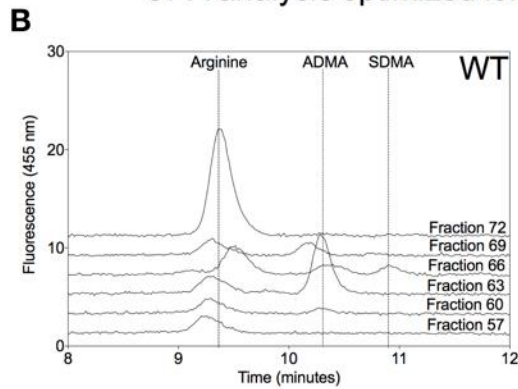
3.3 Amino acid analysis confirms the global accumulation of MMA and SDMA levels with PRMT1 loss

To confirm the above findings using an antibody-independent approach, we performed amino acid analysis for wild-type and PRMT1 knockout MEFs. To do this, we untreated or treated *Prmt1^{fl/-}* ER-Cre MEFs with 4-hydroxytamoxifen (OHT) for 7 days, harvested whole cell lysates and acid hydrolyzed proteins to obtain amino acids. To quantify methylated arginine residues, we have developed a novel two-dimensional approach that takes advantage of the high-resolution of cation-exchange and reverse-phase columns coupled to the sensitivity of the fluorescent labeling (Figures 12 and 13). PRMT1 wild-type or knockout acid hydrolysates were first separated by high-resolution cation exchange chromatography. The fractions obtained were then labeled with *o*-phthaldialdehyde (OPA) to enable the detection of picomole levels of amino acids after a second step of separation using two conditions of reverse-phase HPLC to quantitate MMA, SDMA, and ADMA relative to the level of arginine (Figure 14). From this study, we were able to measure the changes in different types of arginine methylation upon PRMT1 loss accurately (Table 2). The loss of PRMT1 has caused a five-fold increase in MMA levels, a three-fold increase in SDMA levels, and a 50% reduction in ADMA levels. Consistent with the above antibody studies, amino

A Cation exchange chromatography



OPA analysis optimized for SDMA and ADMA quantitation



OPA analysis optimized for MMA quantitation

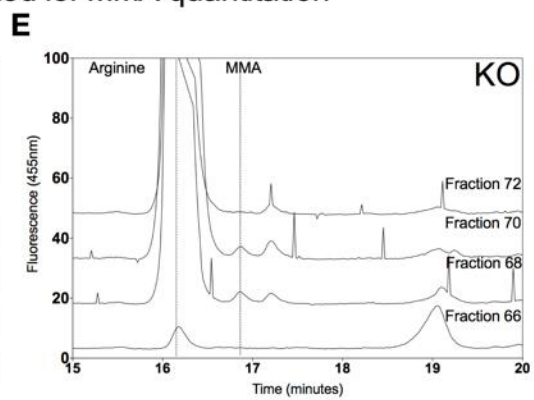
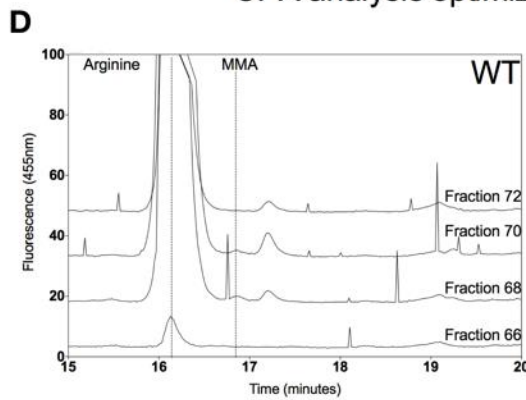


Figure 12: Quantification of MMA, ADMA, SDMA and arginine levels in protein hydrolysates of wild-type and PRMT1-knockout MEFs.

Cell pellets from wild-type and PRMT1 knockout MEFs were acid hydrolyzed and the resulting amino acids were separated by high-resolution cation exchange chromatography. **(A)** Control chromatograph showing the standards (1 μ mol) of ADMA, SDMA and MMA/arginine with ninhydrin detection. Cell hydrolysates were then chromatographed without standard amino acids and fractions analyzed by reverse-phase HPLC after derivatization with OPA for fluorescence quantification as described in "Methods". HPLC conditions were optimized to separate the large pool of arginine from ADMA and SDMA in wild-type **(B)** and PRMT1 knockout **(C)** and from MMA in wild-type **(D)** and PRMT1 knockout **(E)** samples. The total amount of a given species was quantified by summing the integrated area under the curve for all HPLC fractions containing the respective species that are consistent with the migration on the cation-exchange column.

Experiment for figure 12 was performed by Grace Huang and Dr. Alexander Patananan from Dr. Steven Clarke's lab, UCLA. Wild-type and PRMT1 knockout MEF extracts for the amino acid analysis were provided by us.

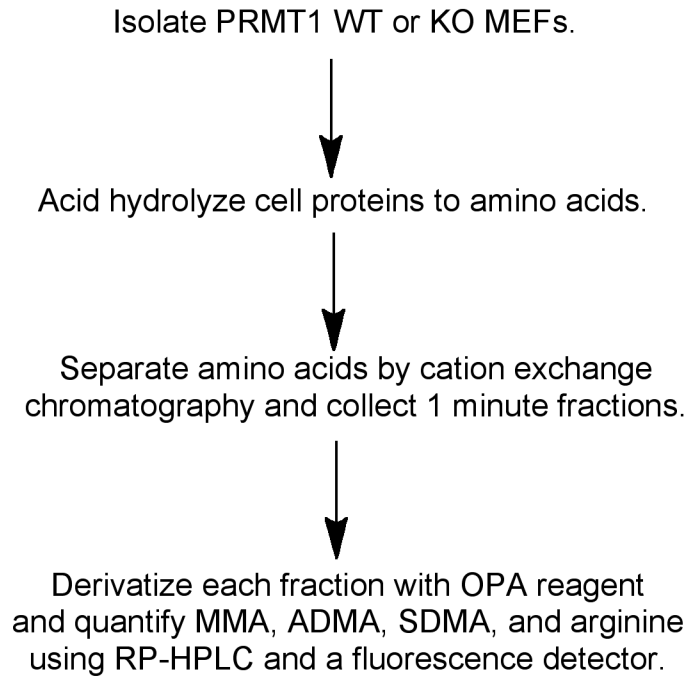


Figure 13: Workflow for the two-dimensional quantification of MMA, ADMA, SDMA, and arginine in MEFs.

Figure 13 flowchart was made by Dr. Steven Clarke's lab, UCLA.

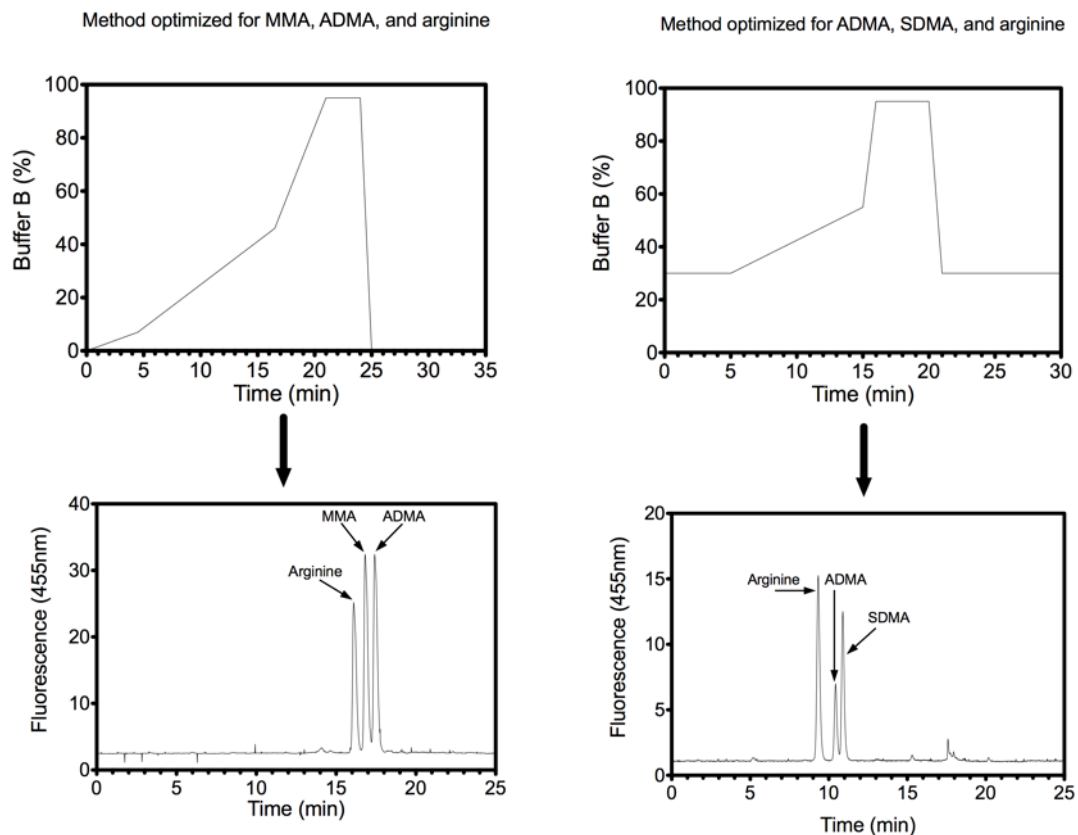


Figure 14: Reverse-phase HPLC methods optimized to quantify OPA-derivatives of arginine, MMA, ADMA, and SDMA.

Experiment for figure 14 was performed by Grace Huang and Dr. Alexander Patananan from Dr. Steven Clarke's lab, UCLA.

acid analysis showed that both MMA and SDMA levels rise with the loss of the major protein arginine methyltransferase. Additionally, these studies also demonstrate the prevalence of arginine methylation in MEFs. We found that about 0.4% of arginine residues are asymmetrically di-methylated, 0.01% of arginine residues are mono-methylated, and 0.03% of arginine residues are symmetrically di-methylated in MEFs (Table 2). Therefore, ADMA is the predominant mark of methylation in MEFs. We have enlisted here the MMA, ADMA, and SDMA levels in wild-type MEFs obtained from this study as well as those in rat brain and liver shown previously in the literature (Table 3). It is noteworthy that while ADMA and SDMA levels are comparable in MEFs and rat brain and liver, MMA levels are significantly lower in MEFs.

Residue analyzed	Experiment #	PRMT1 WT	PRMT1 KO	Average fold change (KO to WT)
		Residues per 1000 arginine residues		
MMA	Experiment 1	0.16	0.83	4.73
	Experiment 2	0.07	0.30	
ADMA	Experiment 1	4.36	3.14	0.52
	Experiment 2	3.69	1.76	
	Experiment 3	3.98	1.49	
SDMA	Experiment 1	0.34	0.94	2.76

Table 6: Average fold change in MMA, ADMA and SDMA levels upon the loss of PRMT1.

Table 6 was generated by Dr. Steven Clarke's lab, UCLA.

Cells	MMA	ADMA	SDMA	Reference
	Average number of residues per 1000 arginine residues			
Wild-type MEFs	0.12	4.01	0.34	This study
PRMT1 KO MEFs	0.57	2.13	0.94	This study
Rat brain	2.04	3.60	0.99	1, 2
Rat liver	0.65	2.95	0.35	1, 2
Rat brain nuclear fraction	1.98	10.1	1.10	1, 2

Table 7: Comparison of the relative levels of MMA, ADMA, and SDMA in different mammalian cells.

Values from rat brain and liver were taken from Matsuoka (1972)¹ as translated by Paik and Kim (1980)², and converted from μ mol per g protein assuming an average arginine residue content of 5% in proteins.

References for table 7:

1. Matsuoka, M. [Epsilon - N - methylated lysine and guanidine - N - methylated arginine of proteins. 3. Presence and distribution in nature and mammals]. Seikagaku 44, 364-70 (1972).
2. Paik, W.K. & Kim, S. Natural occurrence of various methylated amino acid derivatives. (ed. Meister, A.) (John Wiley & sons, New York, 1980).

Table 7 was generated by Dr. Steven Clarke's lab, UCLA.

Chapter 4: CARM1 Methylates Mediator to Promote Estrogen Receptor-Regulated Transcription

4.1 Developing and characterizing CARM1 Substrate antibodies

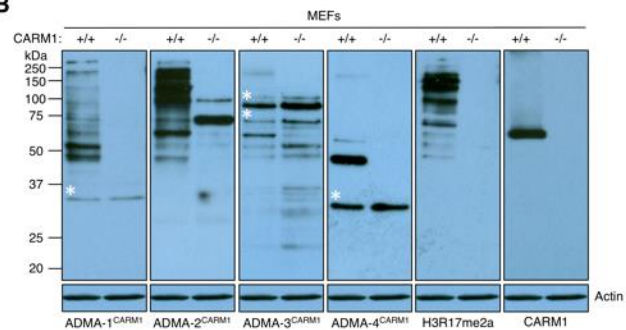
Methyl-specific antibodies (both ADMA and SDMA) have previously been used to identify PRMT substrates (Boisvert et al, 2003; Guo et al, 2014). However, these antibodies cannot enrich CARM1 substrates because CARM1 does not methylate the glycine and arginine-rich (GAR) motifs. Indeed, the alignment of methylation motifs of known CARM1 substrates does not create a consensus sequence that could be used for *in silico* prediction of additional candidate substrates, although the motif does seem to be proline-rich (Figure 35). Thus, to facilitate the identification of CARM1 substrates, a peptide cocktail of six different CARM1-methylated motifs (Figure 15A) was used to immunize rabbits to obtain CARM1 substrate antibodies, henceforth referred to as ADMA^{CARM1} antibodies. The four polyclonal antibodies were affinity purified over a column containing the six peptides.

To characterize ADMA^{CARM1} antibodies, we performed Western analysis on the whole cell lysates from wild-type (WT) and CARM1 knockout (KO) mouse embryonic fibroblasts (MEFs) (Figure 15B). ADMA-1^{CARM1} and ADMA-2^{CARM1} recognized a slew of bands in the WT lane, but displayed minimal immunoreactivity in the KO lane. ADMA-3^{CARM1} showed the loss of one band, but also a slightly increased signal in the KO lane relative to the WT lane, suggesting that it might recognize proteins methylated by CARM1 and other Type I PRMTs, compensating the loss of CARM1 in KO cells. ADMA-4^{CARM1} seemed to be less immunoreactive than the other three antibodies, recognizing only a single CARM1 substrate. As anticipated, the H3R17me2a antibody cross-reacted with a number of proteins in WT cells, which are absent in CARM1 KO cells. Interestingly, some proteins were recognized in WT and KO cells at similar levels (indicated by asterisks). Next, we tested the antibodies on

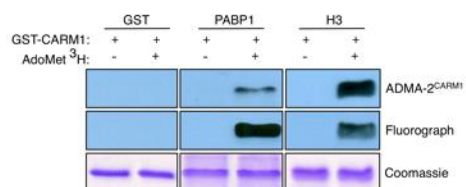
A

CARM1 substrates	Methylation motifs
PABP1	CHPGA1 (Rme2a) PAAPR
PABP1	CRPAAP (Rme2a) PPFST
TARPP	CTSQQY (Rme2a) PLASV
H3R17	CGGKAP (Rme2a) KQLAT
CAS3	CAVYPV (Rme2a) SAYPQ
CBP	CAPMGP (Rme2a) AASPM

B



D



C

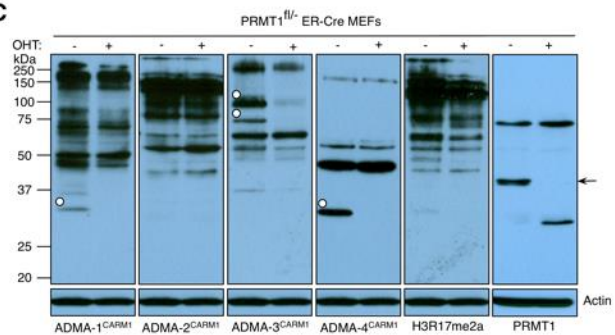


Figure 15: Characterization of CARM1 substrate antibodies.

(A) The list of peptides used to generate CARM1 Substrate antibodies. **(B)** Whole cell extracts from CARM1 wild-type (+/+) and knockout (-/-) MEFs were subjected to western analysis with α ADMA^{CARM1}, α H3R17me2a and α CARM1 antibodies. The asterisks on the gels indicate the positions of the proteins present in both cell lines. Actin blot serves as a loading control. **(C)** *Prmt1*^{fl/-} ER-Cre MEFs were untreated or treated with 4-hydroxytamoxifen (OHT, 2 μ M) for 8 days. Whole cell extracts were immunoblotted with α ADMA^{CARM1}, α H3R17me2a and α PRMT1 antibodies. The solid circles on the gels indicate the positions of the proteins specific to PRMT1 wild-type (OHT -) MEFs. The arrow points to the position of the PRMT1 protein. Actin blot serves as a loading control. **(D)** GST, PABP1 and H3 were methylated *in vitro* by recombinant CARM1 in the absence or presence of tritium-labeled AdoMet and subjected to western analysis with α ADMA-2^{CARM1} antibody (top panel), fluorography (middle panel) and Coomassie Brilliant Blue staining (bottom panel). GST serves as a negative control. *CARM1 substrate antibodies used in figures 15B-D were generated by Cell Signaling Technology.*

WT and PRMT1-deficient MEFs. Most proteins were recognized at similar levels in both cell lines. However, some protein bands were specific to WT cells, not PRMT1-deficient cells (indicated by solid circles) (Figure 15C). It is noteworthy that these PRMT1-specific proteins migrated at the same positions as the non-specific proteins observed in CARM1 MEFs (asterisks in Figure 15B). This suggests that while the ADMA^{CARM1} antibodies primarily recognize CARM1 substrates, they can also recognize a few PRMT1 substrates. We next tested the ability of some of the ADMA^{CARM1} antibodies to recognize *in vitro* methylated CARM1 substrates. PABP1 and H3 were *in vitro* methylated by CARM1 in the absence or presence of tritium-labeled AdoMet. Methylation efficiency was monitored by fluorography (Figure 15D, middle panel), and duplicate blots were subjected to western blotting using the ADMA^{CARM1} antibodies. We found that the ADMA-2^{CARM1} antibody recognized PABP1 and H3 in a methyl-specific fashion (Figure 15D, top panel).

The antibodies were also tested on peptide arrays that harbor a collection of histone tail modifications, including those deposited by CARM1, PRMT1, PRMT5 and PRMT6. This peptide microarray currently harbors over 300 modified histone tail peptides. The methylated arginine motifs include the H3R2, H3R8, H3R17, H3R26 and H4R3 sites. Peptides representing the mono- and di-methylated forms of these motifs are present on the array. The dimethyl-H3R17 antibody (Millipore) only recognizes H3R17me2a peptide on the array. ADMA-2^{CARM1} behaves very similarly to dimethyl-H3R17 antibody, in terms of site-specific recognition as well as overall signal intensity. ADMA-3^{CARM1} also recognizes H3R17me2a, but weakly (Figure 16). Although ADMA-1^{CARM1} and ADMA-4^{CARM1} did not recognize arginine methylated histone marks, they seemed to be effective in recognizing non-histone substrates (refer to Figure 17). All antibodies show low levels of non-specific recognition, as observed with H4 unmodified and H3K4me2/T6p peptides (highlighted in red and green, respectively). These results independently confirm the establishment of a panel of four.

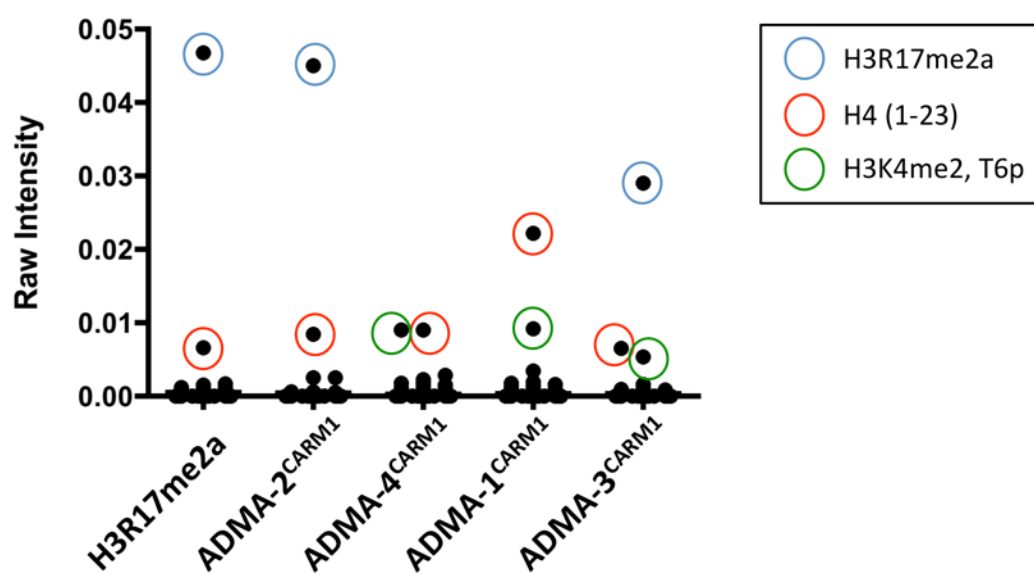


Figure 16: Histone peptide array analysis of CARM1 substrate antibodies.

The five CARM1 substrate antibodies were tested on peptide arrays that harbor a collection of over 300 histone tail modifications, including H3R2, H3R8, H3R17, H3R26 and H4R3 (Un-, mono- and di-methylated forms) sites. X-axis shows the names of antibodies tested. Y-axis represents raw binding intensity of the histone peptides with each antibody.

Experiment for figure 16 was performed by Dr. Scott Rothbart, a previous post-doc from Dr. Brian Strahl's lab, UNC, Chapel Hill.

different rabbit polyclonal antibodies that recognize arginine methylated proteins that are specific to CARM1

4.2 Using ADMA^{CARM1} antibodies to identify CARM1 substrates

A combined immunoprecipitation (IP) and mass spectrometric (MS) approach was employed to identify CARM1 substrates, using an approach developed for the identification of tyrosine phosphorylation sites (Rush et al, 2005). Briefly, proteins were extracted from WT MEFs and digested with trypsin. The resulting complex peptide mixture was partitioned into three fractions by reversed-phase solid-phase extraction, and each fraction was treated with one of the four ADMA^{CARM1} antibodies, immobilized on agarose beads. After washing, peptides were eluted and analyzed by nanoflow LC-MS/MS. The resulting spectra were assigned to peptide sequences using the program Sequest. Lists of credible methylpeptide sequence assignments were generated. Using this approach, 112 different proteins were identified as putative CARM1 substrates. All the identified methylation sites have been submitted to the PhosphoSitePlus database (www.phosphosite.org). *(We sent the WT MEF extracts to Dr. John Rush at Cell Signaling Technology, who performed the Immunoprecipitation-Mass Spectrometry experiments on those extracts using CARM1 substrate antibodies.)* We selected ten proteins for further evaluation based on the number of identified methylated peptides in the MS data, and the potential involvement of the candidate CARM1 substrates in different aspects of chromatin regulation, transcription and RNA processing (Figure 17A). Out of the ten identified substrates, PABP1 (Lee & Bedford, 2002), CA150/TCERG1 (Cheng et al, 2007) and SRC-3 (Feng et al, 2006) were described previously as *in vivo* CARM1 substrates, thus validating the approach. SF3B4 (Cheng et al, 2007), SRC-1 (Feng et al, 2006) and SRC-2 (Feng et al, 2006) were shown to be methylated by CARM1 *in vitro*. GPS2, KMT2D, SLM2 and MED12 were identified as

A

CARM1 Substrate	Function
KMT2D* (Histone-Lysine N-methyltransferase 2D)	H3K4 mono- and trimethylation
GPS2* (G Protein Pathway Suppressor 2)	Component of SMRT corepressor complexes
SLM2* (Sam68-Like Mammalian 2)	RNA binding protein
MED12* (Mediator complex subunit 12)	Component of the Mediator coregulator complex
SRC-1 (Steroid Receptor Coactivator-1)	Transcriptional coactivator for nuclear hormone receptors
SRC-2 (Steroid Receptor Coactivator-2)	Transcriptional coactivator for nuclear hormone receptors
SRC-3 (Steroid Receptor Coactivator-3)	Transcriptional coactivator for nuclear hormone receptors
PABP1 (Poly(A)-Binding Protein 1)	Translation initiation factor
TCERG1/CA150 (Transcription Elongation Regulator 1)	Transcription elongation
SF3B4 (Splicing Factor 3B, Subunit 4)	Pre-mRNA splicing

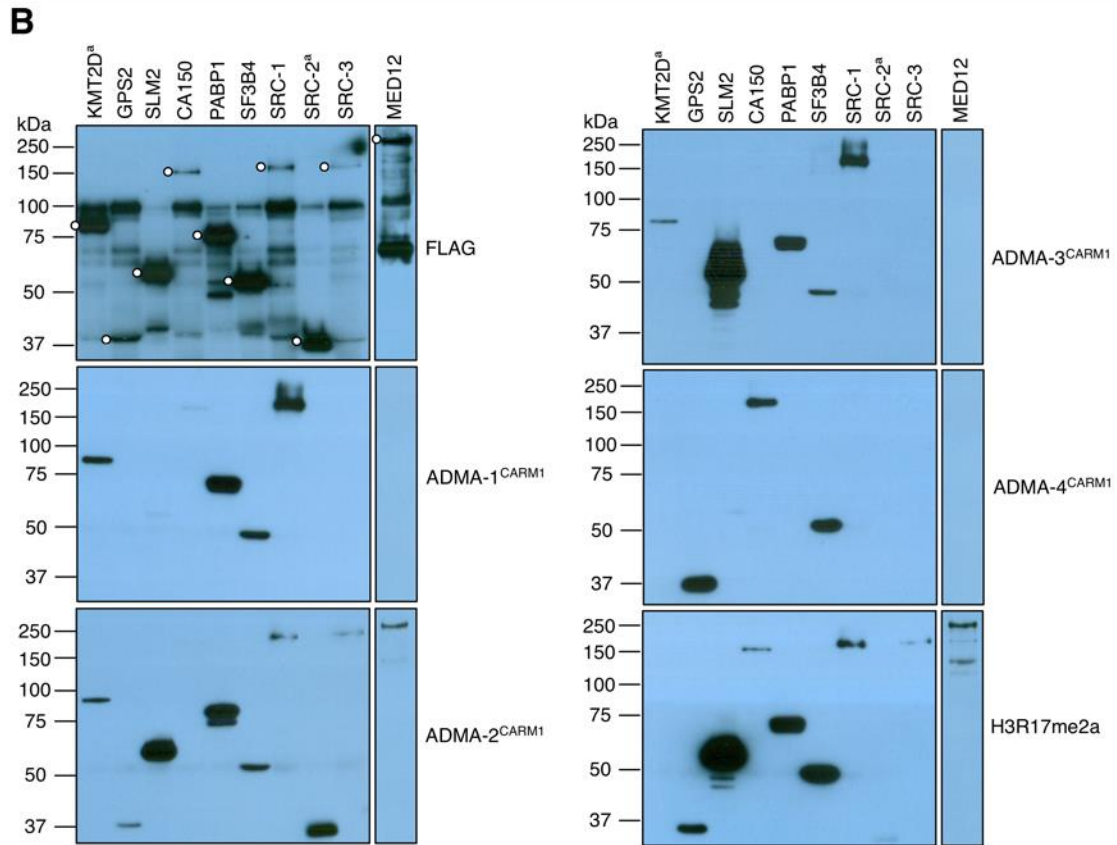


Figure 17: Identification of novel CARM1 substrates.

(A) A table showing the list of CARM1 substrates, identified from the □ADMA^{CARM1} IP-MS screen, and their functions. The proteins, denoted by an asterisk, were identified as CARM1 substrates for the first time in this study.

(B) The positive hits obtained from the screen were transiently transfected into HEK293T cells and immunoprecipitated with αFLAG antibody. Western analysis was performed, first with αFLAG to gauge the expression of the FLAG-tagged proteins (indicated by solid circles), and then with the αADMA^{CARM1} antibodies. KMT2D^a (3619-4285 aa) and SRC-2^a (1037-1295 aa) represent fragments of the full-length KMT2D and SRC-2 proteins.

potential CARM1 substrates for the first time in this study. GPS2 (G-protein Pathway Suppressor 2) is an integral component of the NCoR/SMRT/HDAC3 complex (Wong et al, 2014b). The mixed-lineage leukemia 4 methyltransferase (KMT2D) is responsible for depositing histone H3K4me1/2 marks at enhancers (Ford & Dingwall, 2015; Lee et al, 2013). SLM2 is a KH domain containing protein that has been implicated in the regulation of alternative splicing (Traunmuller et al, 2014). To confirm that the identified proteins were indeed recognized by the methyl-specific antibodies that we developed and used in the screen, we FLAG-tagged the ten selected proteins, overexpressed them in HEK293T cells, and then immunoprecipitated them using an anti-FLAG antibody. Western analysis was performed on the immunoprecipitates, first with an anti-FLAG antibody to confirm the expression of FLAG-tagged proteins, and then with the ADMA^{CARM1} antibodies (Figure 17B). Importantly, all ten proteins were recognized by at least one of the four different ADMA^{CARM1} antibodies, and no single antibody recognized all the tagged proteins. These results demonstrate that none of the four ADMA^{CARM1} antibodies are totally pan CARM1 substrate antibodies, but they clearly recognize different subsets of CARM1 substrates.

In Figure 15B, we demonstrated that the ADMA^{CARM1} antibodies primarily recognize CARM1 substrates, but they are also able to engage a few PRMT1 substrates (Figure 15C). To be sure that the new methylated proteins that we identified are indeed CARM1 and not PRMT1 substrates, we performed further analysis in CARM1 knockout and knock-down cell lines that we had previously established (Yadav et al, 2003; Yang et al, 2010). We immunoprecipitated endogenous MED12 from CARM1 WT and KO MEFs, and then performed Western blot analysis using ADMA^{CARM1} and H3R17me2a antibodies (Figure 18C). Both cell lines had the same amount of MED12, but only MED12 isolated from CARM1 expressing cells was immunoreactive with the two methyl-specific antibodies. This indicates that arginine methylation of MED12 is CARM1-dependent. Additionally, we tested the antibodies on purified Mediator complex (Figure 18B), and found that they recognize two

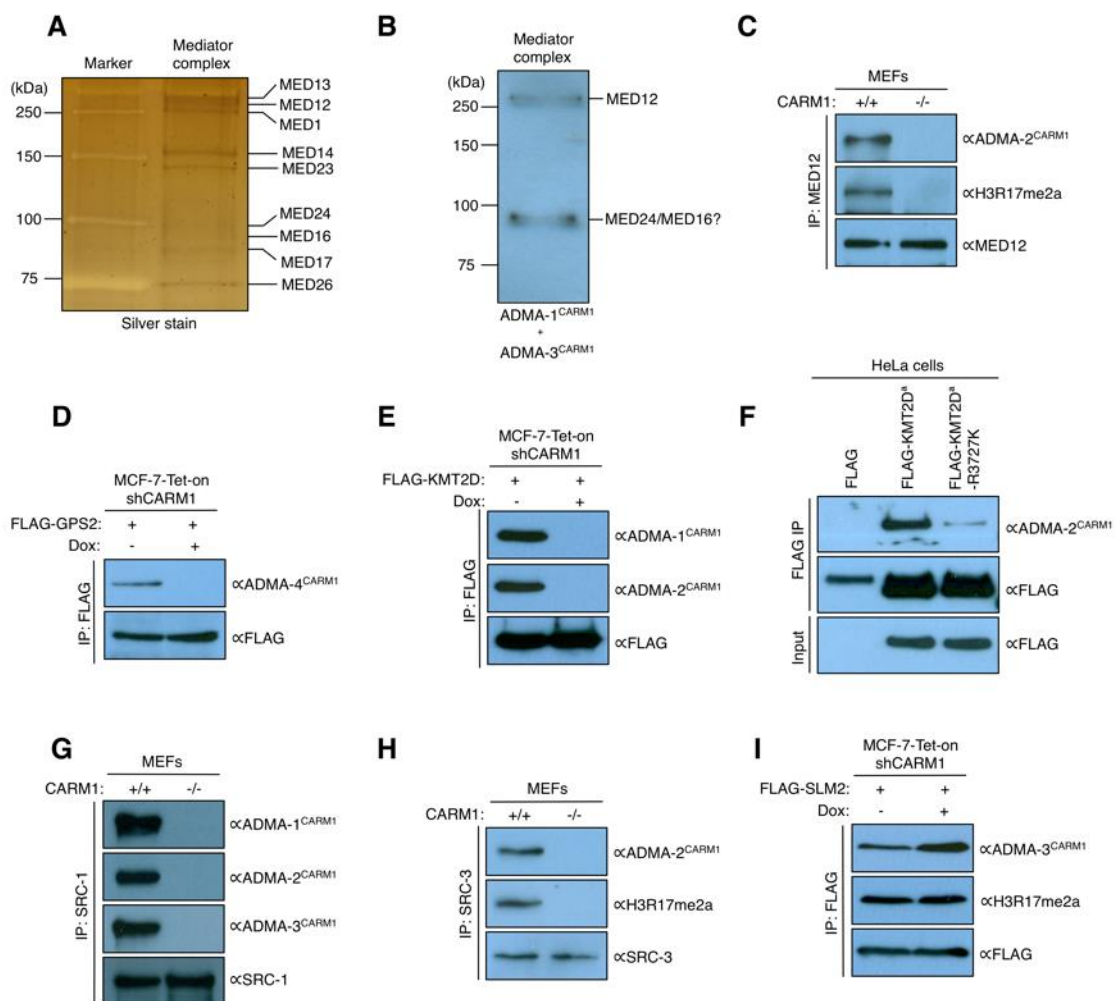


Figure 18: Validation of CARM1 substrates.

(A) Silver stained SDS-PAGE gel analysis of the purified Mediator complex (1 μ g). **(B)** Western analysis of the purified Mediator complex (1 μ g) using α ADMA-1^{CARM1}+ α ADMA-3^{CARM1} antibodies. **(C, G, H)** Whole cell lysates from CARM1 wild-type (+/+) and knockout (-/-) MEFs were immunoprecipitated with antibodies against MED12, SRC-1 or SRC-3 proteins, and the eluted samples were subjected to western blotting with α ADMA^{CARM1} and α H3R17me2a antibodies. α MED12, α SRC-1, and α SRC-3 blots (bottom panels) demonstrate equal expression of these proteins in CARM1 wild-type (+/+) and knockout (-/-) MEFs. **(D, E and I)** MCF-7-Tet-on-shCARM1 cells were untreated or treated with doxycycline (1 μ g/ml) for 8 days and transiently transfected with FLAG-KMT2D, -GPS2 and -SLM2, separately. Total cell lysates were immunoprecipitated with α FLAG antibody and the eluted samples were subjected to western blotting with α ADMA^{CARM1} and α FLAG antibodies. **(F)** HeLa cells were transiently transfected with FLAG control, FLAG-KMT2D^a or FLAG-KMT2D^a-R3727K. Total cell lysates were immunoprecipitated with α FLAG antibody and the eluted samples were subjected to western analysis with α ADMA^{CARM1} and α FLAG antibodies. α FLAG blot of the input samples (bottom panel) shows equal expression of the wild-type and mutant KMT2D^a proteins. KMT2D^a represents a fragment (3619-4285 aa) of the full-length KMT2D protein (NP_003473).

Purified Mediator complex used in figures 18A and 18B was kindly provided by Dr. Cheng-Ming Chiang, UT Southwestern.

proteins – one that migrates at the same position as MED12 and another at around 90kDa (which could be MED24 or MED16, presumed based on the silver stained complex (Figure 18A)). This suggests that MED12 may not be the sole target for CARM1 in the Mediator complex. GPS2, KMT2D and SLM2 were not tested in this assay because we were unable to find specific antibodies that were able to immunoprecipitate the respective endogenous proteins. We thus overexpressed FLAG-GPS2 in control and CARM1-knockdown cells, and then performed Western blotting of the FLAG immunoprecipitates using ADMA^{CARM1} antibodies to show that GPS2 is specifically recognized in control cells, but not in CARM1-knockdown cells (Figure 18D). In the case of KMT2D, owing to its large size (5537 aa), we cloned a fragment (3619-4285 aa) of the full-length KMT2D protein, which harbors the mass spectrometry identified methylation site (R3727). We also engineered a R3727K mutation at this site in the FLAG-KMT2D^a construct (QuikChange II XL Site-Directed Mutagenesis Kit, Agilent Technologies), and found that the ADMA^{CARM1} signal is significantly reduced in the R3727K-MLL2^a mutant, relative to the wildtype-MLL2^a protein, indicating that R3727 is a major site for CARM1 methylation (Figures 18E and 18F). Finally, we also confirmed that steroid receptor coactivators SRC-1 (Figure 18G) and SRC-3 (Figure 18H) are recognized in a CARM-dependent fashion by the ADMA^{CARM1} antibodies. Interestingly, when SLM2 was tested in CARM1 knockdown cell lines, we did not observe a loss of methylation (Figure 18I), although this protein is recognized by a number of CARM1 substrate antibodies. Instead, we observed an increased signal with ADMA-3^{CARM1}, which indicates overcompensation by another type I enzyme. Hence, SLM2 may be targeted by more than one PRMT.

4.3 Mediator subunit 12 is methylated at Arginine 1899 by CARM1 *in vivo*

The mass spectrometry studies identified MED12-R1899 as a major site of CARM1 methylation. To characterize the methylation site in more detail, we raised two independent

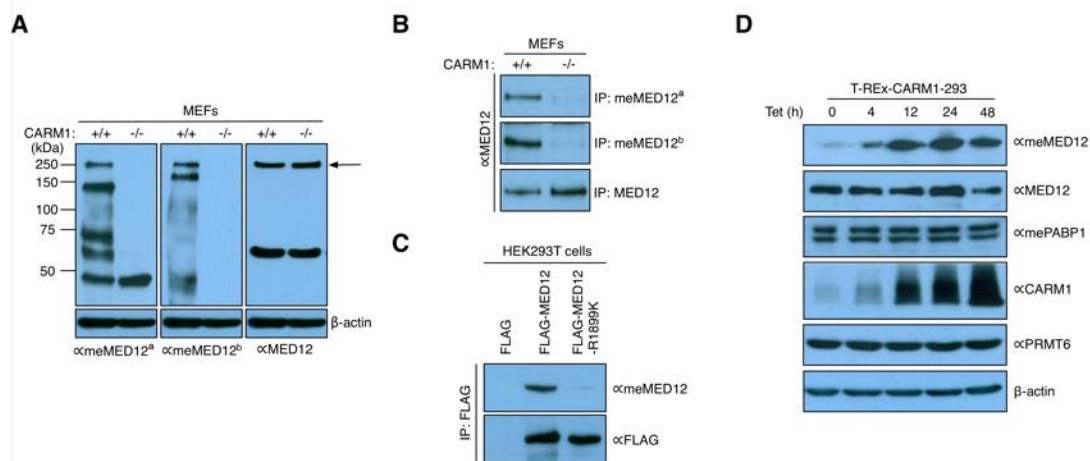


Figure 19: Characterization of the meMED12 antibodies.

(A) Whole cell extracts from CARM1 wild-type (+/+) and knockout (-/-) MEFs were subjected to western analysis with α meMED12^a, α meMED12^b and α MED12 antibodies. The arrow points to the position of the MED12 protein. Actin blot serves as a loading control. **(B)** CARM1 wild-type (+/+) and knockout (-/-) MEFs were immunoprecipitated with α meMED12^a, α meMED12^b and α MED12 antibodies and the eluted samples were subjected to western blotting with α MED12 antibody. **(C)** HEK293T cells were transiently transfected with FLAG, FLAG-MED12 or FLAG-MED12-R1899K (NP_005111). Total cell lysates were immunoprecipitated with α FLAG antibody and the eluted samples were subjected to western analysis with α meMED12^a and α FLAG antibodies. **(D)** T-REx-CARM1-293 cells were treated with tetracycline and harvested after 0, 4, 12, 24, and 48h. Whole cell extracts were immunoblotted with the indicated antibodies. β -actin blot serves as a loading control.

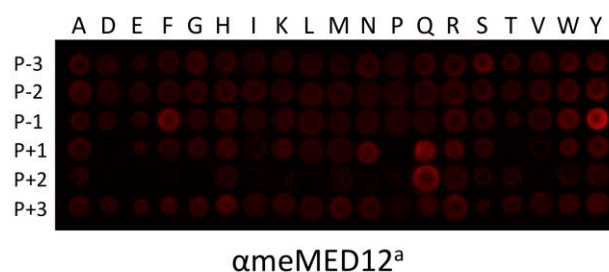
Methyl-MED12 antibodies used in figures 19A-D were generated by Cell Signaling Technology.

antibodies against a MED12-R1899me2a peptide. Western blot analysis of CARM1 WT and KO MEF extracts showed that both antibodies detect a 240kDa protein (the size of MED12) and a few other potential substrates, in a CARM1-dependent manner (Figure 19A). MeMED12^b was more selective and only recognized one additional band of about 200kDa. To confirm that the 240kDa protein is MED12, we immunoprecipitated methylated MED12 from WT and CARM1 KO MEF lysates with the meMED12 antibodies and blotted with the MED12 (Bethyl) antibody. We found that both meMED12 antibodies selectively enriched MED12 protein from WT cells (Figure 19B). To confirm that the meMED12^a antibodies are site-specific, we made a R1899K point mutation (QuikChange II XL Site-Directed Mutagenesis Kit, Agilent Technologies) in the full-length FLAG-MED12 construct, immunoprecipitated the wild-type and mutant forms from transiently expressing HEK293T cells and blotted with meMED12^a antibody. The antibody detected the wild-type form of FLAG-MED12 strongly, but not the mutant form (Figure 19C). All these data clearly show that MED12 is methylated by CARM1 at R1899.

To further characterize the binding specificity of meMED12 antibodies, we tested them on the Oriented Peptide Array Library (OPAL). In this oriented KGXXXXRme2aXXXXGK-biotin peptide library, X denotes degenerate position and central-R is asymmetrically dimethylated (Figure 20A). For example, the position P-4 is fixed (Z) in the KGZXXXRXXXXGK-biotin library, 19 different libraries will be synthesized, and each library will have one of the 19 amino acids (excluding cysteine) fixed at position Z. For the next row, the Z position moves to P-3 (three residues up from the fixed arginine), and again 19 different libraries are synthesized. A total of 152 (19 amino acids x 8 positions) library pools were synthesized and printed onto a streptavidin-coated glass slide. When meMED12 antibody is incubated with this OPAL, we observed strong binding at P+1 and P+2 positions, where Glutamine (Q) was selected (Figure 20B). Tyrosine (Y) was preferred strongly at P-1 position, and Phenylalanine (F) weakly. Weaker binding was also observed at P-3 position,

⁻⁴ ⁻³ ⁻² ⁻¹ ⁺¹ ⁺² ⁺³ ⁺⁴
 K G X X X X R_(me2a) X X X X G K - biotin
 ↑
 fixed

MED12 methylation motif → S V Y R_(me2a) Q Q Q
OPAL-derived motif → S X Y/F R_(me2a) Q Q X



HUMAN	EPSSYKTSVYRQQQPAVPQGG
MOUSE	EPSSYKTSVYRQQQTPVPQGG
RAT	EPSSYKTSVYRQQQTPVPQGG
CHIMPANZEE	EPSSYKTSVYRQQQPAVPQGG
RHESUS MACAQUE	EPSSYKTSVYRQQQPAVPQGG
COW	EPASYKTSVYRQQQPAVPQGG
DOG	EP-SYKTSVYRQQQTPVPQGG
CHICKEN	DP-SYKPAVYR-QQPPVSQGG

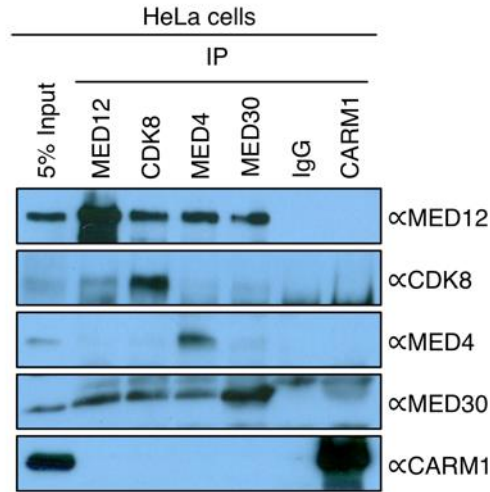
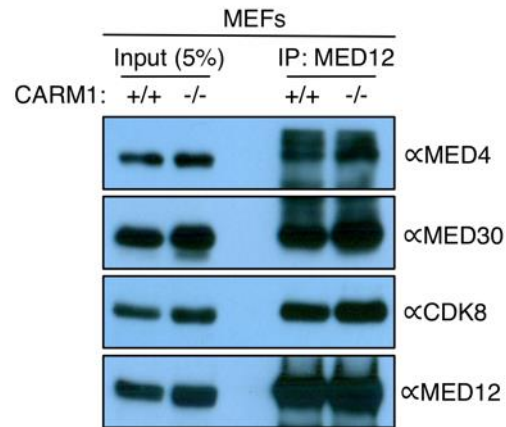
(A) Degenerate peptide sequence used to synthesize OPAL peptide array library. **(B)** The OPAL library, containing 152 peptide (KGXXXXRme2aXXXXGK) pools, is incubated with α meMED12^(a&b) antibodies and detected using a fluorescently labeled secondary antibody. X represents random amino acids (except cysteine). **(C)** Alignment showing high conservation of MED12 methylation motif (SVYRQQQ) among vertebrates.

71

where Serine (S) was selected. The motif preferred by the meMED12 antibody (S-X-Y/F-Rme2a-Q-Q-X) is highly comparable with the MED12 methylation motif (S-V-Y-Rme2a-Q-Q-Q), hence confirming the antibody's binding specificity. We also aligned the Human MED12 methylation motif with the MED12 sequences of various vertebrates and found that R1899 is highly conserved among these species (highlighted in black) (Figure 20C). R1899 flanking amino acids recognized by the meMED12 antibody (highlighted in grey) were also conserved.

CARM1 occasionally interacts with its substrates (Feng et al, 2006; Kowenz-Leutz et al, 2010; Wang et al, 2014a). To determine if CARM1 interacts with the Mediator complex, we performed reciprocal co-immunoprecipitation experiments between CARM1 and Mediator subunits (MED12, MED4, MED30, and CDK8) from HeLa cells. We found that CARM1 does not interact with the Mediator complex (Figure 21A). Thus, CARM1 and MED12 are likely transiently engaged. We also tested if MED12 methylation has a role in Mediator complex assembly. Co-immunoprecipitations were performed between MED12 and other Mediator subunits in WT and CARM1 KO MEFs. We found that the MED12 antibody co-immunoprecipitated Mediator subunits (MED4, MED30, and CDK8) from WT and KO cells at similar levels. This suggests that MED12 is incorporated into the Mediator complex, irrespective of its methylation status (Figure 21B).

Since MED12 belongs to the CDK8 module, we wanted to determine if R1899 methylation of MED12 affects the kinase activity of CDK8. So, we immunoprecipitated the CDK8 subcomplex using CDK8 or MED12 antibodies from wild-type versus CARM1 knockout cells and used as an enzyme source to perform *in vitro* phosphorylation of recombinant histone H3. Immunoprecipitates (MED12 or CDK8) from both wild-type and CARM1 knockout cells phosphorylated the histone H3 (at S10) at similar levels, as observed by the pH3S10 immunoblot (Figure 22). This suggests that MED12 methylation has no effect on CDK8 kinase activity towards H3.

A**B****Figure 21: CARM1 - Mediator interactions**

(A) HeLa whole cell lysates were subjected to immunoprecipitation using IgG or antibodies specific for MED12, CDK8, MED4, MED30 and CARM1. Western blotting was performed on the immunoprecipitates using antibodies against CARM1 or the indicated Mediator subunits.

(B) Whole cell extracts from CARM1 wild-type (+/+) and knockout (-/-) MEFs were immunoprecipitated with α MED12 antibody and subjected to western analysis using antibodies specific for the indicated mediator subunits.

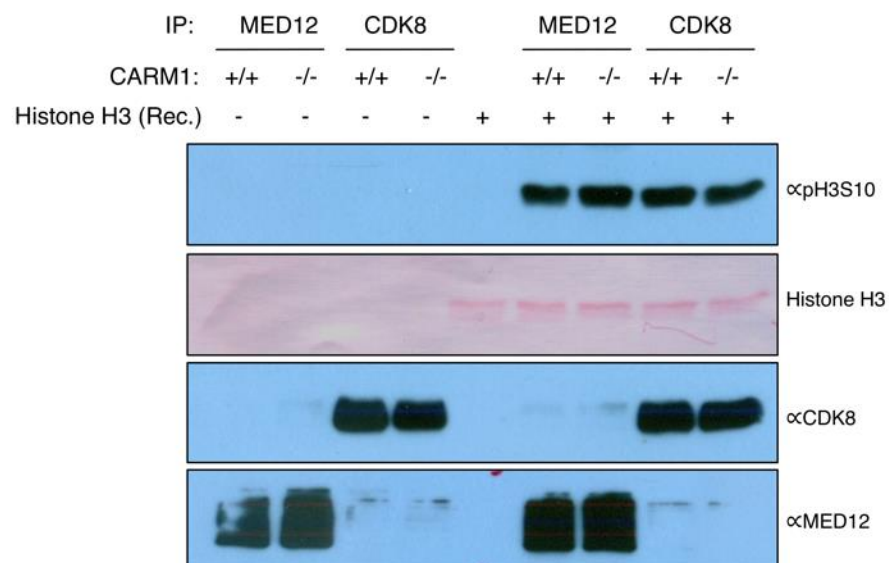


Figure 22: MED12 methylation does not affect CDK8 kinase activity.

Recombinant H3 protein is *in vitro* phosphorylated using MED12 or CDK8 immunoprecipitates from wild-type (+/+) or CARM1 knockout (-/-) MEFs in the presence of the phosphate donor, adenosine-5'-triphosphate, and immunoblotted with α pH3S10, α CDK8 and α MED12 antibodies. Ponceau stained blot shows equal loading of H3 protein.

Arginine methylated proteins, PABP1 and SAP145, are thought to be fully methylated in cells (Yang et al, 2015; Zeng et al, 2013), suggesting that these are not regulatable signaling nodes. To test if MED12 is fully methylated in cells, we employed the tetracycline-inducible CARM1-Flp-In HEK293 cell system (Cheng et al, 2007). Upon the induction of CARM1 expression, we observed an increase in MED12 methylation levels, as detected by the meMED12^a antibody (Figure 19D). On the other hand, methylated PABP1 levels did not change with CARM1 induction, as expected. Therefore, MED12 is not fully methylated in cells, and the dynamic changes in methylation levels upon CARM1 expression point toward a regulatory role for this R1899 methylation. Thus, transient association of CARM1 with MED12 at enhancer elements may induce local methylation of the R1899 site to facilitate the docking of an effector molecule.

4.4 Methylated MED12 interacts with the effector molecule TDRD3

Effector molecules for both ADMA and SDMA motifs are Tudor-domain containing proteins (Cote & Richard, 2005; Gayatri & Bedford, 2014). For example, the Tudor domain of SMN binds spliceosomal proteins like SmB (Brahms et al, 2001; Friesen et al, 2001) and SAP145 (Yang et al, 2015), and TDRD3 was shown to bind the CARM1 histone code mark, H3R17me2a (Yang et al, 2010). To determine if MED12 interacts with any of the known methylarginine “reading” Tudor domain-containing proteins, we synthesized biotin-tagged, unmodified and methylated, MED12 peptides and validated them by an *in vitro* methylation assay. As expected, recombinant CARM1 methylated the unmodified MED12 peptide *in vitro* but not the methylated peptide, which has no methyl-acceptor position (Figure 23A). This experiment also independently confirms that the MED12 R1899 site is a good CARM1 methylation motif. These peptides were then used to pull-down GST-fused Tudor domains

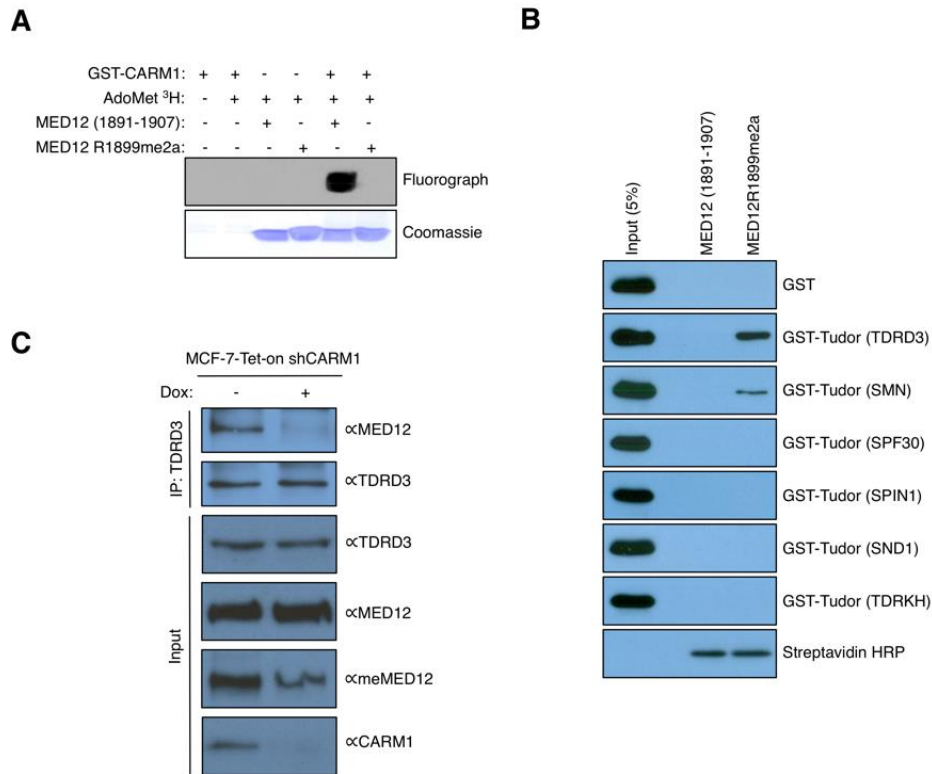


Figure 23: MED12 - TDRD3 interactions

(A) Fluorograph (top panel) and Coomassie Brilliant Blue staining (bottom panel) of the peptides *in vitro* methylated by recombinant CARM1 in the presence of tritium-labeled AdoMet. **(B)** The peptides were used to pull down tudor domains of the indicated proteins. The input samples and the eluted samples were immunoblotted with α GST antibody. Streptavidin HRP blot serves as a peptide loading control. **(C)** MCF-7-Tet-on-shCARM1 cells were untreated or treated with doxycycline (1 μ g/ml) for 8 days. Nuclear extracts were subjected to immunoprecipitation with α TDRD3 antibody and the eluted samples were detected by western blotting with α MED12 and α TDRD3. The input samples were immunoblotted with α TDRD3, α MED12, α meMED12^a and α CARM1.

Figure 23C – Experiment performed and figure organized by Dr. Yanzhong Yang, a previous post-doc from Bedford lab, UT M.D. Anderson Cancer Center.

of TDRD3, SMN, SPF30, TDRKH, SPIN1 and SND1, the six best-characterized methylarginine “reading” Tudor domain-containing proteins (Gayatri & Bedford, 2014). Pull-down experiments demonstrated that the Tudor domains of TDRD3 bound strongly to the methylated form of the MED12 peptide, and SMN bound weakly (Figure 23B). Next, we endeavored to confirm that MED12 interacts with TDRD3 in cells, and that this interaction is CARM1-dependent. To do this, we used CARM1-inducible knockdown cells, and immunoprecipitated TDRD3 from CARM1 WT and KD cells. TDRD3 co-immunoprecipitated MED12 from WT but not KD cells (Figure 23C). Input controls show that CARM1 was efficiently knocked-down and that MED12 methylation levels were decreased. These data establish that TDRD3 interacts with MED12 in a CARM1-dependent manner.

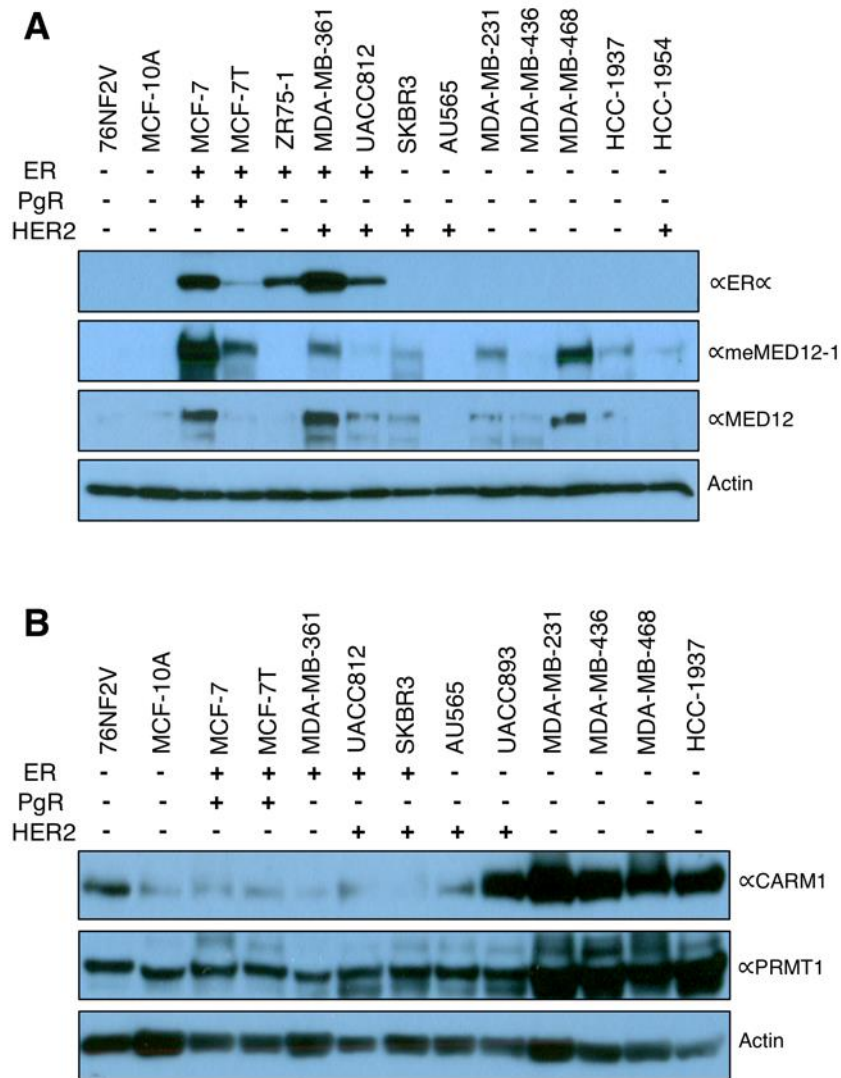


Figure 24: MED12 methylation status in breast cancer subtypes.

Western analysis was performed on a panel of 14 breast cancer cell lines using **(A)** αERα, αmeMED12-1 (also called meMED12^a), αMED12, **(B)** αCARM1 and αPRMT1 antibodies. β-actin blots serve as loading controls.

4.5 Genome-wide analysis of CARM1, MED12 and H3R17me2a in MCF-7 cells

To perform methyl-MED12 ChIP-seq studies, we wanted to choose a cell line with relatively high levels of MED12 methylation. Hence, we obtained whole cell extracts for a panel of 14 breast cancer subtypes (obtained from MD Anderson characterized cell line core facility) and tested for total- and methylated-MED12 levels. We found that MED12 is variably expressed across different cell lines, and it is highly methylated in the ER α positive MCF-7 cell line (Figure 24A). However, we did not observe any correlation between R1899 methylation levels and CARM1 expression levels or the hormone receptor status (Figure 24B).

In order to determine the chromatin distribution of methylated MED12 in MCF-7 cells, we developed two methyl-specific MED12 antibodies (meMED12^{a&b}). In addition to methylated MED12, the antibodies recognized at least one other CARM1 substrate (Figure 19A). Owing to their non-specific nature, ChIP-seq experiments for the methylated form of MED12 could not be attempted with these antibodies. Hence, to indirectly define methylated MED12 chromatin associated regions, we performed ChIP-seq analysis using MED12 (total), CARM1, and H3R17me2a antibodies. The H3R17me2a antibody (Millipore) recognizes a number of different CARM1 substrates, including MED12 (Figure 18C), SRC-3 (Figure 18H), CA150 (Cheng et al, 2007), and SmB (Cheng et al, 2007). The H3R17me2a antibody is not totally pan, because it does not recognize the methyl-motifs on KMT2D and SRC2 (Figure 17B). Therefore, ChIP-seq with this antibody provides a genomic readout for most CARM1 activity, not just for the histone mark alone. From the ChIP-seq data, we detected 992 MED12 binding sites, 743 CARM1 binding sites, and 726 peaks enriched for CARM1 activity in proliferating MCF-7 cells, grown in phenol red-containing media. We observed a 33% (410 out of total 1234 binding sites) overlap of the CARM1, MED12, and CARM1 activity profiles (Figure 25A). Analysis of the overlapping peaks identified a number of estrogen-regulated genes. We then compared our ChIP-seq data with the binding profiles

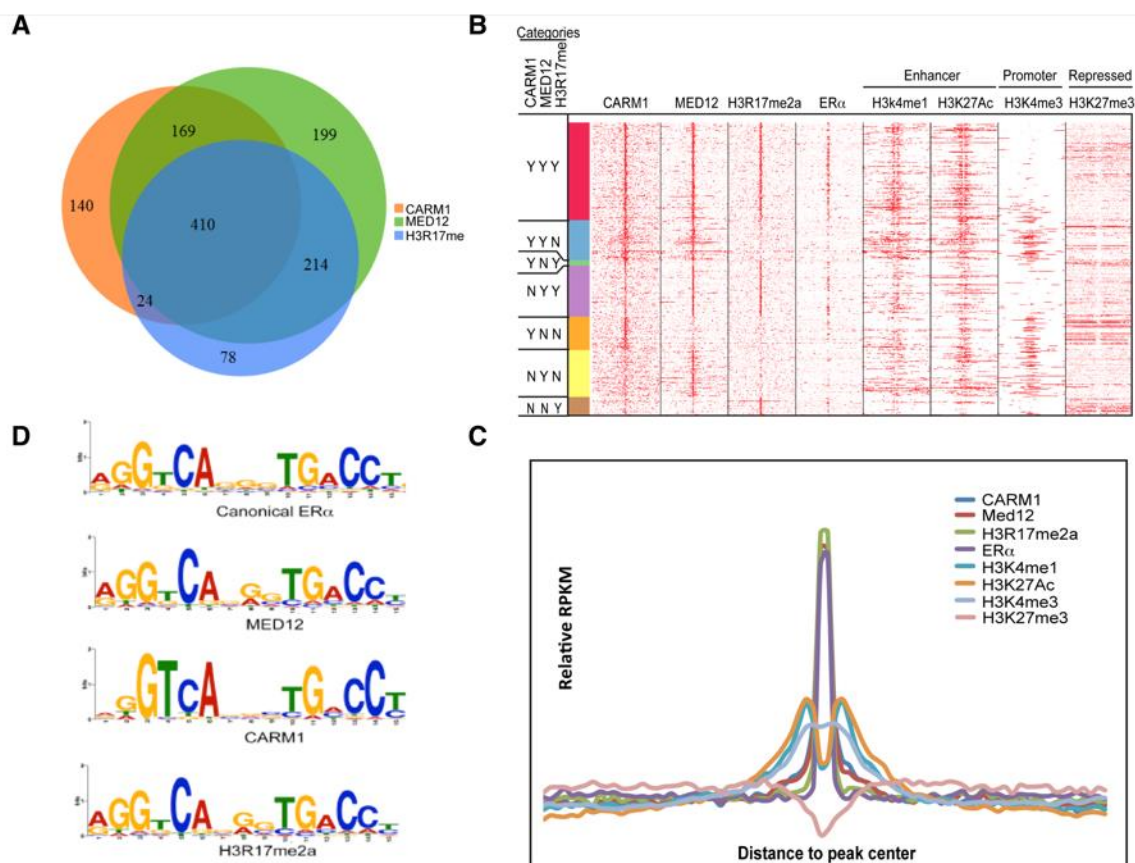
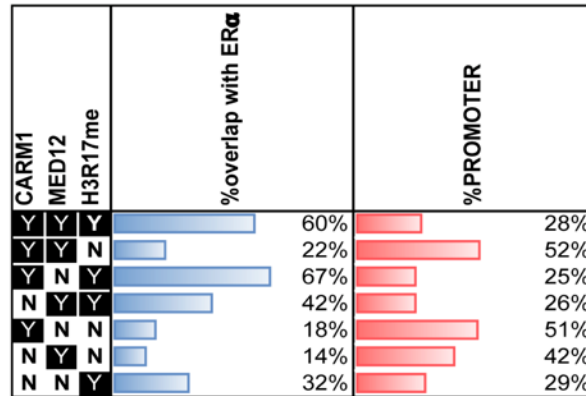


Figure 25: ChIP-seq analysis of CARM1, MED12, and H3R17me2a in MCF-7 cells.

(A) Venn diagram showing an overlap between CARM1-, MED12- and H3R17me2a-binding sites on the MCF-7 genome. **(B & C)** Heatmap and distribution figures depict profiles for genome-wide localization of CARM1, MED12, H3R17me2a, ER α , enhancer (H3K4me1 & H3K27ac), promoter (H3K4me3) and repressor (H3K27me3) marks. Categories: YYY – peaks co-occupied by CARM1, MED12 and H3R17me2a, YYN – peaks co-occupied by CARM1 and MED12, YNY – peaks co-occupied by CARM1 and H3R17me2a, NYY – peaks co-occupied by MED12 and H3R17me2a, YNN, NYN and NNY – peaks occupied by CARM1, MED12, and H3R17me2a, respectively. **(D)** Comparison of the binding motifs for MED12, CARM1, H3R17me2a, and ER α . Motif analysis was done using MEME suite.

Figure 25A-D – ChIP-seq experiments were performed by Dr. Donghang Cheng from The University of Texas MD Anderson Cancer Center. ChIP-seq data analysis was performed by Dr. Yue Lu from The University of Texas MD Anderson Cancer Center.

A



B

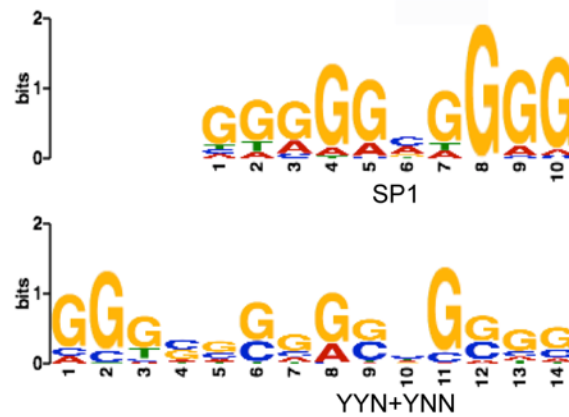


Figure 26: Overlap between ER peaks and promoter peaks

(A) Percentage of peaks overlapping ER α binding sites and percentage of peaks in promoter; ER α peaks were called by MACS at p -value $1e-10$. Promoter was defined as -5000bp to +500bp from transcription start site (TSS).

(B) Comparison between the binding motifs of SP1 and YYN+YNN peaks.

Figure 26 was generated by Dr. Yue Lu from The University of Texas MD Anderson Cancer Center.

of ER α and various histone modifications associated with enhancer (H3K4me1 and H3K27ac), promoter (H3K4me3) and repressed (H3K27me3) regions (Figure 25B). ChIP-seq peaks from all these experiments correlate highly with functional enhancers, moderately with active promoters, but show no overlap with the repressed regions. In addition, our ChIP-seq data also displayed good overlap between H3R17me2a, active enhancer marks and the enhancer-bound protein, MED12, which confirms the ChIP-on-chip studies performed by the Miles Brown group that reported CARM1 activity predominantly at enhancer regions in MCF-7 cells (Lupien et al, 2009). Importantly, 60% of the peaks co-occupied by CARM1, MED12 and H3R17me2a (Category YYY) overlap with ER α peaks, indicating that these Mediator-bound regions targeted by CARM1 are ER α -specific enhancers. The H3K27ac and H3K4me1 marks decorate the edges of active enhancers, creating a trough where the TFs and coregulators are enriched. It is in this trough that we see CARM1, MED12, CARM1 activity and ER α signals (Figure 25C). In addition, motif analysis of CARM1, MED12 and CARM1 activity peaks revealed a consensus sequence that is almost identical to the ER α -binding motif (Figure 25D). It is noteworthy that a subset of peaks, which are weak in ER α and H3R17me2a signal, associated with active promoters (i.e. Categories YYN and YNN overlap well with H3K4me3 signal) (Figure 25B & 26A). We speculate that these peaks may constitute a distinct class of CARM1-regulated genes that do not associate with ER α . Indeed, Motif analysis under this subset of H3K4me3 peaks identified a binding motif for SP1 (Figure 26B), suggesting that this basal transcription factor may also make use of CARM1's coactivator activity.

To highlight the degree of co-occupancy of CARM1, MED12, and CARM1 activity at EREs, we focused on the well-characterized ER α target, GREB1, which has four well-defined EREs (Carroll et al, 2006) (Figure 27A). Similar tight overlap of these three ChIP-seq profiles are also seen at the TFF1, IGFBP4, and FKBP4 loci (Figures 28A-C). The peak

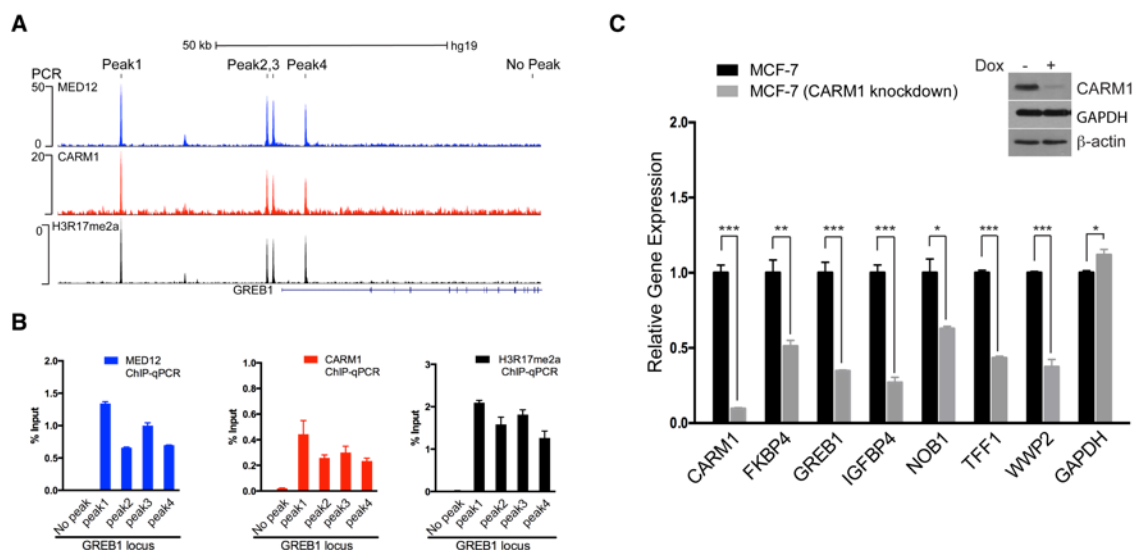


Figure 27: Regulation of ChIP-seq target genes by MED12 methylation.

(A) ChIP-seq peaks demonstrating the enrichment of MED12, CARM1, and H3R17me2a signals at the GREB1 gene locus. **(B)** ChIP-qPCR analysis of the association of MED12, CARM1, and H3R17me2a with GREB1 gene. **(C)** MCF-7-Tet-on-shCARM1 cells were untreated or treated with doxycycline (1 µg/ml) for 8 days. Total RNA was extracted and RT-PCR was performed using primers specific for the genes shown. GAPDH acts as a negative control. Target gene expression was normalized to Actin. Error bars represent standard deviation based on three independent experiments. * (p<0.05), ** (p<0.01) and *** (p<0.001).

Figure 27 – Experiments were performed by Dr. Donghang Cheng from The University of Texas MD Anderson Cancer Center.

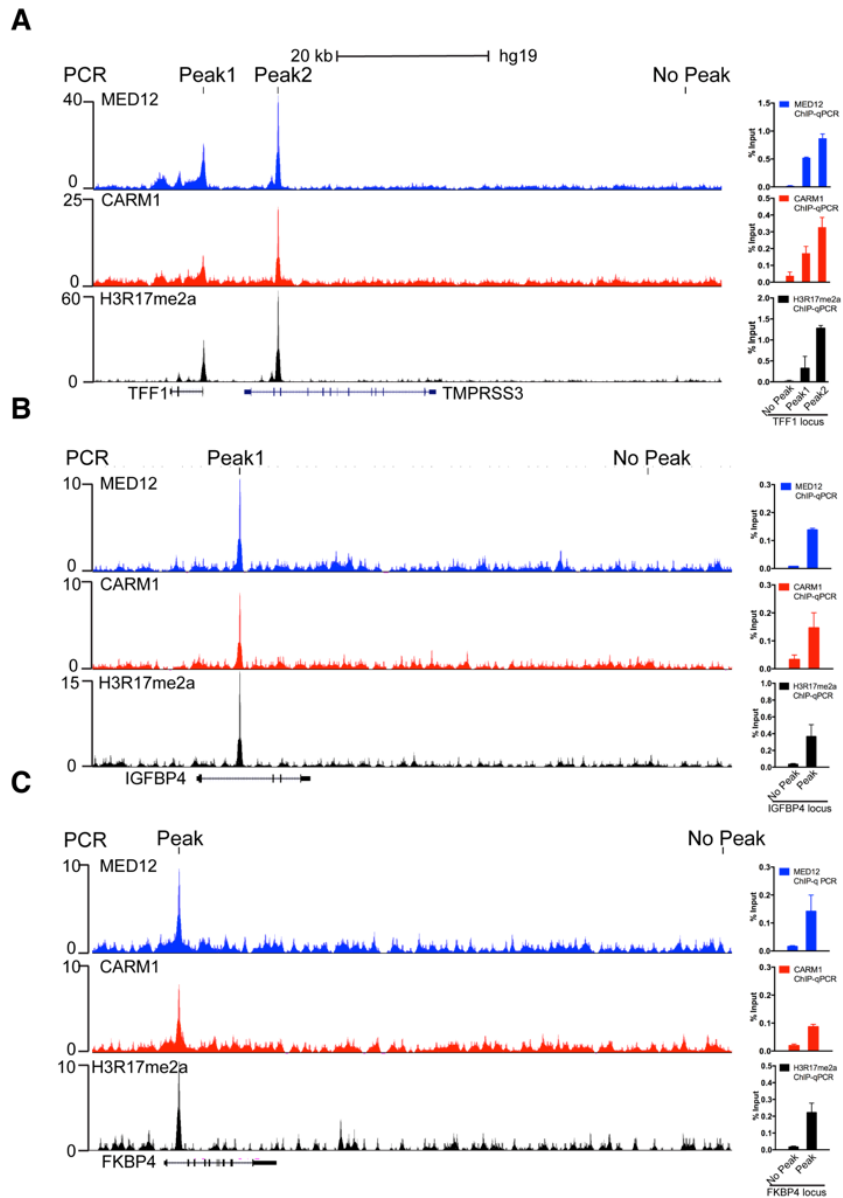


Figure 28: Confirmation of ChIP-seq peaks for the target genes.

ChIP-seq peaks and qPCR analysis demonstrating the enrichment of MED12, CARM1, and H3R17me2a signals at TFF1 **(A)**, IGFBP4 **(B)**, and FKBP4 **(C)** gene loci in MCF-7 cells.

Figure 27 – Experiments were performed by Dr. Donghang Cheng from The University of Texas MD Anderson Cancer Center.

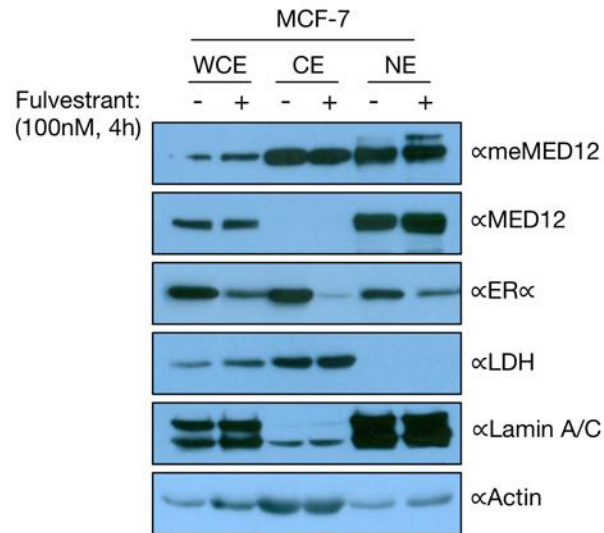


Figure 29: MED12 methylation levels do not correlate with ER levels.

MCF-7 cells were untreated or treated with Fulvestrant (100 nM) for 4 h. Whole cell, cytoplasmic and nuclear extracts were harvested and immunoblotted with α meMED12^a, α MED12, α ER α antibodies. LDH, Lamin A/C, and β -actin blots serve as loading controls.

correlation between CARM1, MED12 and H3R17me2a was confirmed by ChIP-qPCR (Figure 27B & 28). Next, six target genes that displayed strong overlap of all three ChIP-seq profiles (GREB1, TFF1, IGFBP4, FKBP4, NOB1 and WWP2), were tested for their dependency on CARM1 for optimal E2-induced expression. To do this, a Tet-inducible CARM1 shRNA-knockdown cell line was used. CARM1 knockdown significantly reduced the expression of all six tested genes (Figure 27C). Since MED12 occupancy and CARM1 activity is prominent at EREs, we speculated that MED12 methylation may be triggered through the ER α pathway. To address this question, we treated MCF-7 breast cancer cells with an ER α antagonist, Fulvestrant. With the reduction of ER α levels, we found that MED12 methylation remained stable (Figure 29), indicating that this methylation event is not downstream of the ER α pathway.

4.6 The dynamics of CARM1 and MED12 recruitment to EREs

It is well established that ER α orchestrates the ordered and cyclical assembly of transcriptional coactivators and chromatin remodelers at EREs (Metivier et al, 2003). The first cycle of transcription, which is established within 15 minutes of E2-treatment, involves the recruitment of PRMT1, but not CARM1. Mediator is not part of this first round either. Subsequent cycles of transcription initiation that have an interval of about 40 minutes recruit CARM1 preferentially over PRMT1. To gain an understanding of the dynamics of CARM1 and MED12 subcellular localization after MCF7 cells were treated with estrogen, we investigated the timing of nuclear accumulation of these factors, and potential alterations in the modified state of MED12. ER α rapidly translocates into the nucleus in response to E2 (Figure 30A), as expected. Interestingly, and previously unreported, the pool of nuclear CARM1 increases after 1 hour of E2-treatment, perhaps to support the “productive” cycles of transcription, which seem to favor the use of CARM1 over PRMT1 (Metivier et al, 2003). Nuclear MED12 levels

do not fluctuate after E2-treatment, and no dramatic increase in nuclear MED12 methylation is observed during this time course (Figure 30A). Next, we asked if methylated MED12 was recruited to EREs. Again, using the four GREB-linked EREs we find that methylated MED12 recruitment peaks at 1-hour after E2-treatment (Figure 30B), which is the same timing as Mediator recruitment (Metivier et al, 2003). The same holds true for TFF1, TGFBP4, and FKBP4 (Figure 31A-C). Also, using a biotin-DNA pull-down assay (Foulds et al, 2013), we can demonstrate the *in vitro* assembly of an ER α /CARM1/MED12 complex on wild-type ERE (Figure 30C). Finally, we wanted to attempt to determine whether un-methylated MED12 is recruited to ERE, and subsequently becomes methylated due to the co-recruitment of CARM1. To do this, we chose to use a reporter/imaging system that allows the quantification of both ER α and co-regulator recruitment to an ERE array (Bolt et al, 2013). This system makes use of a HeLa cell line that has an array of EREs (over 100 copies) from the rat prolactin (PRL) gene integrated into a single genomic locus, and also stably express GFP-ER α . When these cells are E2-treated you observe the rapid recruitment of GFP-ER α to a single spot within the nucleus – the PRL array. Immunofluorescence can be used to establish the recruitment dynamics of co-regulators to this array. We found that MED12 is recruited to the PRL array (Figure 30D), allowing us to use this approach. We compared the recruitment dynamics of ER α , total MED12 and methylated MED12. The timing of the recruitment of both MED12 and methylated MED12 is very similar to that of ER α , suggesting that either MED12 is recruited in the methylated state, or that methylation occurs concomitantly with recruitment.

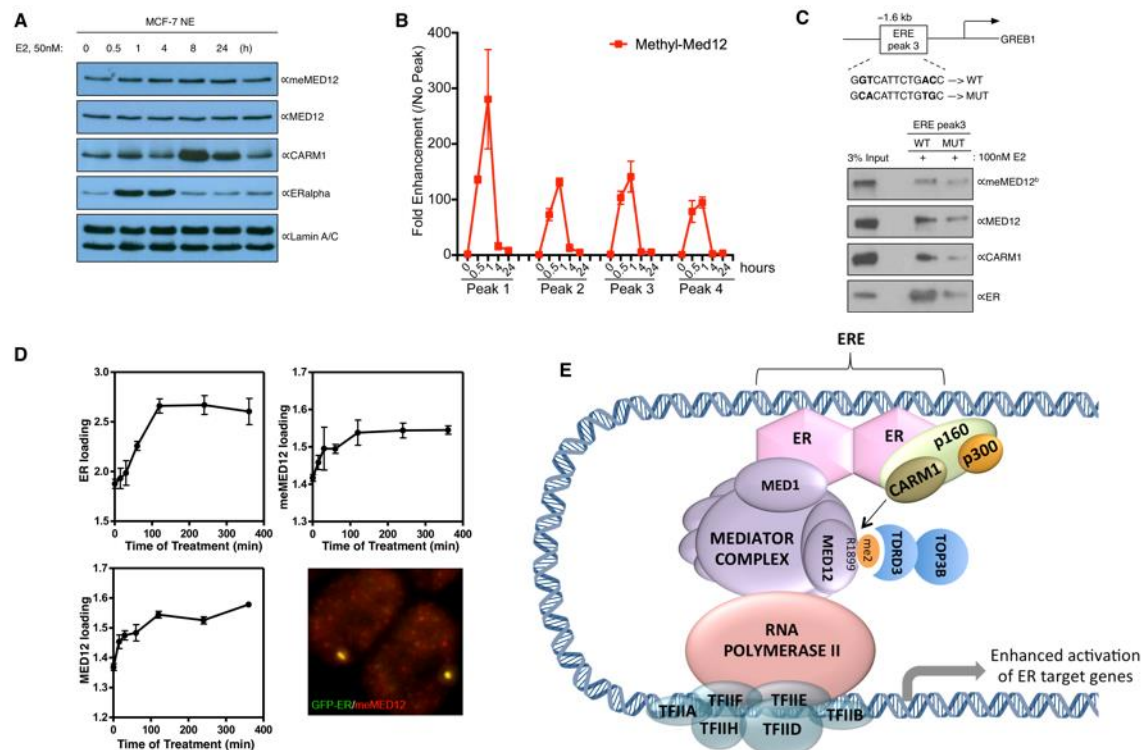


Figure 30: E2-dependent recruitment of methylated MED12 to the ER-target gene, GREB1.

(A) MCF-7 cells were cultured in phenol red-free DMEM supplemented with 10% charcoal dextran-stripped FBS for 3 days and treated with E2 (50 nM) for 0, 0.5, 1, 4, and 24 hours. Nuclear extracts were subjected to Western analysis using αmeMED12^a, αMED12, αCARM1, αERα, and αLamin A/C antibodies. **(B)** MCF-7 cells were cultured in phenol red-free DMEM supplemented with 10% charcoal dextran-stripped FBS for 3 days and treated with E2 (50 nM) for 0, 0.5, 1, 4, and 24 hours. ChIP experiments were performed with αmeMED12^b antibody. Immunoprecipitated DNA was analyzed by qPCR using primers specific for the GREB1 gene. Data represent mean of three independent experiments. The y-axis is the fold change of mean values between peaks and no peak. The x-axis is the hours of E2 treatment. **(C)** Schematic showing the wild-type (WT) and mutated (MUT) ERE1 fragment (peak 3) of the GREB1 gene used for the pull-down experiment. The four nucleotides of the ERE1 fragment written in bold characters are mutated, which attenuates its binding to ERα. Biotinylated WT

and MUT fragments were used to pull down endogenous ER-coregulator complexes from the MCF-7 nuclear extracts. The input and the eluted samples were immunoblotted with α meMED12^b, α MED12, α CARM1, and α ER α antibodies. **(D)** GFP-ER:HeLa:PRL cells were treated with 10 nM E2 for the indicated times. The recruitment of methylated MED12, total MED12, and ER to the PRL array was measured using α meMED12^b, α MED12, and α GFP antibodies. Image shows overlap between GFP-ER and meMED12^b after 1 h of E2 treatment.

Figure 30B – Experiment performed and figure organized by Dr. Donghang Cheng, UT M.D. Anderson Cancer Center

Figure 30C – Experiment performed and figure organized by Dr. Charles Foulds from Dr. Bert O'Malley lab, Baylor College of Medicine

Figure 30D – Experiment performed and figure organized by Dr. Fabio Stossi from Dr. Michael Mancini lab, Baylor College of Medicine

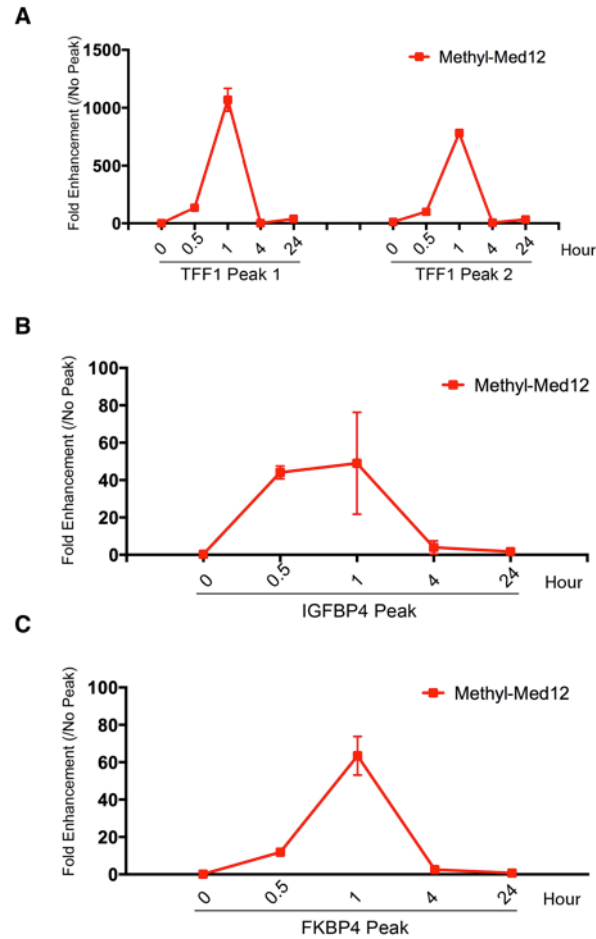


Figure 31: E2-dependent recruitment of methylated MED12 to TFF1, IGFBP4, and FKBP4 EREs.

(A, B, and C) MCF-7 cells were cultured in phenol red-free DMEM supplemented with 10% charcoal dextran-stripped FBS for 3 days and treated with E2 (50nM) for 0, 0.5, 1, 4, and 24 hours. ChIP experiments were performed with α meMED12^b antibody. Immunoprecipitated DNA was analyzed by qPCR using primers specific for TFF1, IGFBP4 and FKBP4 genes. Data represent mean of three independent experiments. The y-axis is the fold change of mean values between peaks and no peak. The x-axis is the hours of E2 treatment.

Figure 31 – Experiment performed and figure organized by Dr. Donghang Cheng, UT M.D. Anderson Cancer Center

Chapter 5: Discussion

Sections 5.1 – 5.3 serve as the discussion for Chapter 3

5.1 Substrate specificity of PRMTs

It is well established that arginine residues within RGG/RG sequences, termed Glycine- and Arginine-rich (GAR) motifs, are preferred sites of methylation for most PRMTs. Some of the examples include GAR1, hnRNPA1, hnRNPU, hnRNPK, fibrillarin and nucleolin (Thandapani et al, 2013b). Of the nine known PRMT enzymes, PRMT1, 3, 5, 6, and 8 methylate arginines within GAR motifs, however, not exclusively, as they also have non-GAR substrates. These non-GAR substrates (E.g. PGC α , ER, FOXO, histones H3, and H4) are perhaps recognized by PRMTs based on their tertiary structure (Di Lorenzo & Bedford, 2011; Le Romancer et al, 2008; Teyssier et al, 2005; Yamagata et al, 2008). CARM1 is a unique enzyme, as it does not methylate GAR containing proteins, it rather methylates PGM (proline-, glycine- and methionine-rich) motifs, which are mainly found in splicing factors (Bedford et al, 1998). It also methylates other substrates that have no obvious common recognition motif. (Cheng et al, 2007). Many CARM1 substrates (PABP1, SmB', CA150, U1C, and SF3B4) are also symmetrically dimethylated by PRMT5 (Cheng et al, 2007). Similarly, many GAR and non-GAR substrates can also be common targets for Type I and Type II enzymes. For example, the GAR substrate, nucleolin, is methylated by PRMT1 and PRMT5 (Bedford & Richard, 2005; Teng et al, 2007). The non-GAR protein, histone H4 (at R3), is a common target for both Type I (PRMT1, 6, and 8) and Type II (PRMT5) enzymes. H4R3me2a is associated with actively transcribed promoters, whereas the H4R3me2s mark colocalizes with repressive marks in ChIP analysis (An et al, 2004; Wang et al, 2001; Wang et al, 2008). This example clearly shows the existence of competition among PRMTs for the same substrates. But, how commonly this happens, especially in non-histone substrates, is unclear. In addition,

GAR and PGM motifs containing multiple arginine residues may also undergo dual modifications (ADMA and/or SDMA), which may attribute them different functions.

5.2 Investigating the MMA mark

PRMT7 is the only known Type III enzyme, which has the ability to exclusively monomethylate arginine residues within substrates (Zurita-Lopez et al, 2012). The enzyme purified from insect cells had robust activity and was able to methylate all core histones, preferentially H2B (at R29, 31 and 33) (Feng et al, 2013). This provided the first evidence that MMA is not only a precursor of ADMA and SDMA, but also a mark that could perhaps be read by effector molecules and have potential biological roles. However, the catalytic efficiency (K_{cat}/K_m) of PRMT7 is around 1000 fold lower than those for other PRMTs (PRMT1, 3, 6) (Feng et al, 2013). This suggests two possible scenarios. One is that PRMT7 only methylates a select few substrates. Since PRMTs work in a distributive fashion, the other possibility is that PRMT7 may act as a priming enzyme by transferring the first methyl group to the substrate, which will then be taken over by another PRMT for asymmetric or symmetric dimethylation. This is perhaps the likely scenario because of the following reason. Fibrillarin, myelin basic protein, and Smd3 are proteins known to be dimethylated by PRMT1 and PRMT5. However, when these proteins are subjected to *in vitro* methylation by PRMT7, they undergo monomethylation (Zurita-Lopez et al, 2012). This suggests that PRMT7 may prime the substrates of PRMT1 or PRMT5 for dimethylation. There could also be a third possibility where PRMT7 is a monomethylator as well as a priming enzyme. One of the ways to understand this issue is to measure the extent of total mono-methylation in wild-type and PRMT7-null cells. In addition, we also wanted to search for any possible PRMTs with Type III

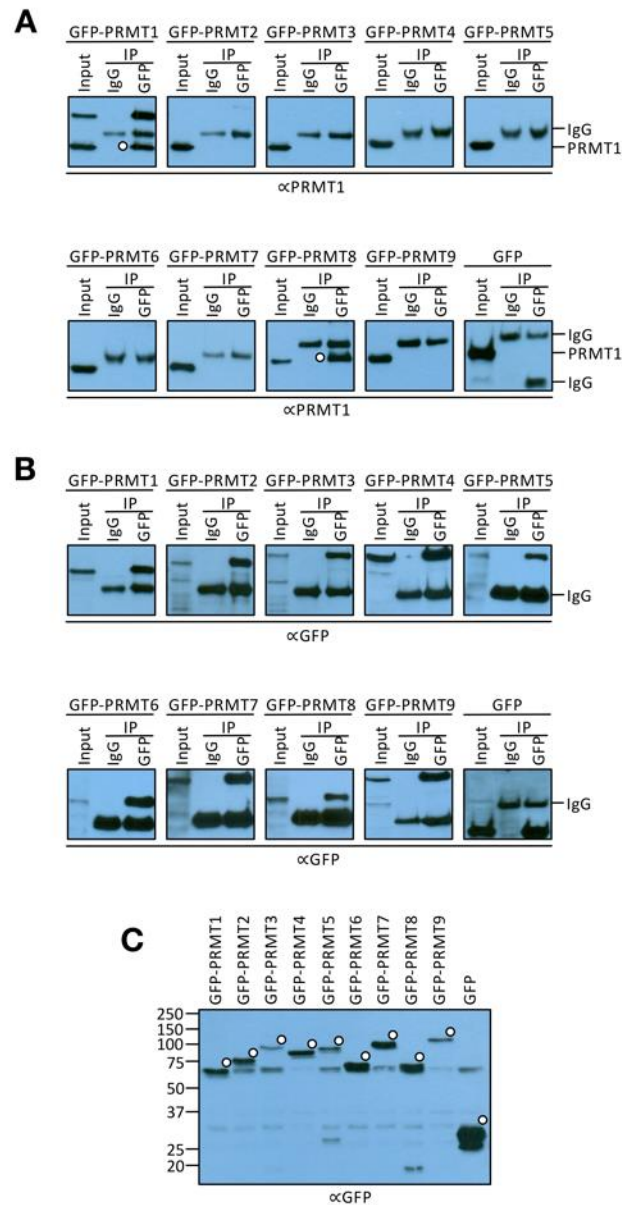


Figure 32: Co-immunoprecipitation of GFP-PRMTs with endogenous PRMT1.

HEK293 cells transiently expressing GFP or GFP-PRMTs (PRMT1-9) fusion proteins were immunoprecipitated with α GFP or α IgG antibodies and subjected to Western analysis with α PRMT1 **(A)** or α GFP **(B)** antibodies. Solid white dots indicate PRMT1 protein co-immunoprecipitated by GFP-PRMT1 and GFP-PRMT8 **(C)** Western analysis of the input samples using α GFP antibody. *Experiment for figure 32 was performed by Dr. Surbhi Dhar (a previous post-doc from Dr. Mark Bedford's lab, UT M.D. Anderson Cancer Center)*

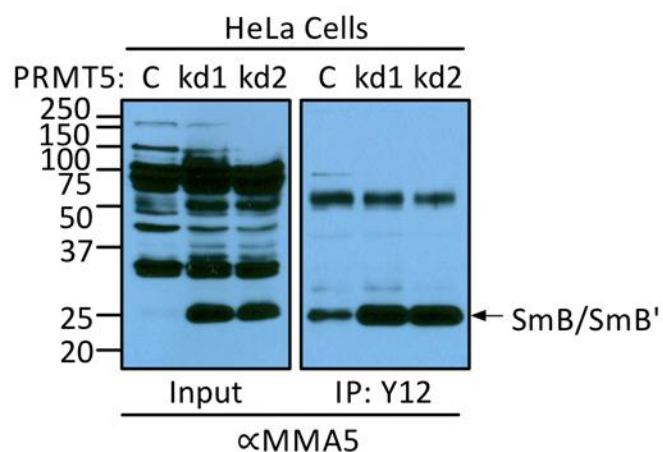


Figure 33: Hyper-monomethylation of SmB/SmB' upon PRMT5 loss.

Whole cell extracts from HeLa-shControl (C) and HeLa-shPRMT5 (kd1 and kd2) cells were immunoprecipitated with Y12 antibody. The input samples and the Y12 immunoprecipitates were subjected to Western analysis with α MMA5 antibody.

activity in addition to PRMT7. Furthermore, we wanted to study how the dynamics of three types of arginine methylation change upon the loss of major PRMTs (PRMT1 and PRMT5)? To address these questions, we generated pan antibodies that recognize monomethylated arginine residues within substrates and studied the methylation patterns in cell lines knocked out/down for various PRMTs.

5.3 The dominant ADMA activity of PRMT1 keeps the global MMA and SDMA levels in check.

The ratios of different arginine methylation types in a variety of cell types were estimated to be 1500:3:2:1 for Arg:ADMA:MMA:SDMA (Matsuoka, 1972). However, upon the loss of PRMT1, we found that there were global increases in MMA and SDMA levels (Figure 34). Since PRMT1 constitutes for about 90% of total ADMA activity, the absence of it leaves a large number of substrates unmethylated, making them available for Type II and III enzymes. This highlights the extent of competition that exists among different methylation types. We speculated that PRMT1 may heterodimerize with PRMT7 or another PRMT, which may act as a priming enzyme for PRMT1 and it monomethylates substrates in the absence of PRMT1. To test this, we transfected HEK293T cells with GFP-PRMTs (PRMT1-9), performed a GFP immunoprecipitation followed by Western analysis with PRMT1 antibody. We found that PRMT1 interacted with itself and PRMT8, an enzyme only expressed in brain (Figure 32) (Lee et al, 2005a). Hence, we concluded that PRMT1 might not function in concert with a priming enzyme. Although, we did not observe major MMA changes in cell lines depleted for PRMT3, 4, 5, and 6, there was a specific doublet of bands that migrated at 25kDa in PRMT5 KD cells that was absent in PRMT WT cells (Figure 9D). Based on the size, we speculated the doublet to be SmB/SmB', which is a well-studied PRMT5 target (Pesiridis et al, 2009). Western analysis of SmB/SmB' proteins immunoprecipitated from wild-type and PRMT5

knockdown cells confirmed that these proteins are indeed monomethylated upon PRMT5 knockdown (Figure 32). Since PRMT5 knockdown does not completely deplete the cells of PRMT5, the remaining low levels of enzyme will transfer the first methyl group to the substrate and release, then the enzyme will likely find another unmethylated substrate (because of its large pool size), instead of binding with the already monomethylated substrate to convert to SDMA, thereby hyper-monomethylating the SmB/SmB' proteins. However, this hypothesis does not hold true in the case of PRMT1 knockout cells for two reasons. First, PRMT1 is completely knocked out in these cells. Second, PRMT1 is a partially-processive enzyme (Obianyo et al, 2008), as opposed to PRMT5, which catalyzes in a distributive fashion (Antonyamy et al, 2012).

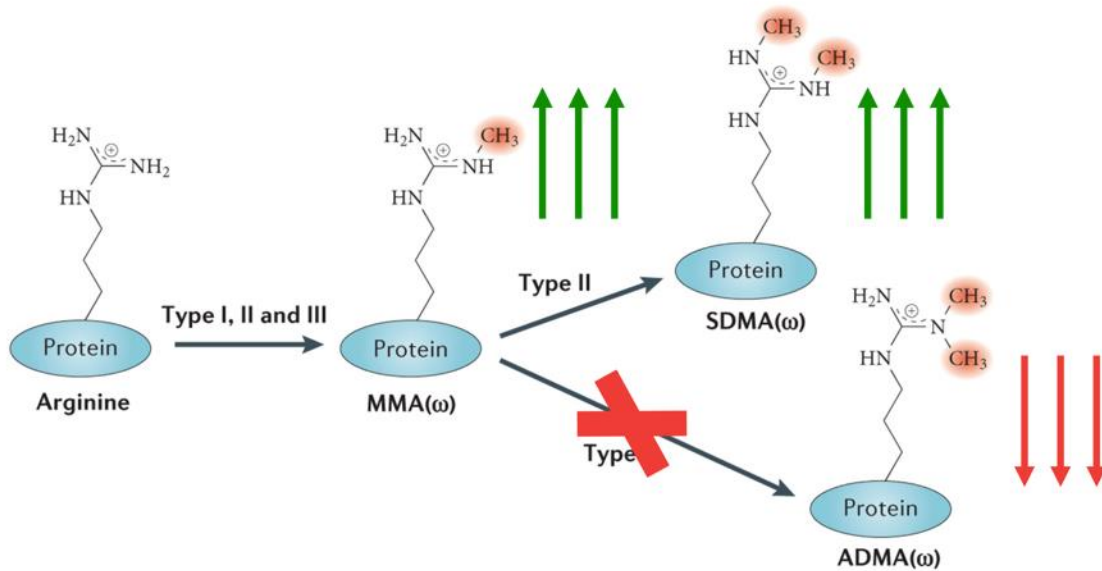


Figure 34: Dynamic interplay between the three types of arginine methylation.

Upon the loss of PRMT1, there are major increases in global MMA and SDMA levels, whereas ADMA levels were reduced. This is likely due to the fact that PRMT1 accounts for more than 90% of ADMA activity and the loss of this enzyme could lead to the accumulation of a number of unmethylated substrates, which then become targets for Type II and Type III enzymes.

*Figure 34 is adapted and modified from Yang Y, Bedford MT (2013) Protein arginine methyltransferases and cancer. Nat Rev Cancer **13**: 37-50.*

Permission has been acquired from the journal to use this figure.

Sections 5.4 – 5.6 serve as the discussion for Chapter 4

5.4 CARM1 methylates a distinct motif

Most PRMTs methylate glycine-arginine-rich (GAR) domains (Thandapani et al, 2013a); CARM1 does not. The ill-defined nature of the CARM1 methylation motif can best be seen when a large number of different CARM1 methylation sites are aligned (Figure 35). There is clearly no obvious motif, except for the propensity for proline residues in the vicinity of the CARM1 methylation site. But even the proline residues are not at a fixed position from the methylated arginine, suggesting that all that is needed is a kink, on either side (or both sides) of the methylation site. Thus, even after the identification of a number of different CARM1 substrates, the methylation motif for this enzyme still remains rather nebulous. Co-crystal structures of CARM1 with H3 and PABP1 peptides were resolved. While substrate arginine makes hydrogen bond interactions with certain key residues in CARM1, residues surrounding the arginine interact through their backbone atoms, suggesting that substrate recognition by CARM1 is largely sequence-independent. However, since the CARM1 crystallization construct used in this study is truncated, it is possible that the missing domains may make additional interactions with the peptide that are necessary for substrate recognition. In addition, the length of the substrate peptides used may also play a role. In fact, long-range interactions between PRMT1 and histone H4 were shown to be critical for substrate binding and catalysis (Osborne et al, 2007). Interestingly, although it is difficult to predict a CARM1 substrate, antibodies developed to one substrate often cross-react with other substrates – so antibodies are able to identify some structural similarity between CARM1 methylation motifs. This “semi-pan” nature of CARM1 substrate antibodies was first realized using the H3R17me2a antibody, which we have shown recognizes

CARM1 Substrate	Methylated motif	Reference
BAF155 (R1064)	PPMPGNILGPRVPLTAPNGMY	(Wang et al, 2014a)
CAS3 (R88)	NPYQTAVYPVRSAYPQQSPYA	(Lee & Bedford, 2002)
CBP (R714)	PNGPLSLPVNRMQVSQGMNSF	(Chevillard-Briet et al, 2002)
CBP (R742)	VQLPQAPMGPRAAASPMNHSVQ	(Chevillard-Briet et al, 2002)
CBP (R768)	SVPGMAISPSRMPQPPNMMGA	(Chevillard-Briet et al, 2002)
CTD (R1810)	TSPSYSPSSPRYTPQSPTYTP	(Sims et al, 2011)
GPS2 (R312)*	GFAATSQPGPRLPFIQHSQNP	(Huang et al, 2015a)
GPS2 (R323)*	LRFIQHSQNPRLFYHKXXXXXX	(Huang et al, 2015a; Jarmalavicius et al, 2010)
H3 (R17)	ARKSTGGKAPRKQLATKAARK	(Bauer et al, 2002; Chen et al, 1999)
H3 (R26)	PRKQLATKAARKSAPATGGVK	(Chen et al, 1999; Schurter et al, 2001)
HuD (R236)	YPGPLHHQAQRFRLDNLLNMA	(Fujiwara et al, 2006)
HuR (R217)	FGGPVHHQAQRFSPMGVDH	(Li et al, 2002)
MED12 (R1899)*	EPSSYKTSVYRQQQPAVPGQ	
MLL2 (R3727)*	QERQLQLQQRMQLAQKLQQ	
p300 (R2142)	NMNPQAGVQRAGLPQQQPQQ	(Lee et al, 2005b)
p300 (580)	QWHEDITQDLRNHLVHKLVQA	(Xu et al, 2001)
PABP1 (R455)	HPFQNMPGAIRPAAPRPPFST	(Lee & Bedford, 2002)
PABP1 (R460)	MPGAIRPAAPRPPFSTMRPAS	(Lee & Bedford, 2002)
Pax7 (R10)	XMAALPGTVPRMMRPAPGQNY	(Kawabe et al, 2012)
Pax7 (R13)	ALPGTVPRMMRPAPGQNYPR	(Kawabe et al, 2012)
Pax7 (R22)	MRPAPGQNYPRTGFPLEVSTP	(Kawabe et al, 2012)
Pax7 (R37)	LEVSTPLGQGRVNQLGGVFIN	(Kawabe et al, 2012)
Sox2 (R113)	KEHPDYKYRPRRKTTLMKKD	(Zhao et al, 2011)
Sox9 (R152)	LWRLLESEKRPFVEEAERLR	(Ito et al, 2009)
Sox9 (R74)	SEEDKFPVCIREAVSQVLKGY	(Ito et al, 2009)
SRC3 (R1171)	RPRNTNPKQLRMQLQQLQGG	(Feng et al, 2006)
TARPP (R650)	QYPTSTSQQYRPLASVQYSAQ	(Kim et al, 2004)

Figure 35: Alignment of CARM1-methylated motifs.

A selection of CARM1-methylated motifs containing 20 amino acids surrounding the central arginine residue was aligned using the MegAlign software (DNASTAR, Inc). The central arginine and the neighboring prolines were highlighted in black and grey, respectively. Asterisk indicates methylation sites identified in this study.

SRC3 (Naeem et al, 2007) and CA150 (Cheng et al, 2007), and here we show also recognizes GPS2, SLM2, PABP1, SF3B4, SRC1 and MED12 (Figure 17B).

The use of methyl-specific antibodies combined with MS-based proteomic analysis has led to the discovery of a number of arginine-methylated proteins (Boisvert et al, 2003; Guo et al, 2014; Ong et al, 2004b). However, these methyl-specific antibodies were raised against GAR-motifs, making them unsuitable for use in enriching CARM1 substrates. To address this issue, we developed antibodies against a mixture of CARM1-methylated motifs and identified over a 100 putative CARM1 substrates by IP-MS (Figures 15 & 17). The enrichment of known CARM1 substrates like SRC3, CA150, and SF3B4, whose methyl-motifs were not used in antibody generation, validates our strategy. The antibodies also enriched for a few known PRMT1 substrates including Sam68 (Cote et al, 2003), G3BP1 (Bikkavilli & Malbon, 2011) and DHX9 (Smith et al, 2004). Secondary screening was performed on a small subset of the identified proteins, using CARM1 knockdown and knockout cells (Figure 18), and we validated three novel CARM1 substrates – GPS2, KMT2D, and MED12. Interestingly, SLM2 methylation is not lost upon CARM1 knockdown (Figure 18I), although this protein is recognized by a number of CARM1 substrate motif antibodies.

All four of these newly confirmed CARM1 substrates have biological activity on or near chromatin. Indeed, GPS2 is a dual-function protein that acts both as a corepressor and coactivator for various transcription factors (Wong et al, 2014a). It has been reported that GPS2 is methylated at R323 (one of the two methyl sites identified in our MS data). Recently, it was found that the H3R17me2a antibody recognizes GPS2 (Huang et al, 2015b), and that PRMT6 can methylate GPS2 *in vitro*, but CARM1 was never tested in this assay. In addition, the site of PRMT6 methylation on GPS2 was mapped to R323 and this methylation seems to be required for GPS2 protein stabilization. Thus, there may be two independent sites of methylation on GPS2 (R312 & R323), and both CARM1 and PRMT6 may compete for this substrate. KMT2D is a lysine methyltransferase, primarily responsible for mono-methylating

H3K4 at active enhancers (Guo et al, 2013; Hu et al, 2013; Lee et al, 2013). We report that KMT2D is arginine methylated at R3727 residue. The functional role of this methylation event is unclear, but it is interesting that KMT2D and CARM1 both have activity at enhancers, and may be “talking” to each other. The RNA-binding protein SLM2 was reported to be arginine methylated by PRMT1 (Cote et al, 2003). Here, we show that SLM2 is also recognized by CARM1 substrate antibodies, suggesting that PRMT1 may not be the sole methyltransferase for this protein. Finally, MED12 was previously identified as an arginine methylated protein in two independent studies. Using hydrophilic interaction liquid chromatography (an antibody-independent approach) to enrich for tryptic peptides that contain methylated arginine residues, the Acuto group identified the same site that we did (R1899) as a prominent site of arginine methylation, although they did not determine the enzyme responsible for the methylation (Uhlmann et al, 2012). Subsequently, Xu group identified MED12 in a screen that used ADMA antibody raised to a redundant XXRme2aXX motif (Guo et al, 2014), to enrich for proteins that were methylated in CARM1 WT but not CARM1 KO breast cancer cell lines (Wang et al, 2014a). Using *in vitro* binding assays, they were able to show that GST-CARM1 interacted with full-length MED12. However, we did not observe a co-immunoprecipitation between endogenous CARM1 and MED12 (Figure 21A). It is possible that the transient interaction needed to achieve methylation is what is detected in the *in vitro* binding assay. Using deletion analysis, they showed that MED12 is methylated at R1862, which is distinct from the site identified in the current study (R1899). Methylation at this site was shown to sensitize breast cancer cells to chemotherapy drugs by enhancing Mediator recruitment to p21 gene locus and suppressing its transcription. Consistent with these reported findings, using the more focused ADMA^{CARM1} antibodies, we also identified MED12 as a methylated protein. We showed that MED12 is methylated by CARM1 and is recruited to the ER α -specific enhancers. We propose that methylated MED12 functions in maximizing ER α -mediated transcription, possibly by recruiting the coactivator, TDRD3.

5.5 CARM1 primarily associates with enhancers, but is also found at promoters

By exploiting the pan nature of the H3R17me2a antibody, CARM1 activity was first mapped in a global fashion by the group of Myles Brown, using a ChIP-on-chip approach (Lupien et al, 2009). They found that the majority (70%) of ER α binding sites are associated with CARM1 activity. Most of the CARM1 activity mapped to intergenic and intronic regions, with less than 3% of this activity associated with proximal promoter regions. Our expanded H3R17me2a ChIP-seq data support these findings.

The association of CARM1 itself with chromatin has been investigated using a reChIP-on-chip approach (Coughlan et al, 2013). In this study from Joe Torchia's group, a promoter array was used for the profiling, so they were not able to investigate enhancer enrichment of CARM1. However, the SRC3/CARM1 protein complex associated not only with promoter proximal EREs, but also with Sp1 and C/EBP1 binding motifs. Importantly, the Sp1 motif is enriched in the YYN and YNN clusters that are associated with CARM1 activity at promoters that are also marked with H3K4me3 signal (Figures 25B & 26B). The reChIP-on-chip experiment focused on identifying promoters that recruited CARM1 through its association with SRC3 (Coughlan et al, 2013). This is likely just a subset of promoters that are engaged by CARM1, because it can be recruited by other SRCs and also directly by other transcription factors themselves. Indeed, CARM1 interacts directly with ER α , and in an estrogen-independent manner in response to cAMP signaling (Carascossa et al, 2010), and also with c-Fos (Fauquier et al, 2008) and C/EBP β (Kowenz-Leutz et al, 2010). CARM1 not only binds, but also methylates C/EBP β and inhibits the association of this transcription factor with the Mediator complex (Kowenz-Leutz et al, 2010). NF- κ B is another transcription factor that directly interacts with CARM1 (Covic et al, 2005), and it was later reported that CARM1 is present at the promoter/enhancer looping joint of a NF- κ B regulated gene (*MCP-1*) (Teferedegne et al, 2006). In this setting, CARM1 was not required for looping, but was required for efficient expression of *MCP-1*. CARM1 also binds directly to the Notch intracellular

domain (NICD), and can be detected at NICD-bound enhancer sites of a number of Notch target genes (Hein et al, 2015). Thus, CARM1 is not a dedicated ER coactivator, but is also recruited by other transcription factors to both proximal promoters and enhancer elements.

CARM1 is not only recruited to chromatin by transcription factors, but also by ATP-dependent remodeling complexes, including the SWI/SNF complex (Xu et al, 2004) and direct interactions with Mi2 α and Mi2 β , components of the NuRD complex (Streubel et al, 2013). Although NuRD is generally considered a transcriptional repressor complex, there is emerging evidence that it can also positively regulate gene expression, particularly in light of recent genomic localization studies that show its enrichment at active promoters and enhancers (Shimbo et al, 2013).

At both enhancer elements and at some proximal promoters, CARM1 methylates a host of different proteins that are detected with the H3R17me2a antibody. However, it is clear that the H3R17me2a antibody does not recognize all CARM1 substrates (Figure 17B – KMT2D & SRC2). This is supported by our ChIP-seq data showing two categories (YYN & YNN) that display strong CARM1 recruitment but very little H3R17me2a antibody ChIP signals (Figure 25B). It is likely that CARM1 activity at these proximal promoter regions will be detected using a different CARM1 substrate antibody. These data support the idea of distinct methylarginine “fingerprints” on transcriptional coactivators, at different gene promoters and enhancers, which was first proposed by the Gronemeyer group (Ceschin et al, 2011). In that study, they showed that three methyl-specific antibodies, raised against different CARM1 methylation sites on the CREB-binding protein (CBP), displayed dissimilar localization signatures at different EREs.

5.6 How does CARM1 methylation of MED12 regulate its function?

CARM1 impacts gene expression pathways at multiple stages; it methylates the SWI/SNF chromatin remodeling protein, BAF155, to modulate chromatin structure at c-Myc-regulated genes. It affects transcription initiation by methylating histone H3, SRCs, and p300/CBP. It also regulates mRNA splicing by methylating CA150 and other splicing factors. Furthermore, CARM1 modifies PABP1, HuR, and HuD to regulate post-splicing events, such as mRNA stability. We demonstrate here that methylation of MED12 provides an additional level of gene expression regulation governed by CARM1. While the Mediator complex broadly regulates transcription, the MED12 subunit is only partially methylated in cells (Figure 19D), suggesting that the Mediator complex targeted by CARM1 may regulate a specific set of transcriptional programs, as opposed to all RNAPII-dependent genes. From ChIP-seq experiments, we defined this specific set of genes to be ER α -dependent. We are currently performing gene expression studies to determine if MED12 methylation enhances the activation of these genes.

Methylation of MED12 signals the recruitment of TDRD3, which may promote transcriptional activation because of TDRD3's coactivator activity (Yang et al, 2010). TDRD3 is in a tightly complex with the topoisomerase, TOP3B (Stoll et al, 2013; Yang et al, 2014). It has been shown that the TDRD3/TOP3B complex is recruited to active chromatin through the ability of the TDRD3 Tudor domain to interact with the H3R17me2a and H4R3me2a marks (Yang et al, 2014). Here we report a third mark that is "read" by TDRD3: MED12R1899me2a. The recruitment of the TDRD3/TOP3B complex could help resolve R-loops at sites of active transcription (Yang et al, 2014), or it could act on ncRNA molecules that are associated with the Mediator complex. Indeed, TOP3B was recently shown to possess both DNA and RNA topoisomerase activities (Xu et al, 2013; Yang et al, 2014). Importantly, Mediator has been shown to associate with at least two classes of non-coding RNAs; 1) activator RNAs (aRNAs, also called ncRNA-a) that increase the transcription of neighboring genes (Lai et al, 2013),

and 2) enhancer RNAs (eRNAs) that correlate with enhancer-promoter looping and gene activation (Hsieh et al, 2014). The recruitment of the TDRD3/TOP3B complex, and its dual topoisomerase activity, may be required for not only reducing R-loop formation in the wake of Pol II at active genes (though a H3R17me2a and H4R3me2a interactions), but also for the “untangling” and “correct” structural presentation of these RNA scaffolds at sites of enhancer-promoter looping (though a MED12R1899me2a interaction) (Figure 30E).

Chapter 6: Future studies

Currently, I am performing gene expression studies to determine if MED12 methylation regulates transcription of ER-target genes. This requires the generation of ER positive breast cancer cell lines depleted of endogenous MED12 and rescued with MED12 wildtype and R1899K constructs. Owing to its large size, overexpression of MED12 plasmid using chemical transfection methods proved difficult to achieve. In addition, RNAi-mediated knockdown of endogenous MED12 was only partially successful. To circumvent these issues, we planned to use lentiviral-mediated transduction method and generate five MCF-7 cell lines that express (i) Scramble shRNA and FLAG-empty (ii) MED12 shRNA and FLAG-empty (iii) MED12 shRNA and shRNA-resistant MED12 wild-type (iv) MED12 shRNA and shRNA-resistant MED12 R1899K and (v) MED12 shRNA and shRNA-resistant MED12 R1862K vectors. These cells will be treated with Estrogen (50 nM, 1 h), validated by Western analysis and tested for gene expression changes by RT-qPCR. We hypothesized that MED12 R1899 methylation enhances ER-mediated transcription and hence, we expect to see reduced ER-target gene expression in mutant (R1899K) cells (iv) compared to their wild-type counterparts (iii). The cell line (v) will determine if the R1862 methylation, identified by the Xu group, is also important in mediating ER signaling (Wang et al, 2015). We do not expect that MED12 methylation will negatively regulate these target genes, for two reasons: CARM1 is a coactivator for nuclear hormone receptors (Chen et al, 1999) and MED12 knockdown reduces the expression of ER target genes and ESR1 gene itself (Prenzel et al, 2012). It is also possible that MED12 methylation may function redundantly in recruiting TDRD3 to NR target gene loci and hence, may not produce a significant effect on transcription. In this unlikely, yet possible scenario, we will focus our efforts of

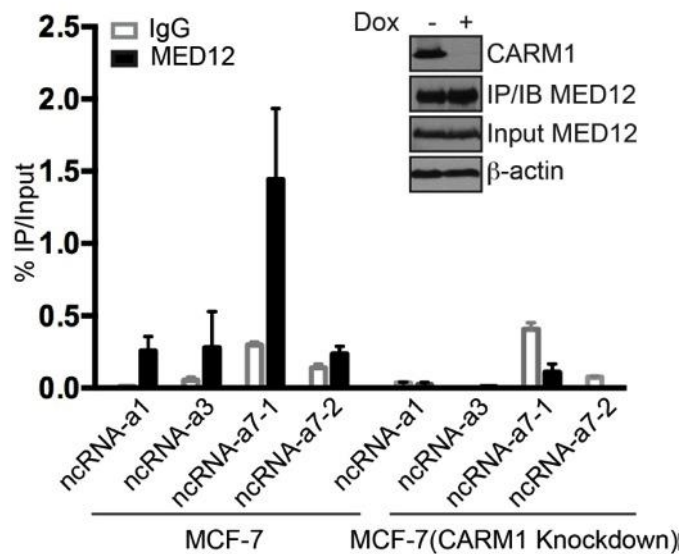


Figure 36: MED12 associates with activating ncRNAs in a CARM1-dependent manner. MCF-7-Tet-on-shCARM1 cells were untreated or treated with doxycycline (1 $\mu\text{g/ml}$) for 8 days. The cells were ultraviolet crosslinked at 254 nm (200 mJ/cm^2) in 10 ml ice-cold PBS, lysed in mild buffer and immunoprecipitated with αMED12 antibody. Total RNA is then extracted from the immunoprecipitates, converted to cDNA and analyzed by RT-qPCR using primer sets specific for ncRNA-a1, -a3 and -a7 genes.

Figure 36 – RIP experiment performed and figure organized by Dr. Donghang Cheng. I did validation of CARM1 KO and MED12 IP-WBs.

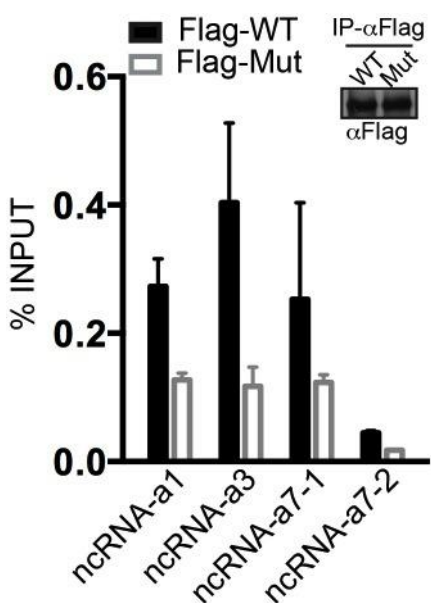


Figure 37: Mutant MED12 shows reduced interaction with activating ncRNAs.

HEK293T cells were transiently transfected with FLAG-MED12-WT or FLAG-MED12-MUT constructs. The cells were ultraviolet crosslinked at 254 nm (200 mJ/cm²) in 10 ml ice-cold PBS, lysed in mild buffer and immunoprecipitated with αFLAG antibody. Total RNA is then extracted from the immunoprecipitates, converted to cDNA and analyzed by RT-qPCR using primer sets specific for ncRNA-a1, -a3 and -a7 genes.

Figure 37 – RIP experiment performed and figure organized by Dr. Donghang Cheng. I did validation of MED12 WT and MUT protein expression.

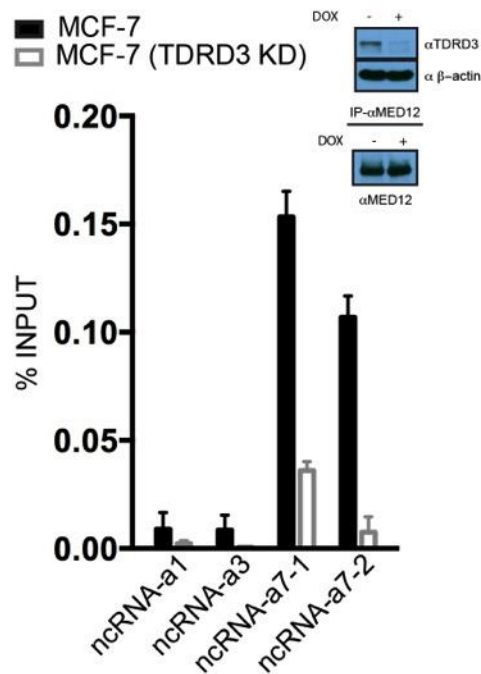


Figure 38: MED12 associates with activating ncRNAs in a TDRD3-dependent manner.

MCF-7-Tet-on-shTDRD3 cells were untreated or treated with doxycycline (1 $\mu\text{g/ml}$) for 8 days. The cells were ultraviolet crosslinked at 254 nm (200 mJ/cm^2) in 10 ml ice-cold PBS, lysed in mild buffer and immunoprecipitated with αMED12 antibody. Total RNA is then extracted from the immunoprecipitates, converted to cDNA and analyzed by RT-qPCR using primer sets specific for ncRNA-a1, -a3 and -a7 genes.

Figure 38 – RIP experiment performed and figure organized by Dr. Donghang Cheng. I did validation of TDRD3 KO and MED12 IP-WBs.

understanding the biological roles of MED12 methylation in the activating ncRNA (ncRNA-a) field. MED12 was shown to associate with activating ncRNA (a1, a3, and a7) (Lai et al, 2013). We performed RNA immunoprecipitation (RIP) experiments and found that MED12 associates with these ncRNAs in a CARM1-dependent manner in MCF-7 cells (Figure 36). We also overexpressed FLAG-MED12 wild-type and mutant (R1899K) in HEK293T cells and found that the methyl-mutant showed reduced association with the three ncRNAs when compared with the wild-type protein (Figure 37). In addition, we showed that methyl-MED12 antibody was able to pull down these ncRNAs in MCF-7 cells (data not shown). Furthermore, we showed that MED12 interaction with ncRNA-a7 is also dependent on TDRD3 (Figure 38). These findings led us to hypothesize that methyl-MED12-associated TDRD3 may act as an interface that links ncRNA-a with their target gene loci to promote their transcription. As a secondary confirmation, we will perform RIP-seq experiments using RNA isolated from MED12 immunoprecipitates of wild-type and CARM1- and TDRD3-knockdown cells. To test our hypothesis, the cell lines (i-iv) will be infected with a lentivirus expressing TK promoter-driven luciferase reporter, which is fused to the ncRNA (a1, a3 or a7) gene driven by its natural promoter. The effect of MED12 methylation on ncRNA target gene activation can be measured by the changes in luciferase activity. In addition, the expression of ncRNA-a target genes (TAL1, STIL, SNAI1, UBE2V1, AURKA, and CSTF1) in cell lines (i-iv) will be also tested. These target genes were shown to be activated by CDK8-mediated phosphorylation of H3S10, a histone mark linked with transcriptional activation (Lai et al, 2013; Nowak & Corces, 2004). We noted earlier that MED12 methylation does not have an effect on Mediator-associated kinase activity (Figure 22) at the global level. However, there may be a MED12 methylation-dependent CDK8 regulation at the gene specific level. Phospho-H3S10 chIP at these target gene loci in wild-type and methyl mutant cell lines will be performed. If the above studies hold true, chromosome conformation capture (3C) should be performed to confirm the

association of ncRNAs with their target gene promoters in MED12 wild-type versus methyl-mutant cell lines.

Chapter 7: Significance

In order to better understand PRMT functions in normal physiology as well as to develop therapeutic targets, many PRMT inhibitors have been identified and some of them have proven effective in ameliorating symptoms in animal disease models (Alinari et al, 2015; Chan-Penebre et al, 2015; Panfil et al, 2015; Sun et al, 2012). Bedford group identified the first class of small molecule inhibitors (AMI series) that specifically targeted PRMTs, but not other AdoMet-dependent methyltransferases (Cheng et al, 2004). AMI-1, which targets PRMT1, 3, 4, and 6, was shown to alleviate asthmatic symptoms in AIP1 (Ag-induced pulmonary inflammation) rat model (Sun et al, 2012). Later on, more selective inhibitors were identified. A PRMT5 inhibitor has been reported to have anti-tumor effects in Mantle cell lymphoma (MCL) xenograft model (Chan-Penebre et al, 2015). While the knowledge of PRMT crystal structures aided in identifying small molecule inhibitors, validating them requires additional tools. Methyl-specific antibodies are proving valuable in assessing the efficacy and selectivity of these PRMT small molecule inhibitors. For example, a pan-SDMA antibody was used to measure the loss of PRMT5 activity in PRMT5 inhibitor-treated MCL cell lines (Chan-Penebre et al, 2015). A selective CARM1 inhibitor was also identified that inhibited methylation of CA150, PABP1, and SmB strongly, however H3 weakly, as detected by the antibodies specific for individual substrates (Cheng et al, 2011). Hence, there is a need for developing better CARM1 inhibitors and CARM1 substrate motif antibodies generated in this study will act as great tools for characterizing their selectivity. Similarly, MMA antibodies generated in the first study can be used to validate loss of PRMT1 activity, which is measured by the increase in monomethylation signal. Recently, we have tested a new set of PRMT inhibitors in our lab. As anticipated, PRMT1 inhibitor treated cells showed an increase in MMA signal and a decrease in ADMA signal (top and middle panels – Figure 39). However, the CARM1 inhibitor did not prove effective in eliminating or

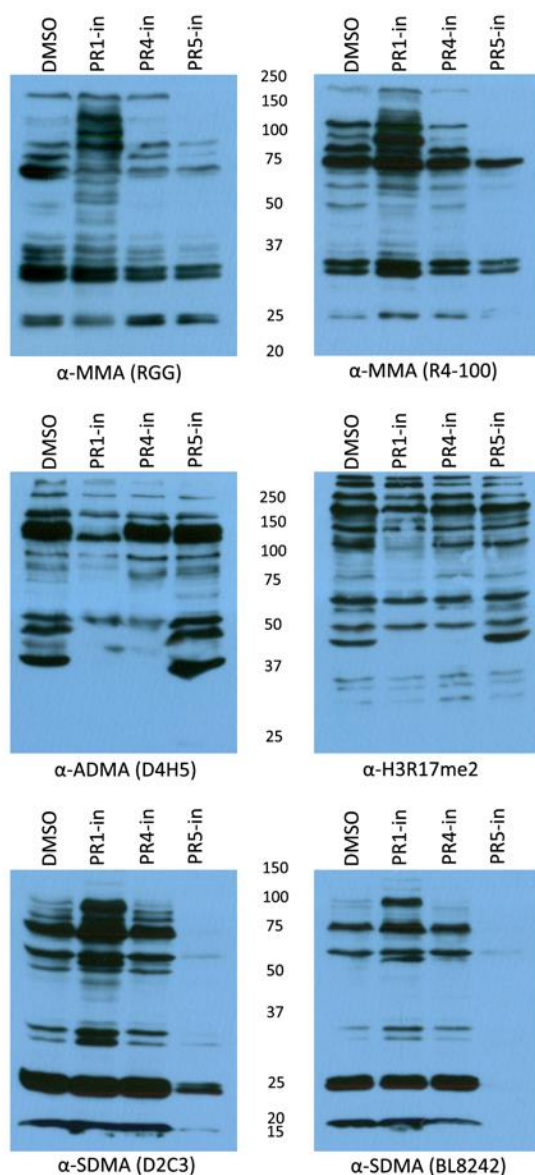


Figure 39: Testing the efficacy of PRMT inhibitors using methyl-specific antibodies.

HeLa cells were treated with DMSO, PRMT1 (1 μ M), PRMT4/CARM1 (2 μ M) or PRMT5 (5 μ M) inhibitors for 4 days. Whole cell extracts were subjected to Western analysis using the specified antibodies.

Figure 39 – Experiment performed and figure organized by Dr. Guozhen Guo

reducing the signal on CARM1 substrates, as detected by H3R17me2a antibody (middle panel – Figure 39). PRMT5 inhibitor showed a dramatic decrease in SDMA signal (bottom panel – Figure 39), proving its efficacy. The same held true for MLL-ENL leukemic cell lines treated with the three PRMT inhibitors (Collaboration with Santos group). In addition, anti-proliferative effects were observed in PRMT5 inhibitor-treated MLL-ENL cell lines (data not shown).

In addition to small molecule inhibitor validation, MMA antibodies can be used to identify novel PRMT1 and PRMT7 substrates. Wild-type, PRMT1 knockout, and PRMT7 knockout MEF extracts can be immunoprecipitated with MMA antibodies and the eluates can be subjected to mass spectrometry to identify differentially recognized proteins.

In the second study involving CARM1 substrate motif antibodies, we have only tested a small subset of the 112 MS-identified potential CARM1 substrates. IP-WB experiments may uncover more unknown substrates, in addition to GPS2, MLL2, and MED12. Unlike p300/CBP and the NCoA family, if methylated MED12 proves to be a dedicated coregulator of ER α signaling, an inhibitor targeting methylated MED12, but not unmodified MED12, may specifically impact ER pathway and possibly hold some therapeutic value. MLL2 (or KMT2D), another substrate identified in this study, is recurrently mutated in multiple cancers. Studying the biological role of MLL2 methylation may clarify its possible tumorigenic functions. It is notable that R3727 and R4198 sites, methylated by CARM1, were mutated in melanoma, lung and pancreatic cancers (TCGA database).

8. References

- Abramovich C, Yakobson B, Chebath J, Revel M (1997) A protein-arginine methyltransferase binds to the intracytoplasmic domain of the IFNAR1 chain in the type I interferon receptor. *EMBO J* **16**: 260-266
- Akoulitchev S, Chuikov S, Reinberg D (2000) TFIIH is negatively regulated by cdk8-containing mediator complexes. *Nature* **407**: 102-106
- Alarcon C, Zaromytidou AI, Xi Q, Gao S, Yu J, Fujisawa S, Barlas A, Miller AN, Manova-Todorova K, Macias MJ, Sapkota G, Pan D, Massague J (2009) Nuclear CDKs drive Smad transcriptional activation and turnover in BMP and TGF-beta pathways. *Cell* **139**: 757-769
- Alinari L, Mahasen KV, Yan F, Karkhanis V, Chung JH, Smith EM, Quinion C, Smith PL, Kim L, Patton JT, Lapalombella R, Yu B, Wu Y, Roy S, De Leo A, Pileri S, Agostinelli C, Ayers L, Bradner JE, Chen-Kiang S, Elemento O, Motiwala T, Majumder S, Byrd JC, Jacob S, Sif S, Li C, Baiocchi RA (2015) Selective inhibition of protein arginine methyltransferase 5 blocks initiation and maintenance of B-cell transformation. *Blood* **125**: 2530-2543
- An W, Kim J, Roeder RG (2004) Ordered cooperative functions of PRMT1, p300, and CARM1 in transcriptional activation by p53. *Cell* **117**: 735-748
- Antonyamy S, Bonday Z, Campbell RM, Doyle B, Druzina Z, Gheyi T, Han B, Jungheim LN, Qian Y, Rauch C, Russell M, Sauder JM, Wasserman SR, Weichert K, Willard FS, Zhang A, Emtage S (2012) Crystal structure of the human PRMT5:MEP50 complex. *Proc Natl Acad Sci U S A* **109**: 17960-17965
- Ashcroft FJ, Newberg JY, Jones ED, Mikic I, Mancini MA (2011) High content imaging-based assay to classify estrogen receptor-alpha ligands based on defined mechanistic outcomes. *Gene* **477**: 42-52
- Bauer UM, Daujat S, Nielsen SJ, Nightingale K, Kouzarides T (2002) Methylation at arginine 17 of histone H3 is linked to gene activation. *EMBO Rep* **3**: 39-44
- Bedford MT, Clarke SG (2009) Protein arginine methylation in mammals: who, what, and why. *Mol Cell* **33**: 1-13
- Bedford MT, Frankel A, Yaffe MB, Clarke S, Leder P, Richard S (2000) Arginine methylation inhibits the binding of proline-rich ligands to Src homology 3, but not WW, domains. *J Biol Chem* **275**: 16030-16036
- Bedford MT, Reed R, Leder P (1998) WW domain-mediated interactions reveal a spliceosome-associated protein that binds a third class of proline-rich motif: the proline glycine and methionine-rich motif. *Proc Natl Acad Sci U S A* **95**: 10602-10607
- Bedford MT, Richard S (2005) Arginine methylation an emerging regulator of protein function. *Mol Cell* **18**: 263-272

Belakavadi M, Fondell JD (2010) Cyclin-dependent kinase 8 positively cooperates with Mediator to promote thyroid hormone receptor-dependent transcriptional activation. *Mol Cell Biol* **30**: 2437-2448

Bikkavilli RK, Malbon CC (2011) Arginine methylation of G3BP1 in response to Wnt3a regulates beta-catenin mRNA. *J Cell Sci* **124**: 2310-2320

Boisvert FM, Cote J, Boulanger MC, Richard S (2003) A proteomic analysis of arginine-methylated protein complexes. *Mol Cell Proteomics* **2**: 1319-1330

Boisvert FM, Dery U, Masson JY, Richard S (2005a) Arginine methylation of MRE11 by PRMT1 is required for DNA damage checkpoint control. *Genes Dev* **19**: 671-676

Boisvert FM, Rhie A, Richard S, Doherty AJ (2005b) The GAR motif of 53BP1 is arginine methylated by PRMT1 and is necessary for 53BP1 DNA binding activity. *Cell Cycle* **4**: 1834-1841

Bolt MJ, Stossi F, Newberg JY, Orjalo A, Johansson HE, Mancini MA (2013) Coactivators enable glucocorticoid receptor recruitment to fine-tune estrogen receptor transcriptional responses. *Nucleic Acids Res* **41**: 4036-4048

Boulanger MC, Liang C, Russell RS, Lin R, Bedford MT, Wainberg MA, Richard S (2005) Methylation of Tat by PRMT6 regulates human immunodeficiency virus type 1 gene expression. *J Virol* **79**: 124-131

Brahms H, Meheus L, de Brabandere V, Fischer U, Luhrmann R (2001) Symmetrical dimethylation of arginine residues in spliceosomal Sm protein B/B' and the Sm-like protein LSm4, and their interaction with the SMN protein. *RNA* **7**: 1531-1542

Carascossa S, Dudek P, Cenni B, Briand PA, Picard D (2010) CARM1 mediates the ligand-independent and tamoxifen-resistant activation of the estrogen receptor alpha by cAMP. *Genes Dev* **24**: 708-719

Carrera I, Janody F, Leeds N, Dubeau F, Treisman JE (2008) Pygopus activates Wingless target gene transcription through the mediator complex subunits Med12 and Med13. *Proc Natl Acad Sci U S A* **105**: 6644-6649

Carroll JS, Meyer CA, Song J, Li W, Geistlinger TR, Eeckhoutte J, Brodsky AS, Keeton EK, Fertuck KC, Hall GF, Wang Q, Bekiranov S, Sementchenko V, Fox EA, Silver PA, Gingeras TR, Liu XS, Brown M (2006) Genome-wide analysis of estrogen receptor binding sites. *Nat Genet* **38**: 1289-1297

Ceschin DG, Walia M, Wenk SS, Duboe C, Gaudon C, Xiao Y, Fauquier L, Sankar M, Vandel L, Gronemeyer H (2011) Methylation specifies distinct estrogen-induced binding site repertoires of CBP to chromatin. *Genes & development* **25**: 1132-1146

Chan-Penebre E, Kuplast KG, Majer CR, Boriack-Sjodin PA, Wigle TJ, Johnston LD, Rioux N, Munchhof MJ, Jin L, Jacques SL, West KA, Lingaraj T, Stickland K, Ribich SA, Raimondi A, Scott MP, Waters NJ, Pollock RM, Smith JJ, Barbash O, Pappalardi M, Ho TF, Nurse K, Oza KP, Gallagher KT, Kruger R, Moyer MP, Copeland RA, Chesworth R, Duncan KW

(2015) A selective inhibitor of PRMT5 with in vivo and in vitro potency in MCL models. *Nat Chem Biol* **11**: 432-437

Chang B, Chen Y, Zhao Y, Bruick RK (2007) JMJD6 is a histone arginine demethylase. *Science* **318**: 444-447

Chen D, Ma H, Hong H, Koh SS, Huang SM, Schurter BT, Aswad DW, Stallcup MR (1999) Regulation of transcription by a protein methyltransferase. *Science* **284**: 2174-2177

Chen X, Niroomand F, Liu Z, Zankl A, Katus HA, Jahn L, Tiefenbacher CP (2006) Expression of nitric oxide related enzymes in coronary heart disease. *Basic Res Cardiol* **101**: 346-353

Cheng D, Cote J, Shaaban S, Bedford MT (2007) The arginine methyltransferase CARM1 regulates the coupling of transcription and mRNA processing. *Mol Cell* **25**: 71-83

Cheng D, Valente S, Castellano S, Sbardella G, Di Santo R, Costi R, Bedford MT, Mai A (2011) Novel 3,5-bis(bromohydroxybenzylidene)piperidin-4-ones as coactivator-associated arginine methyltransferase 1 inhibitors: enzyme selectivity and cellular activity. *J Med Chem* **54**: 4928-4932

Cheng D, Vemulapalli V, Bedford MT (2012) Methods applied to the study of protein arginine methylation. *Methods in enzymology* **512**: 71-92

Cheng D, Yadav N, King RW, Swanson MS, Weinstein EJ, Bedford MT (2004) Small molecule regulators of protein arginine methyltransferases. *J Biol Chem* **279**: 23892-23899

Cheung N, Chan LC, Thompson A, Cleary ML, So CW (2007) Protein arginine-methyltransferase-dependent oncogenesis. *Nat Cell Biol* **9**: 1208-1215

Chevillard-Briet M, Trouche D, Vandel L (2002) Control of CBP co-activating activity by arginine methylation. *EMBO J* **21**: 5457-5466

Cote J, Boisvert FM, Boulanger MC, Bedford MT, Richard S (2003) Sam68 RNA binding protein is an in vivo substrate for protein arginine N-methyltransferase 1. *Mol Biol Cell* **14**: 274-287

Cote J, Richard S (2005) Tudor domains bind symmetrical dimethylated arginines. *The Journal of biological chemistry* **280**: 28476-28483

Coughlan N, Thillainadesan G, Andrews J, Isovich M, Torchia J (2013) beta-Estradiol-dependent activation of the JAK/STAT pathway requires p/CIP and CARM1. *Biochimica et biophysica acta* **1833**: 1463-1475

Covic M, Hassa PO, Sacconi S, Buerki C, Meier NI, Lombardi C, Imhof R, Bedford MT, Natoli G, Hottiger MO (2005) Arginine methyltransferase CARM1 is a promoter-specific regulator of NF-kappaB-dependent gene expression. *EMBO J* **24**: 85-96

Dacwag CS, Bedford MT, Sif S, Imbalzano AN (2009) Distinct protein arginine methyltransferases promote ATP-dependent chromatin remodeling function at different stages of skeletal muscle differentiation. *Mol Cell Biol* **29**: 1909-1921

Daujat S, Bauer UM, Shah V, Turner B, Berger S, Kouzarides T (2002) Crosstalk between CARM1 methylation and CBP acetylation on histone H3. *Curr Biol* **12**: 2090-2097

Davis MA, Larimore EA, Fissel BM, Swanger J, Taatjes DJ, Clurman BE (2013) The SCF-Fbw7 ubiquitin ligase degrades MED13 and MED13L and regulates CDK8 module association with Mediator. *Genes Dev* **27**: 151-156

Deribe YL, Pawson T, Dikic I (2010) Post-translational modifications in signal integration. *Nat Struct Mol Biol* **17**: 666-672

Dhar S, Vemulapalli V, Patananan AN, Huang GL, Di Lorenzo A, Richard S, Comb MJ, Guo A, Clarke SG, Bedford MT (2013) Loss of the major Type I arginine methyltransferase PRMT1 causes substrate scavenging by other PRMTs. *Sci Rep* **3**: 1311

Di Lorenzo A, Bedford MT (2011) Histone arginine methylation. *FEBS Lett* **585**: 2024-2031

Dillon MB, Rust HL, Thompson PR, Mowen KA (2013) Automethylation of protein arginine methyltransferase 8 (PRMT8) regulates activity by impeding S-adenosylmethionine sensitivity. *J Biol Chem* **288**: 27872-27880

Ding N, Tomomori-Sato C, Sato S, Conaway RC, Conaway JW, Boyer TG (2009) MED19 and MED26 are synergistic functional targets of the RE1 silencing transcription factor in epigenetic silencing of neuronal gene expression. *J Biol Chem* **284**: 2648-2656

Ding N, Zhou H, Esteve PO, Chin HG, Kim S, Xu X, Joseph SM, Friez MJ, Schwartz CE, Pradhan S, Boyer TG (2008) Mediator links epigenetic silencing of neuronal gene expression with x-linked mental retardation. *Mol Cell* **31**: 347-359

Donner AJ, Ebmeier CC, Taatjes DJ, Espinosa JM (2010) CDK8 is a positive regulator of transcriptional elongation within the serum response network. *Nat Struct Mol Biol* **17**: 194-201

Donner AJ, Szostek S, Hoover JM, Espinosa JM (2007) CDK8 is a stimulus-specific positive coregulator of p53 target genes. *Mol Cell* **27**: 121-133

El Messaoudi S, Fabrizio E, Rodriguez C, Chuchana P, Fauquier L, Cheng D, Theillet C, Vandel L, Bedford MT, Sardet C (2006) Coactivator-associated arginine methyltransferase 1 (CARM1) is a positive regulator of the Cyclin E1 gene. *Proc Natl Acad Sci U S A* **103**: 13351-13356

Fauquier L, Duboe C, Jore C, Trouche D, Vandel L (2008) Dual role of the arginine methyltransferase CARM1 in the regulation of c-Fos target genes. *FASEB J* **22**: 3337-3347

Feng Q, He B, Jung SY, Song Y, Qin J, Tsai SY, Tsai MJ, O'Malley BW (2009) Biochemical control of CARM1 enzymatic activity by phosphorylation. *J Biol Chem* **284**: 36167-36174

Feng Q, Yi P, Wong J, O'Malley BW (2006) Signaling within a coactivator complex: methylation of SRC-3/AIB1 is a molecular switch for complex disassembly. *Mol Cell Biol* **26**: 7846-7857

Feng Y, Maity R, Whitelegge JP, Hadjikyriacou A, Li Z, Zurita-Lopez C, Al-Hadid Q, Clark AT, Bedford MT, Masson JY, Clarke SG (2013) Mammalian protein arginine methyltransferase 7 (PRMT7) specifically targets RXR sites in lysine- and arginine-rich regions. *J Biol Chem* **288**: 37010-37025

Feng Y, Xie N, Jin M, Stahley MR, Stivers JT, Zheng YG (2011) A transient kinetic analysis of PRMT1 catalysis. *Biochemistry* **50**: 7033-7044

Fischle W, Tseng BS, Dormann HL, Ueberheide BM, Garcia BA, Shabanowitz J, Hunt DF, Funabiki H, Allis CD (2005) Regulation of HP1-chromatin binding by histone H3 methylation and phosphorylation. *Nature* **438**: 1116-1122

Ford DJ, Dingwall AK (2015) The cancer COMPASS: navigating the functions of MLL complexes in cancer. *Cancer genetics* **208**: 178-191

Foulds CE, Feng Q, Ding C, Bailey S, Hunsaker TL, Malovannaya A, Hamilton RA, Gates LA, Zhang Z, Li C, Chan D, Bajaj A, Callaway CG, Edwards DP, Lonard DM, Tsai SY, Tsai MJ, Qin J, O'Malley BW (2013) Proteomic analysis of coregulators bound to ERalpha on DNA and nucleosomes reveals coregulator dynamics. *Mol Cell* **51**: 185-199

Frankel A, Yadav N, Lee J, Branscombe TL, Clarke S, Bedford MT (2002) The novel human protein arginine N-methyltransferase PRMT6 is a nuclear enzyme displaying unique substrate specificity. *J Biol Chem* **277**: 3537-3543

Friesen WJ, Massenet S, Paushkin S, Wyce A, Dreyfuss G (2001) SMN, the product of the spinal muscular atrophy gene, binds preferentially to dimethylarginine-containing protein targets. *Mol Cell* **7**: 1111-1117

Friesen WJ, Wyce A, Paushkin S, Abel L, Rappsilber J, Mann M, Dreyfuss G (2002) A novel WD repeat protein component of the methylosome binds Sm proteins. *J Biol Chem* **277**: 8243-8247

Frietze S, Lupien M, Silver PA, Brown M (2008) CARM1 regulates estrogen-stimulated breast cancer growth through up-regulation of E2F1. *Cancer Res* **68**: 301-306

Fryer CJ, White JB, Jones KA (2004) Mastermind recruits CycC:CDK8 to phosphorylate the Notch ICD and coordinate activation with turnover. *Mol Cell* **16**: 509-520

Fujiwara T, Mori Y, Chu DL, Koyama Y, Miyata S, Tanaka H, Yachi K, Kubo T, Yoshikawa H, Tohyama M (2006) CARM1 regulates proliferation of PC12 cells by methylating HuD. *Mol Cell Biol* **26**: 2273-2285

Galbraith MD, Allen MA, Bensard CL, Wang X, Schwinn MK, Qin B, Long HW, Daniels DL, Hahn WC, Dowell RD, Espinosa JM (2013) HIF1A employs CDK8-mediator to stimulate RNAPII elongation in response to hypoxia. *Cell* **153**: 1327-1339

Gao WW, Xiao RQ, Peng BL, Xu HT, Shen HF, Huang MF, Shi TT, Yi J, Zhang WJ, Wu XN, Gao X, Lin XZ, Dorrestein PC, Rosenfeld MG, Liu W (2015) Arginine methylation of HSP70 regulates retinoid acid-mediated RARbeta2 gene activation. *Proc Natl Acad Sci U S A* **112**: E3327-3336

- Gayatri S, Bedford MT (2014) Readers of histone methylarginine marks. *Biochimica et biophysica acta* **1839**: 702-710
- Ge K, Cho YW, Guo H, Hong TB, Guermah M, Ito M, Yu H, Kalkum M, Roeder RG (2008) Alternative mechanisms by which mediator subunit MED1/TRAP220 regulates peroxisome proliferator-activated receptor gamma-stimulated adipogenesis and target gene expression. *Mol Cell Biol* **28**: 1081-1091
- Ge K, Guermah M, Yuan CX, Ito M, Wallberg AE, Spiegelman BM, Roeder RG (2002) Transcription coactivator TRAP220 is required for PPAR gamma 2-stimulated adipogenesis. *Nature* **417**: 563-567
- Geoghegan V, Guo A, Trudgian D, Thomas B, Acuto O (2015) Comprehensive identification of arginine methylation in primary T cells reveals regulatory roles in cell signalling. *Nature communications* **6**: 6758
- Graham JM, Jr., Schwartz CE (2013) MED12 related disorders. *Am J Med Genet A* **161A**: 2734-2740
- Gui S, Wooderchak WL, Daly MP, Porter PJ, Johnson SJ, Hevel JM (2011) Investigation of the molecular origins of protein-arginine methyltransferase I (PRMT1) product specificity reveals a role for two conserved methionine residues. *J Biol Chem* **286**: 29118-29126
- Guo A, Gu H, Zhou J, Mulhern D, Wang Y, Lee KA, Yang V, Aguiar M, Kornhauser J, Jia X, Ren J, Beausoleil SA, Silva JC, Vemulapalli V, Bedford MT, Comb MJ (2014) Immunoaffinity enrichment and mass spectrometry analysis of protein methylation. *Mol Cell Proteomics* **13**: 372-387
- Guo C, Chen LH, Huang Y, Chang CC, Wang P, Pirozzi CJ, Qin X, Bao X, Greer PK, McLendon RE, Yan H, Keir ST, Bigner DD, He Y (2013) KMT2D maintains neoplastic cell proliferation and global histone H3 lysine 4 monomethylation. *Oncotarget* **4**: 2144-2153
- Hassa PO, Covic M, Bedford MT, Hottiger MO (2008) Protein arginine methyltransferase 1 coactivates NF-kappaB-dependent gene expression synergistically with CARM1 and PARP1. *J Mol Biol* **377**: 668-678
- Hein K, Mittler G, Cizelsky W, Kuhl M, Ferrante F, Liefke R, Berger IM, Just S, Strang JE, Kestler HA, Oswald F, Borggrete T (2015) Site-specific methylation of Notch1 controls the amplitude and duration of the Notch1 response. *Sci Signal* **8**: ra30
- Hittelman AB, Burakov D, Iniguez-Lluhi JA, Freedman LP, Garabedian MJ (1999) Differential regulation of glucocorticoid receptor transcriptional activation via AF-1-associated proteins. *EMBO J* **18**: 5380-5388
- Hong H, Kao C, Jeng MH, Eble JN, Koch MO, Gardner TA, Zhang S, Li L, Pan CX, Hu Z, MacLennan GT, Cheng L (2004) Aberrant expression of CARM1, a transcriptional coactivator of androgen receptor, in the development of prostate carcinoma and androgen-independent status. *Cancer* **101**: 83-89

- Hou Z, Peng H, Ayyanathan K, Yan KP, Langer EM, Longmore GD, Rauscher FJ, 3rd (2008) The LIM protein AJUBA recruits protein arginine methyltransferase 5 to mediate SNAIL-dependent transcriptional repression. *Mol Cell Biol* **28**: 3198-3207
- Hsieh CL, Fei T, Chen Y, Li T, Gao Y, Wang X, Sun T, Sweeney CJ, Lee GS, Chen S, Balk SP, Liu XS, Brown M, Kantoff PW (2014) Enhancer RNAs participate in androgen receptor-driven looping that selectively enhances gene activation. *Proc Natl Acad Sci U S A* **111**: 7319-7324
- Hu D, Gao X, Morgan MA, Herz HM, Smith ER, Shilatifard A (2013) The MLL3/MLL4 branches of the COMPASS family function as major histone H3K4 monomethylases at enhancers. *Mol Cell Biol* **33**: 4745-4754
- Huang J, Cardamone MD, Johnson HE, Neault M, Chan M, Floyd EZ, Mallette FA, Perissi V (2015a) Exchange Factor TBL1 and Arginine Methyltransferase PRMT6 Cooperate in Protecting GPS2 from Proteasomal Degradation. *J Biol Chem*
- Huang J, Cardamone MD, Johnson HE, Neault M, Chan M, Floyd ZE, Mallette FA, Perissi V (2015b) Exchange Factor TBL1 and Arginine Methyltransferase PRMT6 Cooperate in Protecting GPS2 from Proteasomal Degradation. *The Journal of biological chemistry*
- Huang S, Holzel M, Knijnenburg T, Schlicker A, Roepman P, McDermott U, Garnett M, Grernrum W, Sun C, Prahallad A, Groenendijk FH, Mittempergher L, Nijkamp W, Neefjes J, Salazar R, Ten Dijke P, Uramoto H, Tanaka F, Beijersbergen RL, Wessels LF, Bernards R (2012) MED12 controls the response to multiple cancer drugs through regulation of TGF-beta receptor signaling. *Cell* **151**: 937-950
- Iberg AN, Espejo A, Cheng D, Kim D, Michaud-Levesque J, Richard S, Bedford MT (2008) Arginine methylation of the histone H3 tail impedes effector binding. *J Biol Chem* **283**: 3006-3010
- Ito T, Yadav N, Lee J, Furumatsu T, Yamashita S, Yoshida K, Taniguchi N, Hashimoto M, Tsuchiya M, Ozaki T, Lotz M, Bedford MT, Asahara H (2009) Arginine methyltransferase CARM1/PRMT4 regulates endochondral ossification. *BMC Dev Biol* **9**: 47
- Iwasaki H, Yada T (2007) Protein arginine methylation regulates insulin signaling in L6 skeletal muscle cells. *Biochem Biophys Res Commun* **364**: 1015-1021
- Janody F, Treisman JE (2011) Requirements for mediator complex subunits distinguish three classes of notch target genes at the Drosophila wing margin. *Dev Dyn* **240**: 2051-2059
- Jarmalavicius S, Trefzer U, Walden P (2010) Differential arginine methylation of the G-protein pathway suppressor GPS-2 recognized by tumor-specific T cells in melanoma. *FASEB J* **24**: 937-946
- Kang YK, Guermah M, Yuan CX, Roeder RG (2002) The TRAP/Mediator coactivator complex interacts directly with estrogen receptors alpha and beta through the TRAP220 subunit and directly enhances estrogen receptor function in vitro. *Proc Natl Acad Sci U S A* **99**: 2642-2647

- Kawabe Y, Wang YX, McKinnell IW, Bedford MT, Rudnicki MA (2012) CARM1 regulates Pax7 transcriptional activity through MLL1/2 recruitment during asymmetric satellite stem cell divisions. *Cell Stem Cell* **11**: 333-345
- Kim D, Lee J, Cheng D, Li J, Carter C, Richie E, Bedford MT (2010a) Enzymatic activity is required for the in vivo functions of CARM1. *J Biol Chem* **285**: 1147-1152
- Kim J, Lee J, Yadav N, Wu Q, Carter C, Richard S, Richie E, Bedford MT (2004) Loss of CARM1 results in hypomethylation of thymocyte cyclic AMP-regulated phosphoprotein and deregulated early T cell development. *J Biol Chem* **279**: 25339-25344
- Kim JD, Park KE, Ishida J, Kako K, Hamada J, Kani S, Takeuchi M, Namiki K, Fukui H, Fukuhara S, Hibi M, Kobayashi M, Kanaho Y, Kasuya Y, Mochizuki N, Fukamizu A (2015) PRMT8 as a phospholipase regulates Purkinje cell dendritic arborization and motor coordination. *Sci Adv* **1**: e1500615
- Kim JM, Sohn HY, Yoon SY, Oh JH, Yang JO, Kim JH, Song KS, Rho SM, Yoo HS, Kim YS, Kim JG, Kim NS (2005) Identification of gastric cancer-related genes using a cDNA microarray containing novel expressed sequence tags expressed in gastric cancer cells. *Clin Cancer Res* **11**: 473-482
- Kim S, Xu X, Hecht A, Boyer TG (2006) Mediator is a transducer of Wnt/beta-catenin signaling. *J Biol Chem* **281**: 14066-14075
- Kim YR, Lee BK, Park RY, Nguyen NT, Bae JA, Kwon DD, Jung C (2010b) Differential CARM1 expression in prostate and colorectal cancers. *BMC Cancer* **10**: 197
- Kleinschmidt MA, Streubel G, Samans B, Krause M, Bauer UM (2008) The protein arginine methyltransferases CARM1 and PRMT1 cooperate in gene regulation. *Nucleic Acids Res* **36**: 3202-3213
- Kolbel K, Ihling C, Bellmann-Sickert K, Neundorff I, Beck-Sickinger AG, Sinz A, Kuhn U, Wahle E (2009) Type I Arginine Methyltransferases PRMT1 and PRMT-3 Act Distributively. *J Biol Chem* **284**: 8274-8282
- Kowenz-Leutz E, Pless O, Dittmar G, Knoblich M, Leutz A (2010) Crosstalk between C/EBPbeta phosphorylation, arginine methylation, and SWI/SNF/Mediator implies an indexing transcription factor code. *The EMBO journal* **29**: 1105-1115
- Kuhn P, Chumanov R, Wang Y, Ge Y, Burgess RR, Xu W (2011) Automethylation of CARM1 allows coupling of transcription and mRNA splicing. *Nucleic Acids Res* **39**: 2717-2726
- Kwak YT, Guo J, Prajapati S, Park KJ, Surabhi RM, Miller B, Gehrig P, Gaynor RB (2003) Methylation of SPT5 regulates its interaction with RNA polymerase II and transcriptional elongation properties. *Mol Cell* **11**: 1055-1066
- Lahusen T, Henke RT, Kagan BL, Wellstein A, Riegel AT (2009) The role and regulation of the nuclear receptor co-activator AIB1 in breast cancer. *Breast Cancer Res Treat* **116**: 225-237

- Lai F, Orom UA, Cesaroni M, Beringer M, Taatjes DJ, Blobel GA, Shiekhataar R (2013) Activating RNAs associate with Mediator to enhance chromatin architecture and transcription. *Nature* **494**: 497-501
- Lakowski TM, Frankel A (2008) A kinetic study of human protein arginine N-methyltransferase 6 reveals a distributive mechanism. *J Biol Chem* **283**: 10015-10025
- Le Romancer M, Treilleux I, Leconte N, Robin-Lespinasse Y, Sentis S, Bouchekioua-Bouzaghrou K, Goddard S, Gobert-Gosse S, Corbo L (2008) Regulation of estrogen rapid signaling through arginine methylation by PRMT1. *Mol Cell* **31**: 212-221
- Lee DY, Ianculescu I, Purcell D, Zhang X, Cheng X, Stallcup MR (2007) Surface-scanning mutational analysis of protein arginine methyltransferase 1: roles of specific amino acids in methyltransferase substrate specificity, oligomerization, and coactivator function. *Mol Endocrinol* **21**: 1381-1393
- Lee J, Bedford MT (2002) PABP1 identified as an arginine methyltransferase substrate using high-density protein arrays. *EMBO Rep* **3**: 268-273
- Lee J, Sayegh J, Daniel J, Clarke S, Bedford MT (2005a) PRMT8, a new membrane-bound tissue-specific member of the protein arginine methyltransferase family. *J Biol Chem* **280**: 32890-32896
- Lee JE, Wang C, Xu S, Cho YW, Wang L, Feng X, Baldrige A, Sartorelli V, Zhuang L, Peng W, Ge K (2013) H3K4 mono- and di-methyltransferase MLL4 is required for enhancer activation during cell differentiation. *Elife* **2**: e01503
- Lee YH, Coonrod SA, Kraus WL, Jelinek MA, Stallcup MR (2005b) Regulation of coactivator complex assembly and function by protein arginine methylation and demethylation. *Proc Natl Acad Sci U S A* **102**: 3611-3616
- Lehner B, Crombie C, Tischler J, Fortunato A, Fraser AG (2006) Systematic mapping of genetic interactions in *Caenorhabditis elegans* identifies common modifiers of diverse signaling pathways. *Nat Genet* **38**: 896-903
- Lei NZ, Zhang XY, Chen HZ, Wang Y, Zhan YY, Zheng ZH, Shen YM, Wu Q (2009) A feedback regulatory loop between methyltransferase PRMT1 and orphan receptor TR3. *Nucleic Acids Res* **37**: 832-848
- Li H, Park S, Kilburn B, Jelinek MA, Henschen-Edman A, Aswad DW, Stallcup MR, Laird-Offringa IA (2002) Lipopolysaccharide-induced methylation of HuR, an mRNA-stabilizing protein, by CARM1. Coactivator-associated arginine methyltransferase. *J Biol Chem* **277**: 44623-44630
- Li J, Zhao Z, Carter C, Ehrlich LI, Bedford MT, Richie ER (2013) Coactivator-associated arginine methyltransferase 1 regulates fetal hematopoiesis and thymocyte development. *J Immunol* **190**: 597-604
- Lin WJ, Gary JD, Yang MC, Clarke S, Herschman HR (1996) The mammalian immediate-early TIS21 protein and the leukemia-associated BTG1 protein interact with a protein-arginine N-methyltransferase. *J Biol Chem* **271**: 15034-15044

Liu F, Zhao X, Perna F, Wang L, Koppikar P, Abdel-Wahab O, Harr MW, Levine RL, Xu H, Tefferi A, Deblasio A, Hatlen M, Menendez S, Nimer SD (2011) JAK2V617F-mediated phosphorylation of PRMT5 downregulates its methyltransferase activity and promotes myeloproliferation. *Cancer Cell* **19**: 283-294

Lupien M, Eeckhoute J, Meyer CA, Krum SA, Rhodes DR, Liu XS, Brown M (2009) Coactivator function defines the active estrogen receptor alpha cisome. *Mol Cell Biol* **29**: 3413-3423

Majumder S, Liu Y, Ford OH, 3rd, Mohler JL, Whang YE (2006) Involvement of arginine methyltransferase CARM1 in androgen receptor function and prostate cancer cell viability. *Prostate* **66**: 1292-1301

Malik S, Roeder RG (2010) The metazoan Mediator co-activator complex as an integrative hub for transcriptional regulation. *Nat Rev Genet* **11**: 761-772

Malik S, Wallberg AE, Kang YK, Roeder RG (2002) TRAP/SMCC/mediator-dependent transcriptional activation from DNA and chromatin templates by orphan nuclear receptor hepatocyte nuclear factor 4. *Mol Cell Biol* **22**: 5626-5637

Mallappa C, Hu YJ, Shamulailatpam P, Tae S, Sif S, Imbalzano AN (2011) The expression of myogenic microRNAs indirectly requires protein arginine methyltransferase (Prmt)5 but directly requires Prmt4. *Nucleic Acids Res* **39**: 1243-1255

Matsuoka M (1972) [Epsilon-N-methylated lysine and guanidine-N-methylated arginine of proteins. 3. Presence and distribution in nature and mammals]. *Seikagaku* **44**: 364-370

Metivier R, Penot G, Hubner MR, Reid G, Brand H, Kos M, Gannon F (2003) Estrogen receptor- α directs ordered, cyclical, and combinatorial recruitment of cofactors on a natural target promoter. *Cell* **115**: 751-763

Miyata S, Mori Y, Tohyama M (2008) PRMT1 and Btg2 regulates neurite outgrowth of Neuro2a cells. *Neurosci Lett* **445**: 162-165

Mo X, Kowenz-Leutz E, Xu H, Leutz A (2004) Ras induces mediator complex exchange on C/EBP beta. *Mol Cell* **13**: 241-250

Morris EJ, Ji JY, Yang F, Di Stefano L, Herr A, Moon NS, Kwon EJ, Haigis KM, Naar AM, Dyson NJ (2008) E2F1 represses beta-catenin transcription and is antagonized by both pRB and CDK8. *Nature* **455**: 552-556

Naeem H, Cheng D, Zhao Q, Underhill C, Tini M, Bedford MT, Torchia J (2007) The activity and stability of the transcriptional coactivator p/CIP/SRC-3 are regulated by CARM1-dependent methylation. *Molecular and cellular biology* **27**: 120-134

Neault M, Mallette FA, Vogel G, Michaud-Levesque J, Richard S (2012) Ablation of PRMT6 reveals a role as a negative transcriptional regulator of the p53 tumor suppressor. *Nucleic Acids Res* **40**: 9513-9521

- Nicholson TB, Chen T, Richard S (2009) The physiological and pathophysiological role of PRMT1-mediated protein arginine methylation. *Pharmacol Res* **60**: 466-474
- Nowak SJ, Corces VG (2004) Phosphorylation of histone H3: a balancing act between chromosome condensation and transcriptional activation. *Trends Genet* **20**: 214-220
- O'Brien KB, Alberich-Jorda M, Yadav N, Kocher O, Diruscio A, Ebralidze A, Levantini E, Sng NJ, Bhasin M, Caron T, Kim D, Steidl U, Huang G, Halmos B, Rodig SJ, Bedford MT, Tenen DG, Kobayashi S (2010) CARM1 is required for proper control of proliferation and differentiation of pulmonary epithelial cells. *Development* **137**: 2147-2156
- Obianyo O, Osborne TC, Thompson PR (2008) Kinetic mechanism of protein arginine methyltransferase 1. *Biochemistry* **47**: 10420-10427
- Ong SE, Mittler G, Mann M (2004a) Identifying and quantifying in vivo methylation sites by heavy methyl SILAC. *Nature methods* **1**: 119-126
- Ong SE, Mittler G, Mann M (2004b) Identifying and quantifying in vivo methylation sites by heavy methyl SILAC. *Nat Methods* **1**: 119-126
- Osborne TC, Obianyo O, Zhang X, Cheng X, Thompson PR (2007) Protein arginine methyltransferase 1: positively charged residues in substrate peptides distal to the site of methylation are important for substrate binding and catalysis. *Biochemistry* **46**: 13370-13381
- Ou CY, LaBonte MJ, Manegold PC, So AY, Ianculescu I, Gerke DS, Yamamoto KR, Ladner RD, Kahn M, Kim JH, Stallcup MR (2011) A coactivator role of CARM1 in the dysregulation of beta-catenin activity in colorectal cancer cell growth and gene expression. *Mol Cancer Res* **9**: 660-670
- Pal S, Baiocchi RA, Byrd JC, Grever MR, Jacob ST, Sif S (2007) Low levels of miR-92b/96 induce PRMT5 translation and H3R8/H4R3 methylation in mantle cell lymphoma. *EMBO J* **26**: 3558-3569
- Pal S, Vishwanath SN, Erdjument-Bromage H, Tempst P, Sif S (2004) Human SWI/SNF-associated PRMT5 methylates histone H3 arginine 8 and negatively regulates expression of ST7 and NM23 tumor suppressor genes. *Mol Cell Biol* **24**: 9630-9645
- Panfil AR, Al-Saleem J, Howard CM, Mates JM, Kwiek JJ, Baiocchi RA, Green PL (2015) PRMT5 Is Upregulated in HTLV-1-Mediated T-Cell Transformation and Selective Inhibition Alters Viral Gene Expression and Infected Cell Survival. *Viruses* **8**
- Pang L, Tian H, Chang N, Yi J, Xue L, Jiang B, Gorospe M, Zhang X, Wang W (2013) Loss of CARM1 is linked to reduced HuR function in replicative senescence. *BMC Mol Biol* **14**: 15
- Pawlak MR, Scherer CA, Chen J, Roshon MJ, Ruley HE (2000) Arginine N-methyltransferase 1 is required for early postimplantation mouse development, but cells deficient in the enzyme are viable. *Mol Cell Biol* **20**: 4859-4869
- Pesiridis GS, Diamond E, Van Duyne GD (2009) Role of pICLn in methylation of Sm proteins by PRMT5. *J Biol Chem* **284**: 21347-21359

Philibert RA (2006) A meta-analysis of the association of the HOPA12bp polymorphism and schizophrenia. *Psychiatr Genet* **16**: 73-76

Philibert RA, Madan A (2007) Role of MED12 in transcription and human behavior. *Pharmacogenomics* **8**: 909-916

Prenzel T, Kramer F, Bedi U, Nagarajan S, Beissbarth T, Johnsen SA (2012) Cohesin is required for expression of the estrogen receptor-alpha (ESR1) gene. *Epigenetics Chromatin* **5**: 13

Rachez C, Lemon BD, Suldan Z, Bromleigh V, Gamble M, Naar AM, Erdjument-Bromage H, Tempst P, Freedman LP (1999) Ligand-dependent transcription activation by nuclear receptors requires the DRIP complex. *Nature* **398**: 824-828

Rathert P, Dhayalan A, Murakami M, Zhang X, Tamas R, Jurkowska R, Komatsu Y, Shinkai Y, Cheng X, Jeltsch A (2008) Protein lysine methyltransferase G9a acts on non-histone targets. *Nat Chem Biol* **4**: 344-346

Rawal Y, Qiu H, Hinnebusch AG (2014) Accumulation of a threonine biosynthetic intermediate attenuates general amino acid control by accelerating degradation of Gcn4 via Pho85 and Cdk8. *PLoS Genet* **10**: e1004534

Rezai-Zadeh N, Zhang X, Namour F, Fejer G, Wen YD, Yao YL, Gyory I, Wright K, Seto E (2003) Targeted recruitment of a histone H4-specific methyltransferase by the transcription factor YY1. *Genes Dev* **17**: 1019-1029

Risheg H, Graham JM, Jr., Clark RD, Rogers RC, Opitz JM, Moeschler JB, Peiffer AP, May M, Joseph SM, Jones JR, Stevenson RE, Schwartz CE, Friez MJ (2007) A recurrent mutation in MED12 leading to R961W causes Opitz-Kaveggia syndrome. *Nat Genet* **39**: 451-453

Robin-Lespinasse Y, Sentis S, Kolytcheff C, Rostan MC, Corbo L, Le Romancer M (2007) hCAF1, a new regulator of PRMT1-dependent arginine methylation. *J Cell Sci* **120**: 638-647

Rocha PP, Scholze M, Bleiss W, Schrewe H (2010) Med12 is essential for early mouse development and for canonical Wnt and Wnt/PCP signaling. *Development* **137**: 2723-2731

Rush J, Moritz A, Lee KA, Guo A, Goss VL, Spek EJ, Zhang H, Zha XM, Polakiewicz RD, Comb MJ (2005) Immunoaffinity profiling of tyrosine phosphorylation in cancer cells. *Nat Biotechnol* **23**: 94-101

Sandhu HK, Sarkar M, Turner BM, Wassink TH, Philibert RA (2003) Polymorphism analysis of HOPA: a candidate gene for schizophrenia. *Am J Med Genet B Neuropsychiatr Genet* **123B**: 33-38

Sayegh J, Webb K, Cheng D, Bedford MT, Clarke SG (2007) Regulation of protein arginine methyltransferase 8 (PRMT8) activity by its N-terminal domain. *J Biol Chem* **282**: 36444-36453

Schiano C, Casamassimi A, Rienzo M, de Nigris F, Sommese L, Napoli C (2014) Involvement of Mediator complex in malignancy. *Biochim Biophys Acta* **1845**: 66-83

Schurter BT, Koh SS, Chen D, Bunick GJ, Harp JM, Hanson BL, Henschen-Edman A, Mackay DR, Stallcup MR, Aswad DW (2001) Methylation of histone H3 by coactivator-associated arginine methyltransferase 1. *Biochemistry* **40**: 5747-5756

Schwartz CE, Tarpey PS, Lubs HA, Verloes A, May MM, Risheg H, Friez MJ, Futreal PA, Edkins S, Teague J, Briault S, Skinner C, Bauer-Carlin A, Simensen RJ, Joseph SM, Jones JR, Gecz J, Stratton MR, Raymond FL, Stevenson RE (2007) The original Lujan syndrome family has a novel missense mutation (p.N1007S) in the MED12 gene. *J Med Genet* **44**: 472-477

Shalem O, Sanjana NE, Hartenian E, Shi X, Scott DA, Mikkelsen TS, Heckl D, Ebert BL, Root DE, Doench JG, Zhang F (2014) Genome-scale CRISPR-Cas9 knockout screening in human cells. *Science* **343**: 84-87

Shia WJ, Okumura AJ, Yan M, Sarkeshik A, Lo MC, Matsuura S, Komeno Y, Zhao X, Nimer SD, Yates JR, 3rd, Zhang DE (2012) PRMT1 interacts with AML1-ETO to promote its transcriptional activation and progenitor cell proliferative potential. *Blood* **119**: 4953-4962

Shimbo T, Du Y, Grimm SA, Dhasarathy A, Mav D, Shah RR, Shi H, Wade PA (2013) MBD3 localizes at promoters, gene bodies and enhancers of active genes. *PLoS Genet* **9**: e1004028

Sims RJ, 3rd, Rojas LA, Beck D, Bonasio R, Schuller R, Drury WJ, 3rd, Eick D, Reinberg D (2011) The C-terminal domain of RNA polymerase II is modified by site-specific methylation. *Science* **332**: 99-103

Singh V, Miranda TB, Jiang W, Frankel A, Roemer ME, Robb VA, Gutmann DH, Herschman HR, Clarke S, Newsham IF (2004) DAL-1/4.1B tumor suppressor interacts with protein arginine N-methyltransferase 3 (PRMT3) and inhibits its ability to methylate substrates in vitro and in vivo. *Oncogene* **23**: 7761-7771

Smith WA, Schurter BT, Wong-Staal F, David M (2004) Arginine methylation of RNA helicase a determines its subcellular localization. *J Biol Chem* **279**: 22795-22798

Stallcup MR, Kim JH, Teyssier C, Lee YH, Ma H, Chen D (2003) The roles of protein-protein interactions and protein methylation in transcriptional activation by nuclear receptors and their coactivators. *J Steroid Biochem Mol Biol* **85**: 139-145

Stoll G, Pietilainen OP, Linder B, Suvisaari J, Brosi C, Hennah W, Leppa V, Tornaiainen M, Ripatti S, Ala-Mello S, Plottner O, Rehnstrom K, Tuulio-Henriksson A, Varilo T, Tallila J, Kristiansson K, Isohanni M, Kaprio J, Eriksson JG, Raitakari OT, Lehtimaki T, Jarvelin MR, Salomaa V, Hurler M, Stefansson H, Peltonen L, Sullivan PF, Paunio T, Lonnqvist J, Daly MJ, Fischer U, Freimer NB, Palotie A (2013) Deletion of TOP3beta, a component of FMRP-containing mRNPs, contributes to neurodevelopmental disorders. *Nat Neurosci*

Streubel G, Bouchard C, Berberich H, Zeller MS, Teichmann S, Adamkiewicz J, Muller R, Klempnauer KH, Bauer UM (2013) PRMT4 is a novel coactivator of c-Myb-dependent transcription in haematopoietic cell lines. *PLoS Genet* **9**: e1003343

- Stuhlinger MC, Tsao PS, Her JH, Kimoto M, Balint RF, Cooke JP (2001) Homocysteine impairs the nitric oxide synthase pathway: role of asymmetric dimethylarginine. *Circulation* **104**: 2569-2575
- Sun Q, Yang X, Zhong B, Jiao F, Li C, Li D, Lan X, Sun J, Lu S (2012) Upregulated protein arginine methyltransferase 1 by IL-4 increases eotaxin-1 expression in airway epithelial cells and participates in antigen-induced pulmonary inflammation in rats. *J Immunol* **188**: 3506-3512
- Swiercz R, Cheng D, Kim D, Bedford MT (2007) Ribosomal protein rpS2 is hypomethylated in PRMT3-deficient mice. *J Biol Chem* **282**: 16917-16923
- Taatjes DJ (2010) The human Mediator complex: a versatile, genome-wide regulator of transcription. *Trends Biochem Sci* **35**: 315-322
- Tang J, Frankel A, Cook RJ, Kim S, Paik WK, Williams KR, Clarke S, Herschman HR (2000a) PRMT1 is the predominant type I protein arginine methyltransferase in mammalian cells. *J Biol Chem* **275**: 7723-7730
- Tang J, Kao PN, Herschman HR (2000b) Protein-arginine methyltransferase I, the predominant protein-arginine methyltransferase in cells, interacts with and is regulated by interleukin enhancer-binding factor 3. *J Biol Chem* **275**: 19866-19876
- Tee WW, Pardo M, Theunissen TW, Yu L, Choudhary JS, Hajkova P, Surani MA (2010) Prmt5 is essential for early mouse development and acts in the cytoplasm to maintain ES cell pluripotency. *Genes Dev* **24**: 2772-2777
- Teferedegne B, Green MR, Guo Z, Boss JM (2006) Mechanism of action of a distal NF-kappaB-dependent enhancer. *Mol Cell Biol* **26**: 5759-5770
- Teng Y, Girvan AC, Casson LK, Pierce WM, Jr., Qian M, Thomas SD, Bates PJ (2007) AS1411 alters the localization of a complex containing protein arginine methyltransferase 5 and nucleolin. *Cancer Res* **67**: 10491-10500
- Teyssier C, Ma H, Emter R, Kralli A, Stallcup MR (2005) Activation of nuclear receptor coactivator PGC-1alpha by arginine methylation. *Genes Dev* **19**: 1466-1473
- Thandapani P, O'Connor TR, Bailey TL, Richard S (2013a) Defining the RGG/RG motif. *Molecular cell* **50**: 613-623
- Thandapani P, O'Connor TR, Bailey TL, Richard S (2013b) Defining the RGG/RG motif. *Mol Cell* **50**: 613-623
- Traunmuller L, Bornmann C, Scheiffele P (2014) Alternative splicing coupled nonsense-mediated decay generates neuronal cell type-specific expression of SLM proteins. *The Journal of neuroscience : the official journal of the Society for Neuroscience* **34**: 16755-16761
- Tsai KL, Sato S, Tomomori-Sato C, Conaway RC, Conaway JW, Asturias FJ (2013) A conserved Mediator-CDK8 kinase module association regulates Mediator-RNA polymerase II interaction. *Nat Struct Mol Biol* **20**: 611-619

Turunen M, Spaeth JM, Keskitalo S, Park MJ, Kivioja T, Clark AD, Makinen N, Gao F, Palin K, Nurkkala H, Vaharautio A, Aavikko M, Kampjarvi K, Vahteristo P, Kim CA, Aaltonen LA, Varjosalo M, Taipale J, Boyer TG (2014) Uterine leiomyoma-linked MED12 mutations disrupt mediator-associated CDK activity. *Cell Rep* **7**: 654-660

Tutter AV, Kowalski MP, Baltus GA, Iourgenko V, Labow M, Li E, Kadam S (2009) Role for Med12 in regulation of Nanog and Nanog target genes. *J Biol Chem* **284**: 3709-3718

Uhlmann T, Geoghegan VL, Thomas B, Ridlova G, Trudgian DC, Acuto O (2012) A method for large-scale identification of protein arginine methylation. *Molecular & cellular proteomics : MCP* **11**: 1489-1499

Vogl MR, Reiprich S, Kuspert M, Kosian T, Schrewe H, Nave KA, Wegner M (2013) Sox10 cooperates with the mediator subunit 12 during terminal differentiation of myelinating glia. *J Neurosci* **33**: 6679-6690

Wang G, Balamotis MA, Stevens JL, Yamaguchi Y, Handa H, Berk AJ (2005) Mediator requirement for both recruitment and postrecruitment steps in transcription initiation. *Mol Cell* **17**: 683-694

Wang H, Huang ZQ, Xia L, Feng Q, Erdjument-Bromage H, Strahl BD, Briggs SD, Allis CD, Wong J, Tempst P, Zhang Y (2001) Methylation of histone H4 at arginine 3 facilitating transcriptional activation by nuclear hormone receptor. *Science* **293**: 853-857

Wang L, Pal S, Sif S (2008) Protein arginine methyltransferase 5 suppresses the transcription of the RB family of tumor suppressors in leukemia and lymphoma cells. *Mol Cell Biol* **28**: 6262-6277

Wang L, Zeng H, Wang Q, Zhao Z, Boyer TG, Bian X, Xu W (2015) MED12 methylation by CARM1 sensitizes human breast cancer cells to chemotherapy drugs. *Sci Adv* **1**: e1500463

Wang L, Zhao Z, Meyer MB, Saha S, Yu M, Guo A, Wisinski KB, Huang W, Cai W, Pike JW, Yuan M, Ahlquist P, Xu W (2014a) CARM1 methylates chromatin remodeling factor BAF155 to enhance tumor progression and metastasis. *Cancer Cell* **25**: 21-36

Wang M, Fuhrmann J, Thompson PR (2014b) Protein arginine methyltransferase 5 catalyzes substrate dimethylation in a distributive fashion. *Biochemistry* **53**: 7884-7892

Webby CJ, Wolf A, Gromak N, Dreger M, Kramer H, Kessler B, Nielsen ML, Schmitz C, Butler DS, Yates JR, 3rd, Delahunty CM, Hahn P, Lengeling A, Mann M, Proudfoot NJ, Schofield CJ, Bottger A (2009) Jmjd6 catalyses lysyl-hydroxylation of U2AF65, a protein associated with RNA splicing. *Science* **325**: 90-93

Wei TY, Juan CC, Hisa JY, Su LJ, Lee YC, Chou HY, Chen JM, Wu YC, Chiu SC, Hsu CP, Liu KL, Yu CT (2012) Protein arginine methyltransferase 5 is a potential oncoprotein that upregulates G1 cyclins/cyclin-dependent kinases and the phosphoinositide 3-kinase/AKT signaling cascade. *Cancer Sci* **103**: 1640-1650

Wong MM, Guo C, Zhang J (2014a) Nuclear receptor corepressor complexes in cancer: mechanism, function and regulation. *Am J Clin Exp Urol* **2**: 169-187

Wong MM, Guo C, Zhang J (2014b) Nuclear receptor corepressor complexes in cancer: mechanism, function and regulation. *American journal of clinical and experimental urology* **2**: 169-187

Wu Q, Bruce AW, Jedrusik A, Ellis PD, Andrews RM, Langford CF, Glover DM, Zernicka-Goetz M (2009) CARM1 is required in embryonic stem cells to maintain pluripotency and resist differentiation. *Stem Cells* **27**: 2637-2645

Xie Y, Ke S, Ouyang N, He J, Xie W, Bedford MT, Tian Y (2009) Epigenetic regulation of transcriptional activity of pregnane X receptor by protein arginine methyltransferase 1. *J Biol Chem* **284**: 9199-9205

Xu D, Shen W, Guo R, Xue Y, Peng W, Sima J, Yang J, Sharov A, Srikantan S, Fox D, 3rd, Qian Y, Martindale JL, Piao Y, Machamer J, Joshi SR, Mohanty S, Shaw AC, Lloyd TE, Brown GW, Ko MS, Gorospe M, Zou S, Wang W (2013) Top3beta is an RNA topoisomerase that works with fragile X syndrome protein to promote synapse formation. *Nat Neurosci*

Xu W, Chen H, Du K, Asahara H, Tini M, Emerson BM, Montminy M, Evans RM (2001) A transcriptional switch mediated by cofactor methylation. *Science* **294**: 2507-2511

Xu W, Cho H, Kadam S, Banayo EM, Anderson S, Yates JR, 3rd, Emerson BM, Evans RM (2004) A methylation-mediator complex in hormone signaling. *Genes Dev* **18**: 144-156

Xu X, Zhou H, Boyer TG (2011) Mediator is a transducer of amyloid-precursor-protein-dependent nuclear signalling. *EMBO Rep* **12**: 216-222

Yadav N, Cheng D, Richard S, Morel M, Iyer VR, Aldaz CM, Bedford MT (2008) CARM1 promotes adipocyte differentiation by coactivating PPARgamma. *EMBO Rep* **9**: 193-198

Yadav N, Lee J, Kim J, Shen J, Hu MC, Aldaz CM, Bedford MT (2003) Specific protein methylation defects and gene expression perturbations in coactivator-associated arginine methyltransferase 1-deficient mice. *Proc Natl Acad Sci U S A* **100**: 6464-6468

Yamagata K, Daitoku H, Takahashi Y, Namiki K, Hisatake K, Kako K, Mukai H, Kasuya Y, Fukamizu A (2008) Arginine methylation of FOXO transcription factors inhibits their phosphorylation by Akt. *Mol Cell* **32**: 221-231

Yang F, Vought BW, Satterlee JS, Walker AK, Jim Sun ZY, Watts JL, DeBeaumont R, Saito RM, Hyberts SG, Yang S, Macol C, Iyer L, Tjian R, van den Heuvel S, Hart AC, Wagner G, Naar AM (2006) An ARC/Mediator subunit required for SREBP control of cholesterol and lipid homeostasis. *Nature* **442**: 700-704

Yang Y, Bedford MT (2013) Protein arginine methyltransferases and cancer. *Nat Rev Cancer* **13**: 37-50

Yang Y, Hadjikyriacou A, Xia Z, Gayatri S, Kim D, Zurita-Lopez C, Kelly R, Guo A, Li W, Clarke SG, Bedford MT (2015) PRMT9 is a type II methyltransferase that methylates the splicing factor SAP145. *Nat Commun* **6**: 6428

- Yang Y, Lu Y, Espejo A, Wu J, Xu W, Liang S, Bedford MT (2010) TDRD3 is an effector molecule for arginine-methylated histone marks. *Mol Cell* **40**: 1016-1023
- Yang Y, McBride KM, Hensley S, Lu Y, Chedin F, Bedford MT (2014) Arginine Methylation Facilitates the Recruitment of TOP3B to Chromatin to Prevent R Loop Accumulation. *Molecular cell* **53**: 484-497
- Ying Z, Mei M, Zhang P, Liu C, He H, Gao F, Bao S (2015) Histone Arginine Methylation by PRMT7 Controls Germinal Center Formation via Regulating Bcl6 Transcription. *J Immunol* **195**: 1538-1547
- Yoshimoto T, Boehm M, Olive M, Crook MF, San H, Langenickel T, Nabel EG (2006) The arginine methyltransferase PRMT2 binds RB and regulates E2F function. *Exp Cell Res* **312**: 2040-2053
- Yu Z, Chen T, Hebert J, Li E, Richard S (2009) A mouse PRMT1 null allele defines an essential role for arginine methylation in genome maintenance and cell proliferation. *Mol Cell Biol* **29**: 2982-2996
- Zeng H, Wu J, Bedford MT, Sbardella G, Hoffmann FM, Bi K, Xu W (2013) A TR-FRET-based functional assay for screening activators of CARM1. *Chembiochem* **14**: 827-835
- Zhang X, Cheng X (2003) Structure of the predominant protein arginine methyltransferase PRMT1 and analysis of its binding to substrate peptides. *Structure* **11**: 509-520
- Zhao HY, Zhang YJ, Dai H, Zhang Y, Shen YF (2011) CARM1 mediates modulation of Sox2. *PLoS One* **6**: e27026
- Zhao X, Feng D, Wang Q, Abdulla A, Xie XJ, Zhou J, Sun Y, Yang ES, Liu LP, Vaitheesvaran B, Bridges L, Kurland IJ, Strich R, Ni JQ, Wang C, Ericsson J, Pessin JE, Ji JY, Yang F (2012) Regulation of lipogenesis by cyclin-dependent kinase 8-mediated control of SREBP-1. *J Clin Invest* **122**: 2417-2427
- Zhou H, Kim S, Ishii S, Boyer TG (2006) Mediator modulates Gli3-dependent Sonic hedgehog signaling. *Mol Cell Biol* **26**: 8667-8682
- Zhou H, Spaeth JM, Kim NH, Xu X, Friez MJ, Schwartz CE, Boyer TG (2012) MED12 mutations link intellectual disability syndromes with dysregulated GLI3-dependent Sonic Hedgehog signaling. *Proc Natl Acad Sci U S A* **109**: 19763-19768
- Zurita-Lopez CI, Sandberg T, Kelly R, Clarke SG (2012) Human protein arginine methyltransferase 7 (PRMT7) is a type III enzyme forming omega-NG-monomethylated arginine residues. *J Biol Chem* **287**: 7859-7870

9. Vita

Vidyasiri Vemulapalli was born in Vijayawada, Andhra Pradesh, India on January 20, 1986, the daughter of Poornachandra Rao Vemulapalli and Padmavathi Vemulapalli. After completing her work at Narayana Junior College, Vijayawada, Andhra Pradesh, India in 2003, she entered Vellore Institute of Technology in Vellore, Tamil Nadu, India. She received the degree of Bachelor of Science with a major in Biotechnology from Vellore Institute in May 2007. In August 2007, she came to the United States to pursue higher education. She received the degree of Master of Science with a major in Biology from the University of Texas at San Antonio, San Antonio, Texas in May 2009. During her Master's degree program, she did thesis research work in a fungal molecular biology lab as well as worked as a teaching assistant for the cell biology course for the undergraduate program at the University of Texas at San Antonio. In August of 2009, she entered the University of Texas Graduate School of Biomedical Sciences at Houston.